Stratigraphy and Paleoenvironments of Early Postimpact Deposits at the USGS-NASA Langley Corehole, Chesapeake Bay Impact Crater

By C. Wylie Poag and Richard D. Norris

Chapter F of
Studies of the Chesapeake Bay Impact Structure—The USGS-NASA Langley Corehole, Hampton, Virginia, and Related Coreholes and Geophysical Surveys

Edited by J. Wright Horton, Jr., David S. Powars, and Gregory S. Gohn

Prepared in cooperation with the
Hampton Roads Planning District Commission,
Virginia Department of Environmental Quality, and
National Aeronautics and Space Administration Langley Research Center

Professional Paper 1688

U.S. Department of the Interior
U.S. Geological Survey

Contents

Plates

[Plates follow References Cited]

Figures

Tables

Stratigraphy and Paleoenvironments of Early Postimpact Deposits at the USGS-NASA Langley Corehole, Chesapeake Bay Impact Crater

By C. Wylie Poag[1] and Richard D. Norris[2]

Abstract

The USGS-NASA Langley corehole was drilled into the Chesapeake Bay impact crater in Hampton, Va. We used whole and split cores, seismic-reflection surveys (multichannel and single channel), downhole geophysical logs (spontaneous potential and gamma ray), micropaleontology (planktonic and benthic foraminifera and bolboformids), and stable-isotope records ($\delta^{18}O$, $\delta^{13}C$) to interpret the lithic, biotic, paleoenvironmental, and geophysical properties contained in, or represented by, the late synimpact and early postimpact deposits (fallout layer, dead zone, and Chickahominy Formation) overlying the Exmore breccia in the USGS-NASA Langley core.

The initial postimpact deposit in the Langley core (resting above a fallout layer) is a dead zone, barren of indigenous foraminifera, which represents an interval of hostile sea-floor paleoenvironments; the interval length was between less than 1,000 years and 8,000 years. Full recovery of the benthic foraminiferal community was rapid once amenable conditions were reestablished at the beginning of Chickahominy time.

Planktonic foraminifera and bolboformids show that biochronozones P15 and P16-P17 of the late Eocene are represented by the Chickahominy Formation in the Langley corehole. These are the same biochronozones previously documented in the Chickahominy Formation from inside the Chesapeake Bay impact crater at the Exmore and Kiptopeke core sites.

The benthic foraminferal assemblages of the Chickahominy Formation are encompassed in a single biozone (*Cibicidoides pippeni* Zone), which is represented by 126 calcareous and agglutinated species in the Chickahominy Formation in the Langley core. The *Cibicidoides pippeni* Zone can be divided into five subbiozones (*Bathysiphon, Bulimina jacksonensis, Lagenoglandulina virginiana, Uvigerina dumblei,* and *Bolivina tectiformis* Subzones). The most abundant and stratigraphically most persistent species represented in the *Cibicidoides pippeni* assemblage indicate a paleodepth of about 300 meters (~1,000 feet) for the Chickahominy sea floor, which exhibited oxygen deprivation and high flux rates of organic carbon.

At the Langley corehole, the spontaneous-potential and gamma-ray curves allow recognition of four or five lithic subunits, which correlate approximately with those similarly distinguished in three other intracrater coreholes (North, Bayside, Kiptopeke). Lithically, the Chickahominy Formation in the Langley corehole differs from its equivalents in the other three coreholes, however, by having greater permeability and a greater volume of glauconite near the base of the formation.

The late Eocene paleoclimate, as expressed by the postimpact $\delta^{18}O$ record at the Langley corehole, was characterized by three negative excursions of $\delta^{18}O$ (interpreted to represent pulses of atmospheric warmth). A significant negative excursion of $\delta^{13}C$ in the upper part of the Chickahominy Formation is consistent with a net global decrease in carbon burial. These same isotopic successions have been previously recorded in the Kiptopeke corehole, as well as at many other locations around the globe. The isotope record provides evidence that the Chesapeake Bay impact and other late Eocene impacts may have exerted a long-term influence on global climate changes, which culminated in the well-known early Oligocene mass extinction event.

Introduction

The Chesapeake Bay impact crater formed in the late Eocene when a hypervelocity impactor struck the Atlantic continental shelf near the present town of Cape Charles, Va. The impactor was either a comet or an asteroid, but in this chapter, it is referred to by the generic term "bolide." To obtain geological information about the impact and the resultant crater, the U.S. Geological Survey (USGS) and its partners drilled the USGS-NASA Langley corehole in 2000 (see "Acknowledgments").

The USGS-NASA Langley core site is located at lat 37°05'44.28" N., long 76°23'08.96" W. (North American Datum of 1927), at the National Aeronautics and Space Administration (NASA) Langley Research Center in Hampton, Va. The core site is approximately 5 kilometers (km; 3 miles (mi))

[1]U.S. Geological Survey, Woods Hole, MA 02543.
[2]Scripps Institution of Oceanography, La Jolla, CA 92093.

inside the southwestern rim (in the outer part of the annular trough) of the Chesapeake Bay impact crater (figs. F1, F2). Here the Chickahominy Formation is 52.37 meters (m; 171.8 feet (ft)) thick and represents apparently continuous sediment accumulation for most of the final ~2.1 million years (m.y.) of the late Eocene Epoch.

The principal objectives of this study were (1) to establish the immediate effects of the Chesapeake Bay bolide impact on the local benthic biota and to characterize the transition from synimpact to postimpact deposition at the USGS-NASA Langley core site; (2) to qualitatively evaluate the biostratigraphy of principally the benthic foraminiferal assemblages in the Chickahominy Formation in the USGS-NASA Langley core and then to compare the evaluations with the results from previous investigations; and (3) to interpret the postimpact paleoenvironments of the Chickahominy Formation as represented at the USGS-NASA Langley core site.

Methods

We used downhole geophysical logs and cores (whole and split sections) to analyze the general lithostratigraphic aspects of the fallout layer, dead zone, and Chickahominy Formation. To study the foraminiferal suites, we took 66 samples (~85 cubic centimeters each) spaced ~1 m (3 ft) apart (table F1) and prepared them in a standard manner (wet sieved on a 63-micrometer (μm) screen after 15 minutes of boiling in a solution of sodium hexametaphosphate). Oven-dried samples were examined by optical and scanning-electron microscopy. We identified benthic foraminiferal species from available literature where possible (Cushman, 1935; Cushman and Cederstrom, 1945; Charletta, 1980; Jones, 1990), but we also used many provisory trivial names (enclosed in quotation marks in fig. F20, pl. F2, and tables F4–F9) for stratigraphic purposes. These names were previously published by Poag, Koeberl, and Reimold (2004), who studied Chickahominy foraminifera from the Kiptopeke corehole. Because this was not a taxonomic investigation, we did not thoroughly assess the validity or priority of all formal taxonomic names we applied.

We performed stable-isotope analyses for oxygen and organic carbon on the same samples used for foraminiferal analysis (table F2). We used monospecific samples (~3–20 individuals of the benthic foraminifer *Cibicidoides pippeni*) from the >63-μm grain-size fraction. We performed mass spectrometry using a Finnigan MAT 252 instrument with an online automated carbonate reaction Kiel device (Woods Hole Oceanographic Institution). Analytical precision based on repeated analysis of standards (NBS–19, Carrara Marble, and B–1 marine carbonate) was better than ±0.03 per mil (‰) for $\delta^{13}C$ and 0.08‰ for $\delta^{18}O$ relative to the Peedee belemnite (PDB) standard.

We used the magnetobiochronological framework (synthesis of radioisotopes, geomagnetic polarity, planktonic foraminifera, and calcareous nannofossils) of Berggren and others (1995) to guide interpretation and correlation of our biostratigraphic and stable-isotope results (fig. F3).

Previous Work

Several previous studies have documented the physical and biotic characteristics of deposits that record the transition from synimpact sedimentation (fallout zone) to postimpact sedimentation (dead zone and Chickahominy Formation) at sites within and outside the Chesapeake Bay impact crater (Poag, 1997a; Powars and Bruce, 1999; Poag, 2002; Poag, Koeberl, and Reimold, 2004). An initial qualitative stratigraphic study of Chickahominy foraminiferal assemblages was carried out more than 50 years ago (Cushman and Cederstrom, 1945). No subsequent microfossil investigations of the Chickahominy were initiated until cores became available from the Chesapeake Bay impact crater.

After this long hiatus, several new qualitative studies of benthic foraminifera, planktonic foraminifera, and bolboformids were published (Poag and Aubry, 1995; Poag and Commeau, 1995; Poag, 1997a; Poag, Koeberl, and Reimold, 2004; fig. F4). In addition, Poag, Koeberl, and Reimold (2004) presented a *quantitative* stratigraphic analysis and paleoenvironmental interpretation of the Chickahominy benthic foraminiferal assemblages (fig. F5) from the Kiptopeke corehole, located inside the peak ring, near the center of the crater (fig. F1). Poag, Mankinen, and Norris (2003) analyzed the paleomagnetic and stable-isotope records ($\delta^{18}O$ and $\delta^{13}C$) of the Chickahominy Formation at Kiptopeke (figs. F5, F6) and correlated them with other upper Eocene sections around the globe. Poag (2002) and Poag, Koeberl, and Reimold (2004) provided initial assessments of the transition from fallout layer to dead zone to Chickahominy Formation in the USGS-NASA Langley core (fig. F7). Poag, Koeberl, and Reimold (2004, p. 391) extended this evaluation to the Kiptopeke core.

The reader should note that in this chapter, we use the stratigraphic framework and terminology of Poag, Koeberl, and Reimold (2004), in which the brecciated sedimentary crater-fill deposits (underlain by either displaced sedimentary megablocks or crystalline basement rocks, and overlain by the fallout layer) are designated as the *Exmore breccia*. By this designation, the Exmore breccia embraces all but the very top of the *Exmore beds* (as applied in all other chapters of this volume) and includes crater unit B as well (see Gohn and others, this volume, chap. C).

Fallout Layer

Poag (2002) and Poag, Koeberl, and Reimold (2004) showed that at the USGS-NASA Langley corehole, the 52.37-m-thick (171.8-ft-thick) Chickahominy Formation is separated from the Exmore breccia by two thin deposits (3–19 centimeters

Text continues on page F13.

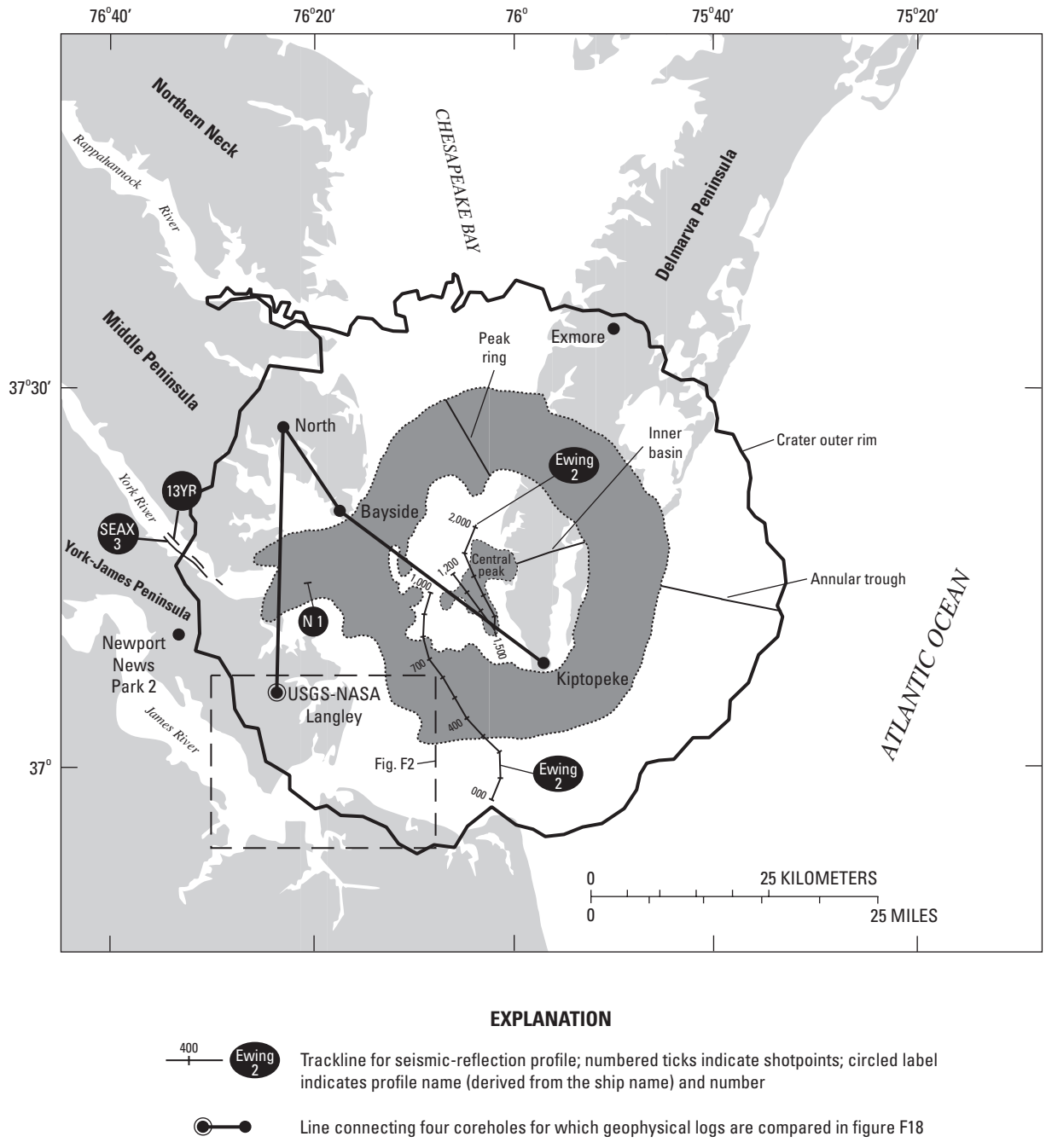

EXPLANATION

400 Ewing 2 — Trackline for seismic-reflection profile; numbered ticks indicate shotpoints; circled label indicates profile name (derived from the ship name) and number

Line connecting four coreholes for which geophysical logs are compared in figure F18

Figure F1. Regional map showing location of the USGS-NASA Langley corehole, four other intracrater coreholes, and one extracrater corehole relative to the principal morphological features of the Chesapeake Bay impact crater. Parts of the crater are defined differently in this chapter than in the other chapters in this volume. Tracklines for most seismic-reflection profiles are labeled as defined in figure F2; N1 indicates a short segment of trackline Neecho 1 (fig. F15); 13YR indicates a multichannel profile furnished by Texaco, Inc. (fig. F9). A detailed map of the USGS-NASA Langley site is shown in figure F2.

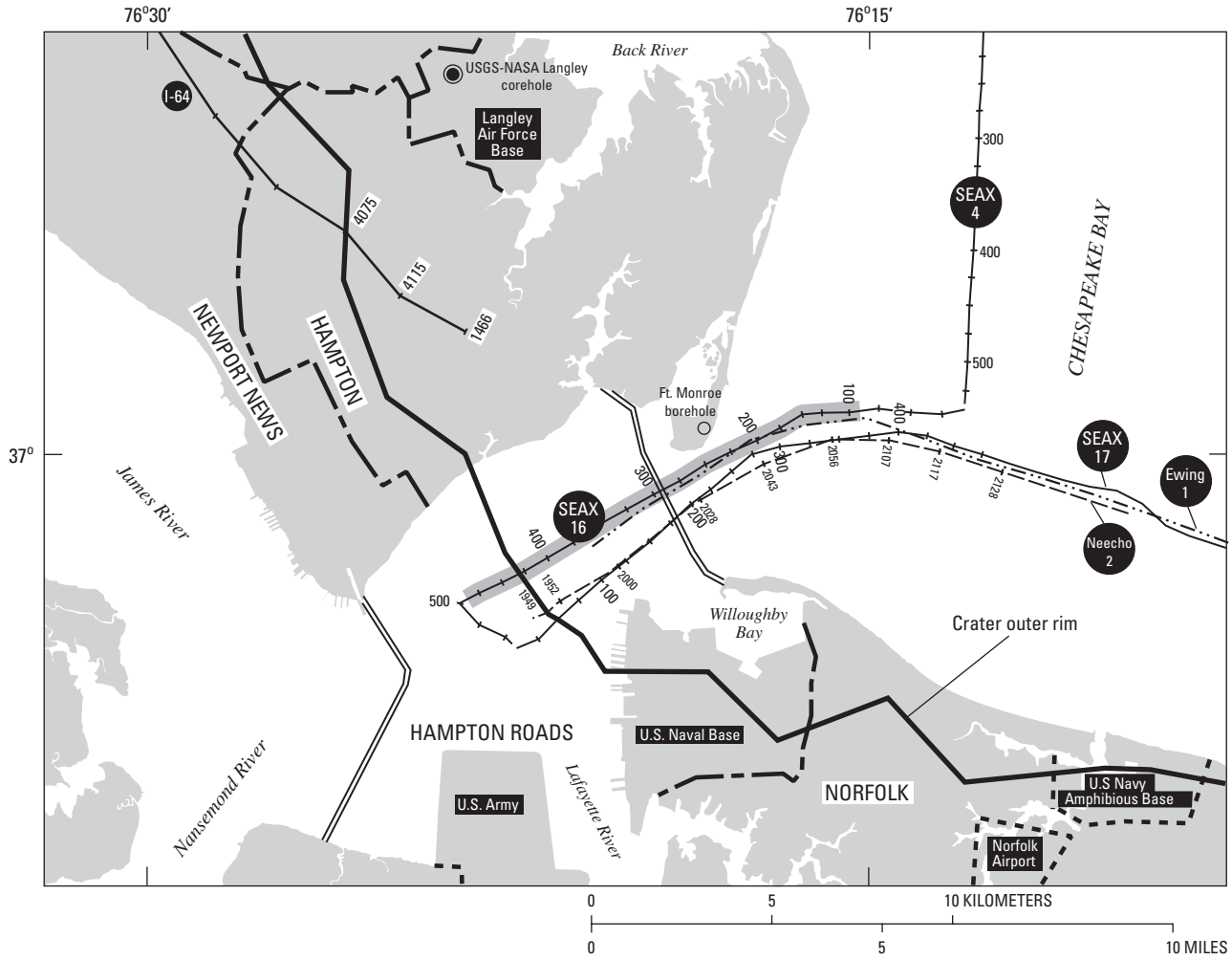

Figure F2. Detailed map showing location of the USGS-NASA Langley corehole, the Fort Monroe borehole, and nearby lines for seismic-reflection profiles. Different line styles are used to differentiate closely spaced tracklines. Offshore profile labels indicate the name of the ship used to collect the profile: Research Vessel (R.V.) *Seaward Explorer* (SEAX); *Neecho*; R.V. *Maurice Ewing*. The shaded segment of profile SEAX 16 is shown in figure F12. I–64 indicates a USGS onshore seismic profile parallel to U.S. Interstate Highway 64. Numbers on I–64, SEAX, and *Ewing* lines are seismic shotpoints; numbers on *Neecho* trackline designate time of day in hours (military time).

Table F1. Numbers and depths of samples collected for analysis of benthic foraminifera in early postimpact deposits in the USGS-NASA Langley core.

[Depths were measured in the field; the datum is ground level. m, meters; ft, feet]

Sample number	Top of sample (m)	Base of sample (m)	Top of sample (ft)	Base of sample (ft)
Drummonds Corner beds				
66	183.00	183.06	600.40	600.60
Chickahominy Formation				
65	183.28	183.34	601.30	601.50
64	183.54	183.60	602.15	602.35
63	183.70	183.76	602.70	602.90
62	184.62	184.68	605.70	605.90
61	185.53	185.59	608.70	608.90
60	186.45	186.60	611.70	611.90
59	187.36	187.42	614.70	614.90
58	188.28	188.34	617.70	617.90
57	189.19	189.25	620.70	620.90
56	190.10	190.16	623.70	623.90
55	191.05	191.13	626.80	627.00
54	191.96	192.02	629.80	630.00
53	192.85	192.91	632.70	632.90
52	193.76	193.82	635.70	635.90
51	194.58	194.64	638.40	638.60
50	195.38	195.44	641.00	641.20
49	196.35	196.41	644.20	644.40
48	197.27	197.33	647.20	647.40
47	198.18	198.24	650.20	650.40
46	199.25	199.31	653.70	653.90
45	200.01	200.07	656.20	656.40
44	201.84	201.90	662.20	662.40
43	202.75	202.81	665.20	665.40
42	203.67	203.73	668.20	668.40
41	204.58	204.64	671.20	671.40
40	205.50	205.56	674.20	674.40
39	206.29	206.35	676.80	677.00
38	207.26	207.32	680.00	680.20
37	208.24	208.30	683.20	683.40
36	209.12	209.18	686.10	686.30
35	210.04	210.10	689.10	689.30
34	210.98	211.04	692.20	692.40
33	211.90	211.96	695.20	695.40
32	212.84	212.90	698.30	698.50
31	213.70	213.76	701.10	701.30
30	214.82	214.88	704.80	705.00
29	215.80	215.86	708.00	708.20
28	216.56	216.62	710.50	710.70
27	219.46	219.52	720.00	720.20
26	220.37	220.43	723.00	723.20
25	221.41	221.47	726.40	726.60
24	222.20	220.26	729.00	729.20
23	223.18	223.24	732.20	732.40
22	224.06	224.12	735.10	735.30
21	224.93	224.99	737.96	738.16

Table F1. Numbers and depths of samples collected for analysis of benthic foraminifera in early postimpact deposits in the USGS-NASA Langley core.—Continued

Sample number	Top of sample (m)	Base of sample (m)	Top of sample (ft)	Base of sample (ft)
Chickahominy Formation—Continued				
20	225.86	225.92	741.00	741.20
19	226.74	226.80	743.90	744.10
18	227.69	227.75	747.00	747.20
17	228.60	228.66	750.00	750.20
16	229.51	229.57	753.00	753.20
15	230.46	230.52	756.10	756.30
14	231.44	231.50	759.30	759.50
13	232.26	232.32	762.00	762.20
12	233.16	233.22	764.95	765.15
11	234.12	234.18	768.10	768.30
10	234.91	234.94	770.70	770.80
9	235.49	235.52	772.60	772.70
8	235.58	235.63	772.90	773.05
Dead zone [The contact between the dead zone and the Chickahominy Formation is near the middle of sample 7 at 235.65 m (773.12 ft), and the contact between the dead zone and the fallout layer is within sample 4 at ~235.84 m (~773.75 ft) (fig. F7)]				
7	235.63	235.67	773.05	773.20
6	235.67	235.72	773.20	773.35
5	235.79	235.82	773.60	773.70
4	235.82	235.85	773.70	773.80
Fallout layer				
3	235.85	235.87	773.80	773.85
Exmore breccia				
2	235.87	235.88	773.85	773.90
1	235.88	235.92	773.90	774.00

Table F2. Stable-isotope data derived from carbonate tests of *Cibicidoides pippeni* extracted from samples of the Chickahominy Formation and the Drummonds Corner beds in the USGS-NASA Langley core.

[Depths are in meters (m) to the tops of samples; depths in feet are in table F1. Delta values for oxygen and organic carbon isotopes are in parts per mil (‰). No data were available for samples 61 and 23 (table F1) from depths of 185.53 m and 223.18 m]

Depth (m)	$\delta^{13}C$ (‰)	$\delta^{18}O$ (‰)	Depth (m)	$\delta^{13}C$ (‰)	$\delta^{18}O$ (‰)	Depth (m)	$\delta^{13}C$ (‰)	$\delta^{18}O$ (‰)	Depth (m)	$\delta^{13}C$ (‰)	$\delta^{18}O$ (‰)
183.00	–7.182	+0.325	195.38	–0.637	–0.124	210.04	–0.954	–0.003	225.86	+0.096	+0.036
183.28	–0.621	+0.184	196.35	–0.286	+0.110	210.98	–0.719	+0.235	226.74	–0.328	+0.275
183.54	–0.616	+0.264	197.27	–0.726	+0.064	211.90	–0.708	–0.001	227.69	+0.073	–0.013
183.70	–0.640	+0.241	198.18	–1.090	+0.111	212.84	–1.190	–0.035	228.60	–0.121	+0.012
184.62	–0.710	+0.344	199.25	–0.765	+0.035	213.70	–0.900	–0.077	229.51	–0.341	–0.029
186.45	–0.938	+0.170	200.01	–0.671	+0.224	214.82	–0.864	–0.078	230.46	–0.407	–0.204
187.36	–0.782	+0.131	201.84	–0.946	+0.334	215.80	–1.066	–0.272	231.44	–0.236	–0.014
188.28	–0.753	–0.044	202.75	–1.329	+0.019	216.56	–0.897	+0.227	232.26	+0.004	–0.029
189.19	–0.526	+0.073	203.67	–0.785	+0.118	219.46	–0.948	+0.201	233.16	–0.189	–0.173
190.10	–0.860	–0.116	204.58	–0.773	–0.276	220.37	–0.975	+0.406	234.12	–0.040	+0.073
191.05	–0.837	–0.047	205.50	–0.736	+0.286	221.41	–1.005	+0.123	234.91	–1.543	–0.246
191.96	–0.704	–0.002	206.29	–0.706	–0.052	222.20	–1.069	+0.087	235.49	–0.702	+0.124
192.85	–0.159	+0.172	207.26	–0.903	–0.149	224.06	–0.172	+0.039	235.58	–0.603	–0.173
193.76	–0.806	+0.013	208.24	–0.922	–0.148	224.93*	–0.106	+0.278			
194.58	–0.449	+0.174	209.12	–0.793	+0.114	224.93*	–0.070	+0.214			

*Two analyses were performed for sample 21 from 224.93 m.

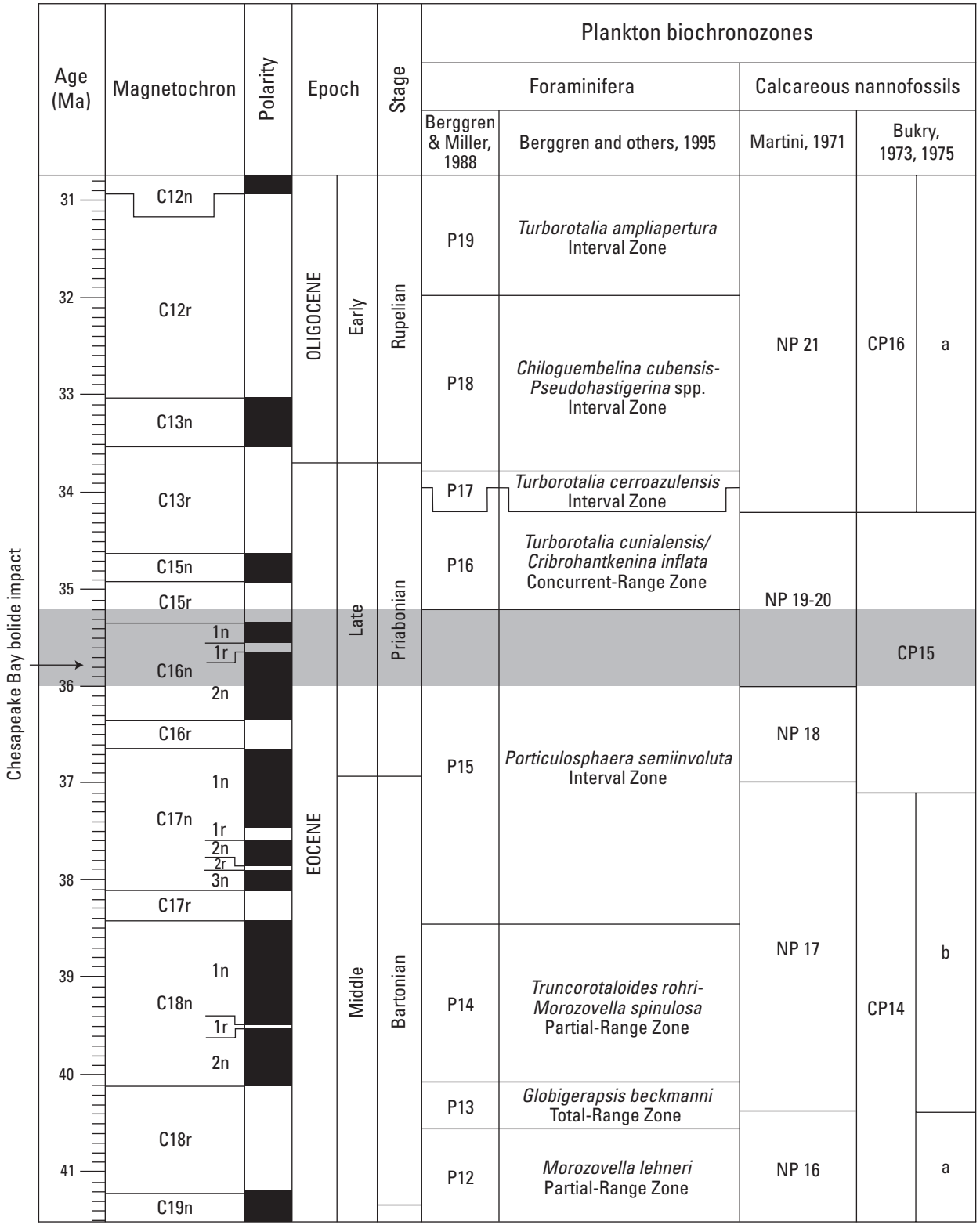

Figure F3. Correlation chart showing magnetobiochronology used in this chapter (modified from Berggren and others, 1995). The shaded band indicates the biochronologic resolution for the age of the Chesapeake Bay impact. The band is the interval of overlap between the top of the planktonic foraminiferal biochronozone P15 and the base of the calcareous nannofossil biochronozone NP 19-20 (35.2–36 Ma). The arrow marks the age of the Chesapeake Bay impact as extrapolated from sediment-accumulation-rate data from the Kiptopeke corehole (modified from Poag, Koeberl, and Reimold, 2004).

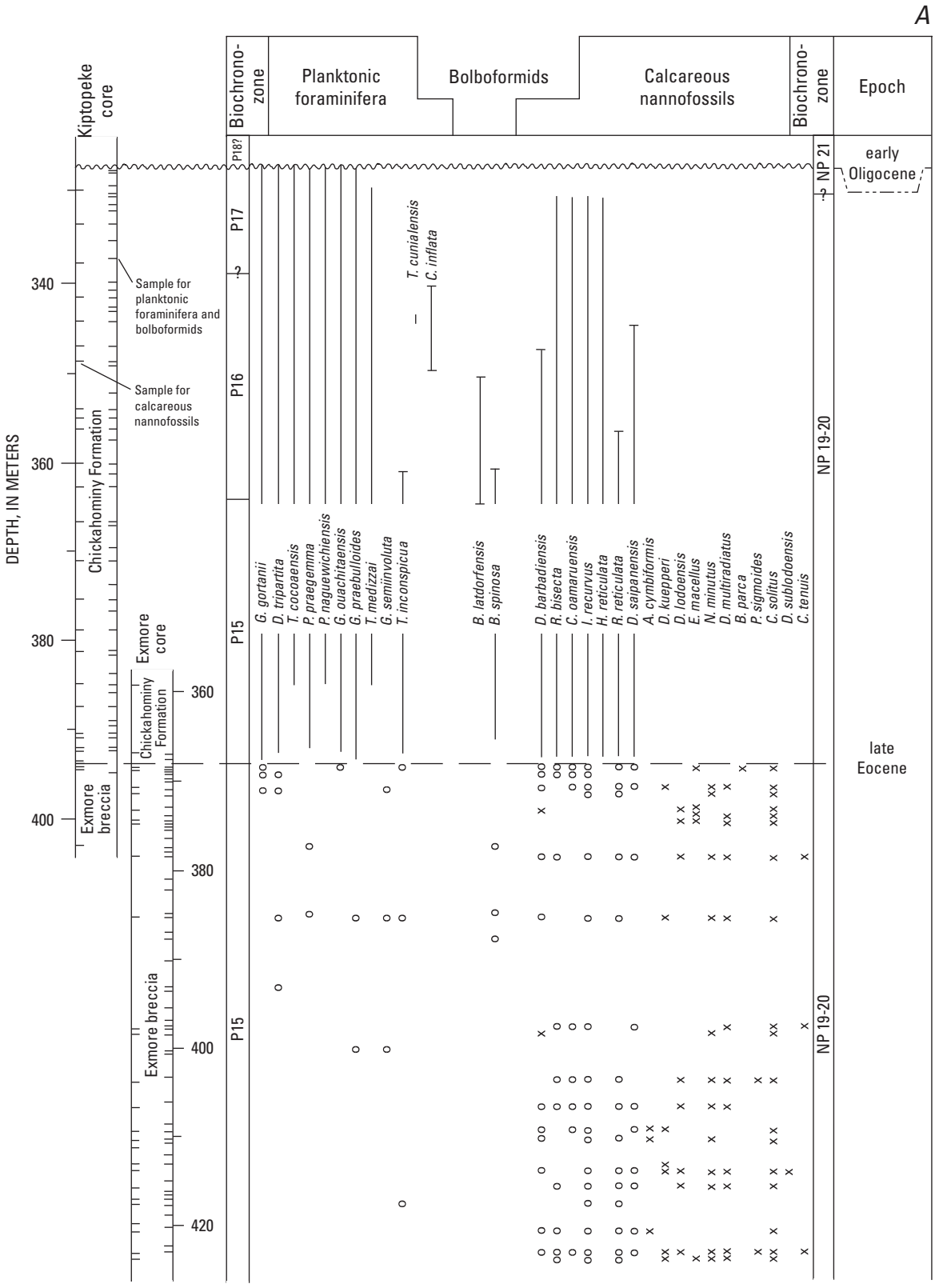

Figure F4. Chart summarizing ranges of principal planktonic foraminifera, bolboformids, and calcareous nannofossils identified in the Chickahominy Formation and the underlying Exmore breccia from the Kiptopeke and Exmore coreholes (from Poag and Aubry, 1995). *A,* Species ranges. *B,* Species names used in figure F4*A*. Ticks inside the core diagrams indicate sample depths for planktonic foraminifera and bolboformids (right) and calcareous nannofossils (left). Symbols for stratigraphically mixed specimens found within the Exmore breccia: o=indigenous late Eocene specimens; x=allogenic specimens (older than late Eocene).

B, Species names used in figure F4*A*

Planktonic Foraminifera

Cribrohantkenina inflata (Howe) 1928
Dentoglobigerina tripartita (Koch) 1926
Globigerina gortanii (Borsetti) 1959
Globigerina ouachitaensis Howe and Wallace, 1932
Globigerina praebulloides Blow, 1959
Globigerinatheka semiinvoluta (Keijzer) 1945
Praetenuitella praegemma Li, 1987
Pseudohastigerina naguewichiensis (Myatyliuk) 1950
Testacarinata inconspicua (Howe) 1939
Testacarinata medizzai (Toumarkine and Bolli) 1975
Turborotalia cocoaensis (Cushman) 1928
Turborotalia cunialensis (Toumarkine and Bolli) 1970

Bolboformids

Bolboforma latdorfensis Spiegler, 1991
Bolboforma spinosa Daniels and Spiegler, 1974

Calcareous Nannofossils

Arkhangelskiella cymbiformis Vekshina, 1959
Broinsonia parca (Stradner, 1963)
Chiasmolithus oamaruensis (Deflandre, 1954)
Chiasmolithus solitus (Bramlette and Sullivan, 1961)
Cruciplacolithus tenuis (Stradner, 1961)
Discoaster barbadiensis (Tan, 1927)
Discoaster kuepperi Stradner, 1959
Discoaster lodoensis Bramlette and Sullivan, 1961
Discoaster multiradiatus Bramlette and Riedel, 1954
Discoaster saipanensis Bramlette and Riedel, 1954
Discoaster sublodoensis Bramlette and Sullivan, 1961
Ellipsolithus macellus (Bramlette and Sullivan, 1961)
Helicosphaera reticulata Bramlette and Wilcoxon, 1967
Isthmolithus recurvus Deflandre, 1954
Neococcolithes minutus (Perch-Nielsen, 1967)
Placozygus sigmoides (Bramlette and Sullivan, 1961)
Reticulofenestra bisecta (Hay, Mohler, and Wade, 1966)
Reticulofenestra reticulata (Gartner and Smith, 1967)

Figure F4. Continued.

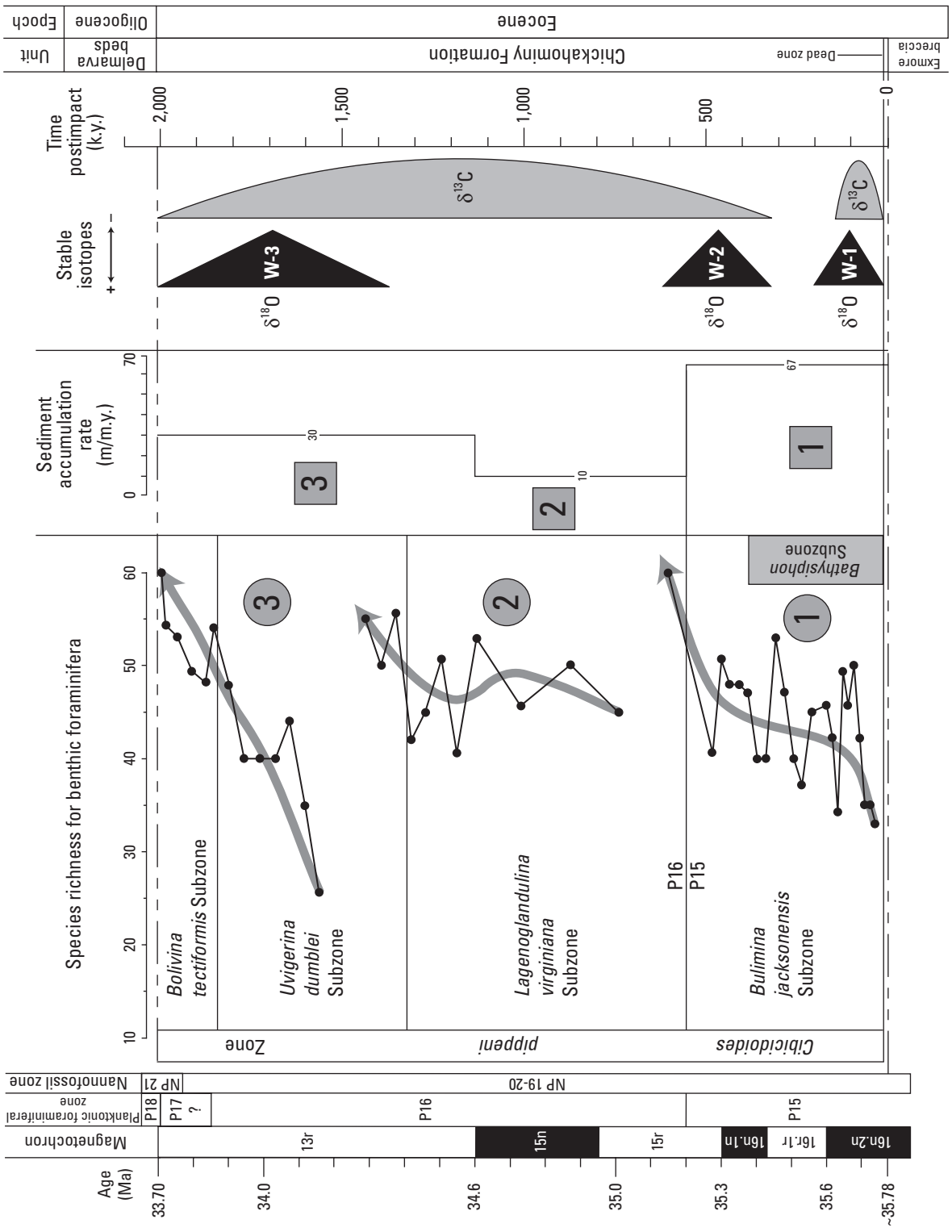

Figure F5. Chart summarizing correlations among magnetostratigraphy, planktonic foraminiferal and calcareous nannofossil zones, benthic foraminiferal subzones, species-richness cycles, sediment accumulation rates, and stable-isotope records ($\delta^{18}O$, $\delta^{13}C$) in the Chickahominy Formation in the Kiptopeke corehole (modified from Poag, Koeberl, and Reimold, 2004, fig. 13.10). W–1, W–2, W–3=pulses of warm global climate based on $\delta^{18}O$; species richness=number of benthic foraminiferal species identified in a sample. Scale at right indicates time in thousands of years (k.y.) postimpact. The three species-richness cycles (numbers in circles) differ slightly from the three depositional episodes (numbers in squares) determined from sediment accumulation rates (Poag, Koeberl, and Reimold, 2004, table 13.1).

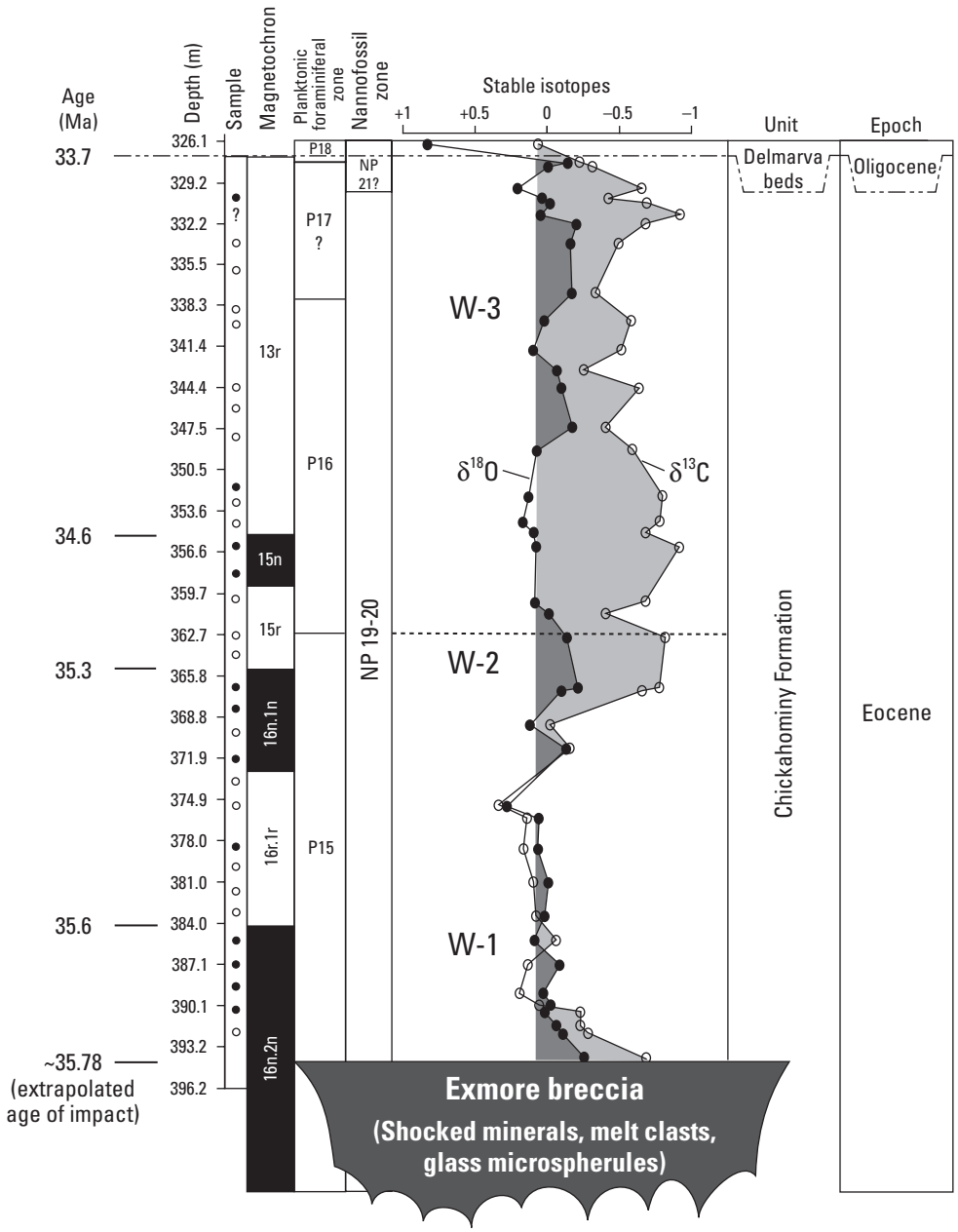

Figure F6. Chart summarizing correlations among magnetostratigraphy, biozones, and stable-isotope records ($\delta^{18}O$, $\delta^{13}C$) for the Chickahominy Formation in the Kiptopeke corehole (modified from Poag, Mankinen, and Norris, 2003). Age of impact was extrapolated by using the sediment accumulation rate of 67 m/m.y. shown in figure F5. In the sample column, open circles indicate reversed polarity; filled circles indicate normal polarity. W–1, W–2, W–3=pulses of warm global climate based on $\delta^{18}O$.

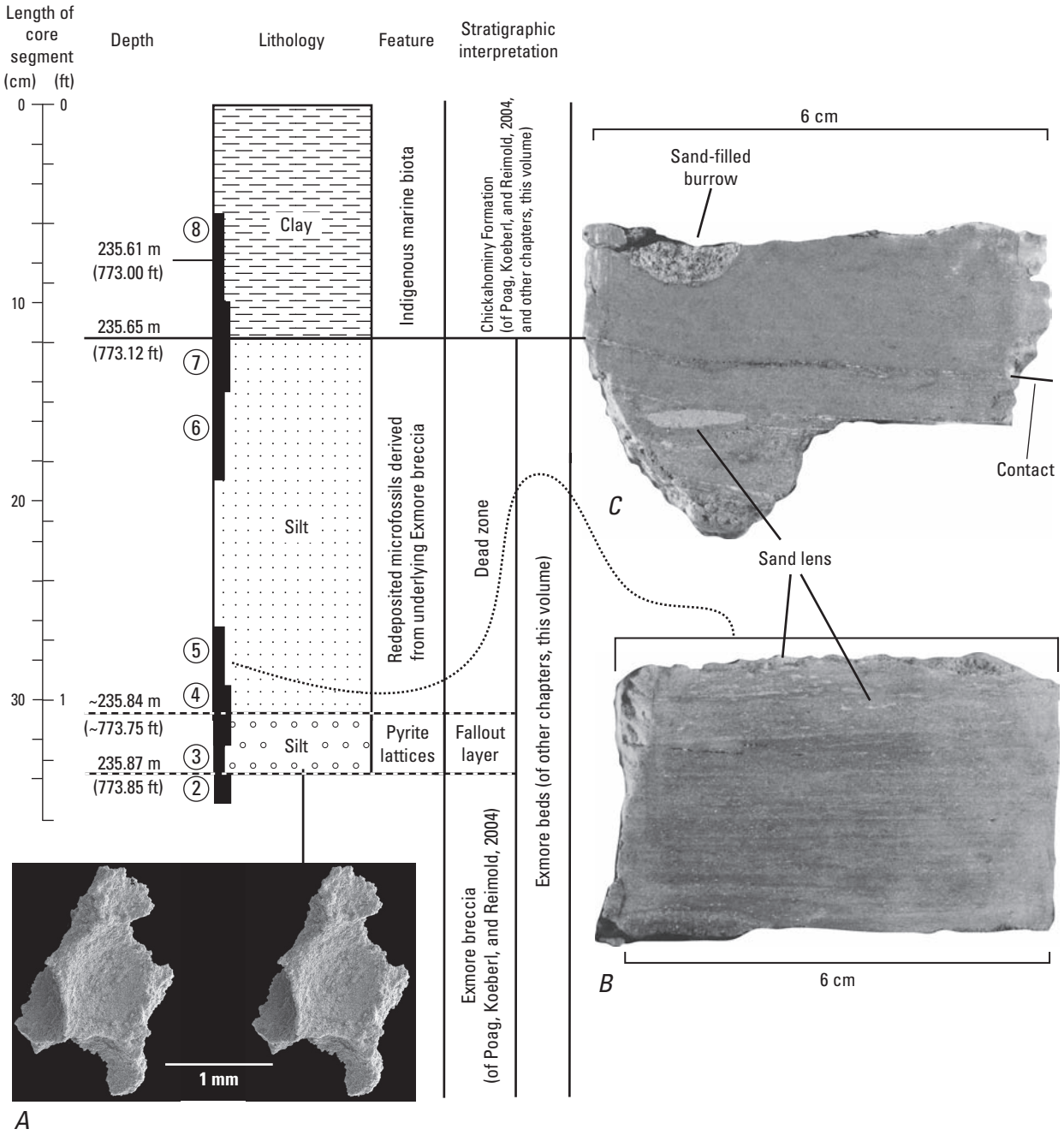

Figure F7. Core log showing stratigraphic interpretation of sediments across the transition from the Exmore breccia to the Chickahominy Formation in the USGS-NASA Langley corehole and images of sampled sediment (modified from figs. 3 and 4 of Poag, 2002). Each solid rectangle at left of the lithology column indicates the position of a sample taken for this study (circled numbers are sample numbers listed in table F1). *A,* Stereopair of scanning-electron micrographs illustrating fragment of pyrite lattice (modified from Poag, 2002, fig. 4). Note hemispherical concavities separated by knife-edge partitions; Poag (2002) inferred that the concavities originally contained glass microspherules, which constituted the fallout layer from the Chesapeake Bay impact. *B,* Split-core sample (sample 5) from near the base of the dead zone (see leader), showing a repetitious succession of submillimeter-scale horizontal laminae of sand, silt, and clay. Photograph from Poag (2002, fig. 3). *C,* Split-core sample (sample 7) containing boundary between clay of the Chickahominy Formation (above) and the dead zone (below). Photograph from Poag (2002, fig. 3). Note coarse sand in the Chickahominy burrow and fine sandy laminae and lenses in the dead zone. Note also that our stratigraphic interpretations of this core interval follow those of Poag, Koeberl, and Reimold (2004). Thus, we recognize the fallout layer and dead zone as a composite transitional interval that separates the Exmore breccia (Exmore beds, in part, of other chapters in this volume) from the Chickahominy Formation.

(cm) or 1.2–7.5 inches (in.) thick) that record the synimpact-postimpact transition. This critical depositional shift began with accumulation of a thin (~3 cm; 1.2 in.) layer of silty clay, containing dozens of well-preserved fragments of pyrite microstructures (fig. F7*A*). The microstructures exhibit smooth-walled, closely spaced, hemispherical pits or depressions, approximately 0.5–1.0 millimeter (mm; 0.02–0.04 in.) in diameter, which are separated from each other by curved, knife-edge partitions. Poag and the Chesapeake Coring Team (2001), Poag, Gohn, and Powers (2001), Poag (2002), and Poag, Koeberl, and Reimold (2004) concluded that the pyrite microstructures originally were parts of a larger pyrite lattice, which had encased a layer of stacked glass microspherules (microtektites) derived from shock-melted silica droplets. Those authors inferred that the glass microspherules had been part of a fallout layer, which originally accumulated in quiet-water conditions following abatement of massive impact-generated turbulence over the crater.

Poag (2002) and Poag, Koeberl, and Reimold (2004) placed the base of the fallout layer at 235.87 m (773.85 ft; fig. F7) in the Langley core. Poag (2002) interpreted the fallout layer to be part of the Exmore breccia (other authors in the present volume assign it to the Exmore beds), whereas Poag, Koeberl, and Reimold (2004) considered the fallout layer to be part of a silt-rich unit that separates the sand-rich Exmore breccia from the clay-rich Chickahominy Formation.

Dead Zone

Above the fallout layer, Poag (2002) and Poag, Koeberl, and Reimold (2004) described a dark-gray, laminated, clayey silt unit, ~0.19 m (~0.63 ft) thick in the Langley core, which they designated as a dead zone (fig. F7). The silt appears to be devoid of indigenous microfossils, though specimens reworked from the Exmore breccia are abundant in thin white laminae and millimeter-scale lenses of micaceous, fine to very fine sand (fig. F7*B,C*). Pyritized burrow casts also are particularly common in the dead zone. Poag (2002) and Poag, Koeberl, and Reimold (2004) interpreted the dead zone to be the initial postimpact marine sedimentary unit, and they inferred quiet-water deposition from the undisturbed geometry of the repetitive, submillimeter-scale**,** horizontal laminae of sand, silt, and clay. Poag (2002) and Poag, Koeberl, and Reimold (2004) placed the conformable lower contact of the dead zone at 235.84 m (773.75 ft) in the Langley core. The upper boundary of the dead zone is a sharp contact with the base of the Chickahominy Formation at 235.65 m (773.12 ft; fig. F7*C*).

Chickahominy Formation

Lithic Characteristics

Poag, Koeberl, and Reimold (2004) described fresh cores of the Chickahominy Formation from several coreholes in the Chesapeake Bay impact crater as typically composed of gray-green clay that weathers to yellowish olive brown and contains variable amounts of finely comminuted glauconite and muscovite (see also Powars and others, this volume, chap. G). The clay is silty to sandy, is richly fossiliferous, and commonly displays fine to coarse (frequently faint) lamination. The biota are mainly marine microfossils (benthic and planktonic foraminifera, calcareous nannofossils, bolboformids, ostracodes, dinoflagellates, radiolarians), but they also include common to abundant remains or evidence of invertebrates (echinoid spines, solitary corals, thin bivalves, scaphopods, pyritized burrow casts) and vertebrates (fish skeletal debris and teeth; see also Edwards and others, this volume, chap. H).

Sediments subjacent to the upper boundary of the Chickahominy Formation are usually intensely burrowed; those near the lower boundary are moderately burrowed. Larger burrows are filled with coarser material (sand) than the Chickahominy itself (clay) and can be identified as far as 2 m (6.6 ft) into the Chickahominy. Burrows at the top of the Chickahominy are filled with glauconitic quartz sand and microfossils reworked downward from the overlying Oligocene Drummonds Corner beds (Langley core) or Delmarva beds (Kiptopeke core). At the base of the Chickahominy Formation, the smallest, most abundant burrows are filled with framboidal pyrite. The largest burrows in this basal interval are filled with quartz sand and mixed microfossil assemblages reworked upward from the Exmore breccia. The presence of the sand-filled burrows causes the upper and lower sediments in the Chickahominy section to fracture and crumble upon drying, in contrast to most of the remainder of the unit, which maintains its dense, massive character.

Seismic Signature

Integrating the lithic core records and downhole geophysical records allows precise correlation between the lithic boundaries of the Chickahominy Formation and their reflection signatures on seismic-reflection profiles (Poag, 1997a; Poag and others, 1999; Poag, Koeberl, and Reimold, 2004). Normally, a significant impedance contrast exists between the relatively consolidated (dense) clay of the Chickahominy Formation and the unconsolidated sands of the overlying unit, which in different areas is the lower Oligocene Drummonds Corner beds or the lower Oligocene Delmarva beds (Powars and others, 1992; Powars and Bruce, 1999; Powars and others, this volume, chap. G). This impedance contrast produces an easily recognized high-amplitude reflection at the upper boundary of the Chickahominy Formation (fig. F8), which can be traced over the entire crater and extends a short distance outside the crater rim.

The lower boundary of the Chickahominy also is characterized by a strong impedance contrast and a resultant high-amplitude reflection where clay of the Chickahominy Formation contacts the underlying unconsolidated silts and sands of the Exmore breccia (figs. F8, F9). Even on profiles where the boundary reflections are weak (fig. F9), the large number of intersections between profiles (Poag and others, 1999; Poag, Koeberl, and Reimold, 2004) assures recognition of both the

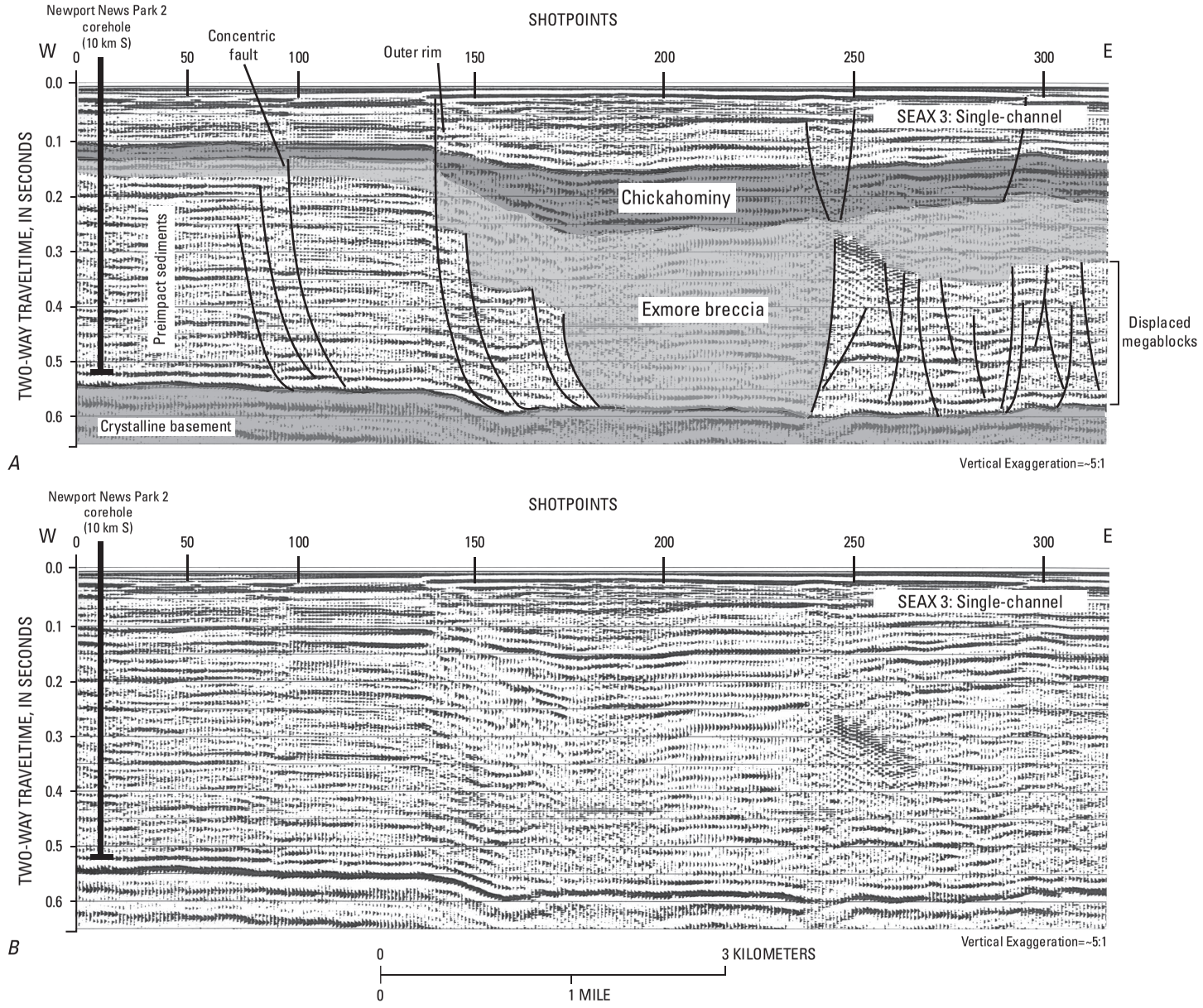

Figure F8. Segment of single-channel seismic-reflection profile SEAX 3 collected by the U.S. Geological Survey (USGS) in collaboration with the National Geographic Society (NGS) in 1996. This profile is one of two parallel seismic-reflection profiles collected in the York River, northwest of the USGS-NASA Langley corehole; it shows that the Chickahominy Formation sags and thickens as it crosses the outer rim of the Chesapeake Bay impact crater. See figure F1 for location of profile. *A,* Interpreted segment of single-channel profile SEAX 3 (from Poag, Koeberl, and Reimold, 2004, fig. 4.9A). *B,* Uninterpreted version of *A.*

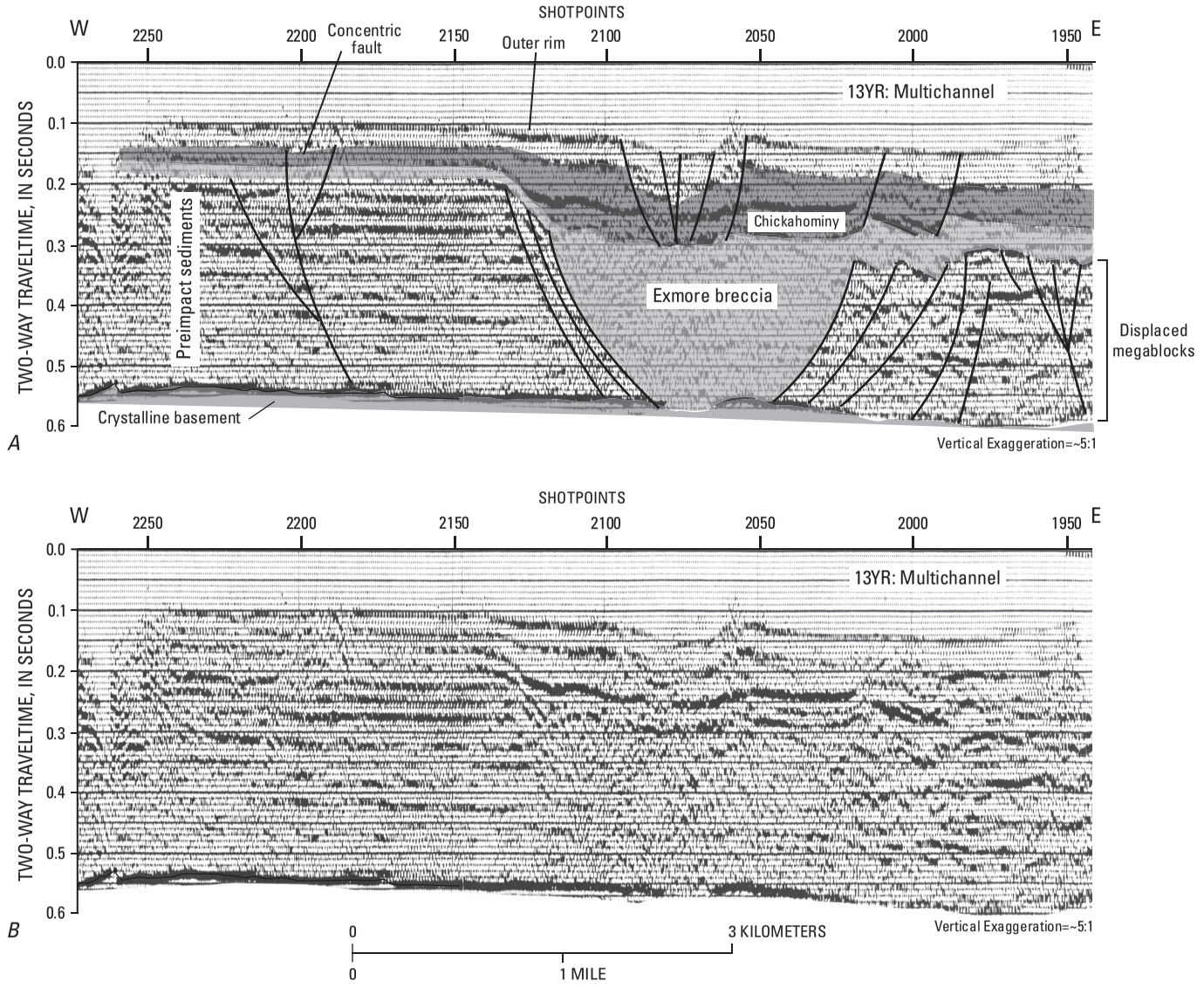

Figure F9. Segment of multichannel seismic-reflection profile 13YR collected by Teledyne Exploration Co. for Texaco, Inc., and Exxon Exploration Co. in 1986 in the York River. It shows that the Chickahominy Formation sags and thickens as it crosses the outer rim of the Chesapeake Bay impact crater. See figure F1 for location of profile. *A,* Interpreted segment of multichannel profile13YR (from Poag, Koeberl, and Reimold, 2004, fig. 4.9B). *B,* Uninterpreted version of *A.*

upper and lower boundaries of the Chickahominy Formation. In the thickest sections of the Chickahominy, internal seismic reflections indicate the probability of meter-scale bedding. In short, the seismostratigraphic signature of the Chickahominy is easy to recognize and to trace over the crater, and, therefore, its present structure (fig. F10), thickness (fig. F11), and distribution can be accurately mapped.

Geometry and Distribution

The structure, morphology, and distribution of the Chickahominy Formation have been influenced strongly by the original irregular geometry of the upper surface of the Exmore breccia and by a long-term subsidence differential between the unconsolidated, water-saturated impact breccia inside the crater and the semiconsolidated, preimpact sedimentary column outside the crater (Poag, Koeberl, and Reimold, 2004). Differential subsidence is partly responsible (along with original bathymetric differences between the crater basin and its peripheral lithotopes) for a much thicker section of Chickahominy inside the crater than outside the crater (figs. F1, F11). In addition, continued differential subsidence during the roughly 34 million years (m.y.) of post-Eocene time, in concert with differential compaction of the underlying breccia, has caused the Chickahominy Formation to sag irregularly over the crater rim (table F3). Thus, the Chickahominy thickens and sags as it crosses into the annular trough and inner basin, just as the underlying Exmore breccia does (figs. F8, F9, F12, F13, F14). Likewise, the Chickahominy mimics the geometry of the underlying Exmore breccia by arching up and thinning over the peak ring and central peak (figs. F13, F14).

Inside the crater, the Chickahominy Formation is ~20 m to >220 m (66 to >720 ft) thick and averages ~100–120 m (330–390 ft) (fig. F11). The thickness varies greatly because the unit fills various pits and troughs in the upper surface of the breccia, which were accentuated by postimpact differential compaction. In general, the formation is thickest where the underlying Exmore breccia is thickest (where the basement surface is deepest) and thins where the Exmore breccia is thinnest (where the basement shallows).

The Chickahominy Formation thickens from 20 m to >90 m (66 to >290 ft) where it crosses the western part of the outer rim, from 20 m to >150 m (66 to >490 ft) across the northern part of the outer rim, and from 20 m to >160 m (66 to >520 ft) across the eastern and southern parts (fig. F11; table F3). The thickest part of the formation (>220 m; >720 ft) occupies the western sector of the inner basin. We have no seismic data for the eastern sector of the inner basin, but a gravity model (Poag, Koeberl, and Reimold, 2004) indicates a similar thickness of Chickahominy there.

The Chickahominy thins over broad areas of the western, northern, and southern sectors of the annular trough; the two locations having the thinnest sections are the area over the southwestern crest of the peak ring and the area over the central peak (figs. F11, F13, F14). The Chickahominy thins rapidly to <10 m (<33 ft) within a few kilometers outside the crater rim, and it is too thin to trace beyond that point on the seismic profiles (fig. F11). The formation is less than 10 m (33 ft) thick in most of the noncored boreholes that have penetrated it outside the crater (Brown and others, 1972; Powars and Bruce, 1999).

Faults and Fault Systems

In addition to producing thickening, thinning, and sagging of the Chickahominy Formation, differential compaction of the Exmore breccia also has created a series of normal-offset faults and fault systems within the postimpact sedimentary section, which break the Chickahominy Formation into discrete fault blocks (figs. F8, F9, F12, F13, F14, F15; Poag, Koeberl, and Reimold, 2004). The throw on most faults decreases upsection, indicating that they are growth faults along which long-term continuous or intermittent movement has occurred (fig. F15). The USGS-NASA Langley corehole crossed a minor branch of one of the postimpact compaction faults, which slices through the Chickahominy Formation at 229.9 m (754.4 ft) depth (fig. F16).

The two most prominent systems of compaction faults are expressed on the seismic profiles as complex intervals of disrupted and offset reflections that derive from distinct grabens located along the outer margins of the annular trough and inner basin (figs. F8, F9, F12, F13). Because these graben structures are present on almost every seismic profile that crosses the outer rim and (or) the outer wall of the inner basin, we infer that they represent parts of two nearly continuous concentric graben systems (ring grabens) that encircle the crater just inside the outer rim and the peak ring (fig. F17).

In addition to the two ring grabens documented on the seismic profiles, more than 700 individual faults and fault clusters (small grabens, horsts, or normal faults) are scattered in mainly concentric orientations throughout the Chickahominy Formation (Poag, Koeberl, and Reimold, 2004; see fig. F17 of this chapter).

Biostratigraphy

Poag and Aubry (1995) established the general biostratigraphic framework for the Chickahominy Formation on the basis of planktonic foraminifera, calcareous nannofossils, and bolboformids from the Kiptopeke core (fig. F4). They concluded that the lower part of the Chickahominy embraces planktonic foraminiferal biochronozone P15 and the upper part represents biochronozone P16-P17. An erosional surface at the top of the Chickahominy Formation is presumed to result from removal of the base of Zone P18, an interval that would represent roughly 0.1 m.y. The P15 zonal marker *Globigerinatheka semiinvoluta* has not been found in the Chickahominy Formation, but specimens of this species are present in the Exmore breccia of the Kiptopeke core. Their presence in the breccia

Text continues on page F26.

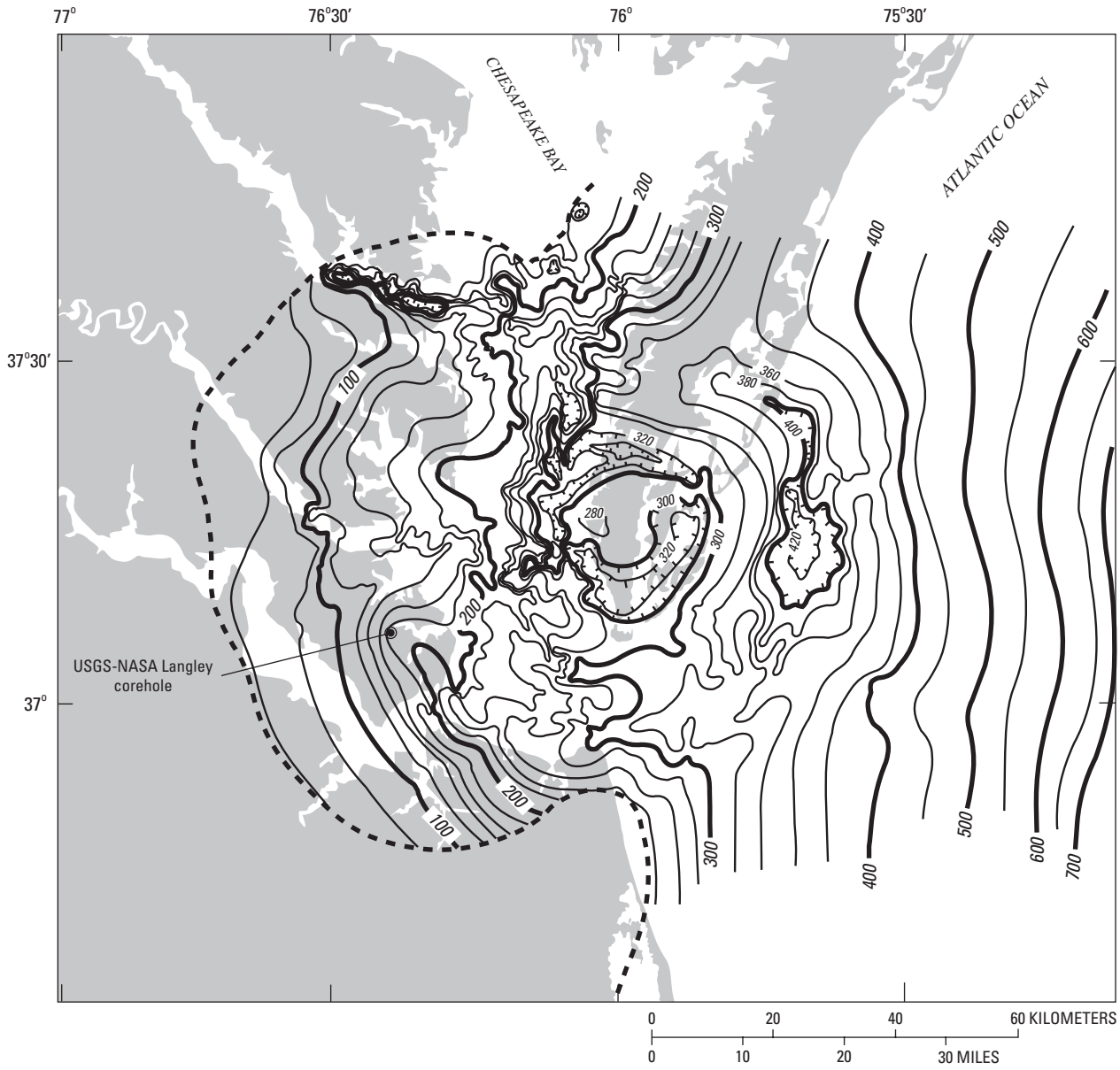

Figure F10. Structure map representing depth to the top of the Chickahominy Formation in the area of the Chesapeake Bay impact crater (fig. F1). Contour intervals are 20 and 50 m (66 and 164 ft); hachured contours indicate depressions. Dashed line is the approximate landward (updip) limit of the Chickahominy Formation. The map is from Poag, Koeberl, and Reimold (2004, fig. 7.8).

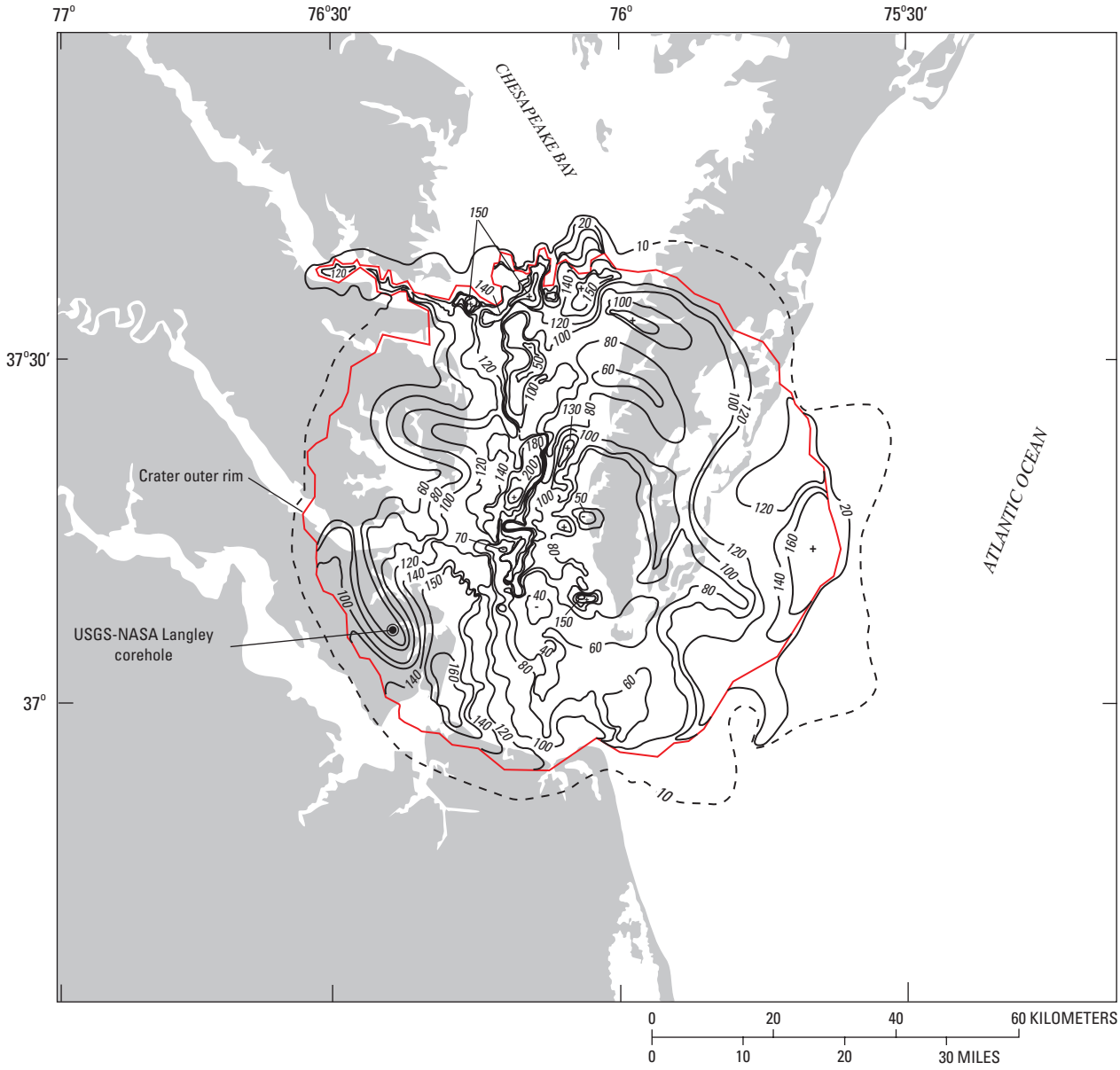

Figure F11. Isopach map of the Chickahominy Formation in the area of the Chesapeake Bay impact crater (fig. F1). Contour intervals are 10 and 20 m (33 and 66 ft); the 10-m contour (dashed where inferred) shows that the Chickahominy extends outside the crater. In places, the outer rim of the crater (red) coincides with various contours. The map is from Poag, Koeberl, and Reimold (2004, fig. 7.9).

Table F3. Elevation, sag, and thickness data for the Chickahominy Formation where it crosses the outer rim of the Chesapeake Bay impact crater.

[Data derived from 25 seismic-reflection profiles and Poag, Koeberl, and Reimold (2004); a few selected profiles are shown in this report (figs. F8, F9, F12). Elevation is depth in meters (m) below sea level (bsl) to the top of the Chickahominy Formation]

Profile name and number	Elevation outside rim (m bsl)	Elevation inside rim (m bsl)	Amount of sag (m)	Thickness outside rim (m)	Thickness inside rim (m)	Thickness increase	
						(m)	(%)
SEAX 2	100	175	75	25	110	85	340
SEAX 3 (fig. F8)	85	120	35	10	90	80	800
Texaco 13YR (fig. F9)	75	120	45	10	90	80	800
SEAX 16 (fig. F12)	110	190	80	15	80	65	433
SEAX 17	125	170	45	10	100	90	900
Neecho 3	110	170	60	10	70	60	600
Texaco 11–PR	120	220	100	40	100	60	150
Texaco 9–CB–F	120	210	90	40	100	60	150
SEAX 12	140	180	40	20	140	120	600
SEAX 13	150	200	50	15	110	95	633
Texaco 10–RR	180	230	50	10	140	130	1,300
Texaco 1–CB	175	200	25	10	90	80	800
SEAX 4	150	180	30	20	100	80	400
SEAX 10	175	220	45	10	130	120	1,200
SEAX 11	160	180	20	10	120	110	1,100
SEAX 5	220	240	20	10	120	110	1,100
SEAX 6	220	270	50	15	70	55	367
SEAX 8	255	310	55	15	60	45	300
SEAX 9	280	320	40	15	100	85	567
SEAX 19	365	390	25	10	120	110	1,100
SEAX 22	370	390	20	10	100	90	900
SEAX 25	350	380	30	30	150	120	400
SEAX 27	315	320	5	20	130	110	550
SEAX 1	365	405	40	20	150	130	650
Ewing 3	310	340	30	25	130	105	420
Average	201	245	44	17	108	91	662

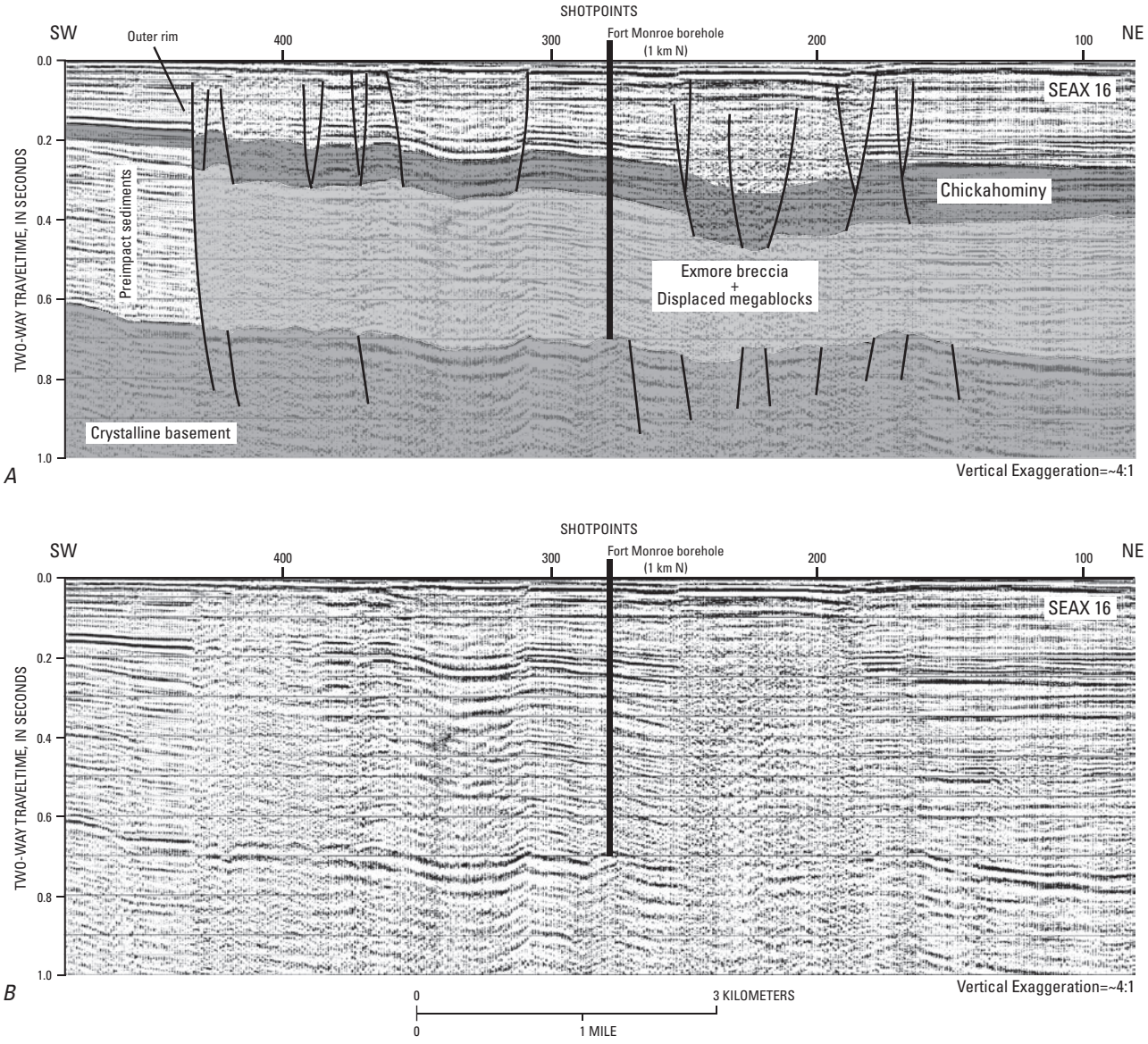

Figure F12. Segment of single-channel seismic-reflection profile SEAX 16 collected by the USGS and the NGS in 1996 in the mouth of the James River. See figure F2 for location of profile. *A,* Interpreted segment of single-channel profile SEAX 16 (from Poag, Koeberl, and Reimold, 2004, fig. 4.11). *B,* Uninterpreted version of *A.*

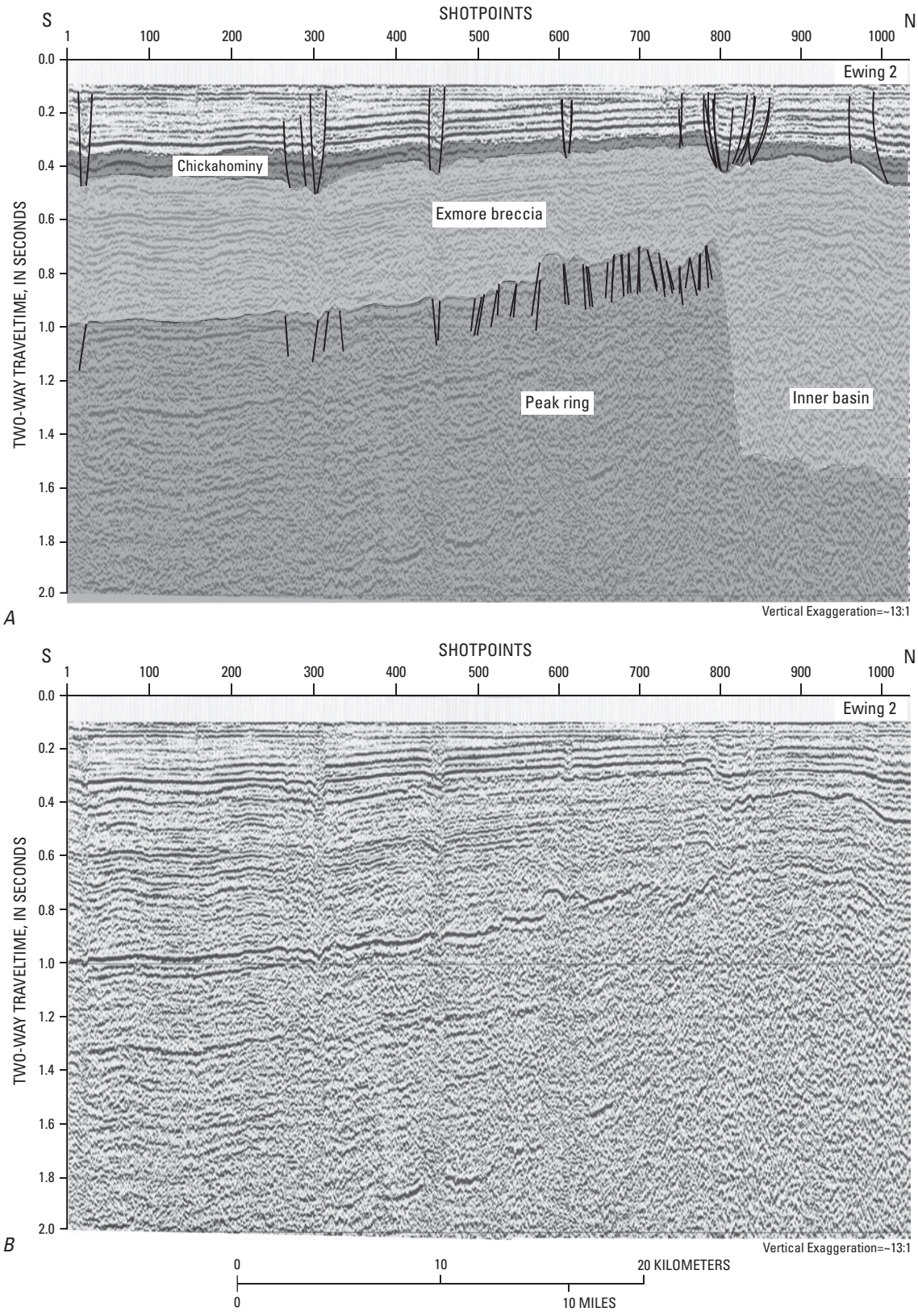

Figure F13. First segment of two-channel seismic-reflection profile Ewing 2 collected in 1998 by the USGS in collaboration with the Lamont-Doherty Earth Observatory (LDEO). The profile segment crosses the peak ring of the Chesapeake Bay impact crater. Note that the Chickahominy Formation thins and rises structurally over basement highs. See figure F1 for location of profile. *A,* Interpreted segment of two-channel profile Ewing 2 (from Poag, Koeberl, and Reimold, 2004, fig. 4.26A). *B,* Uninterpreted version of *A.*

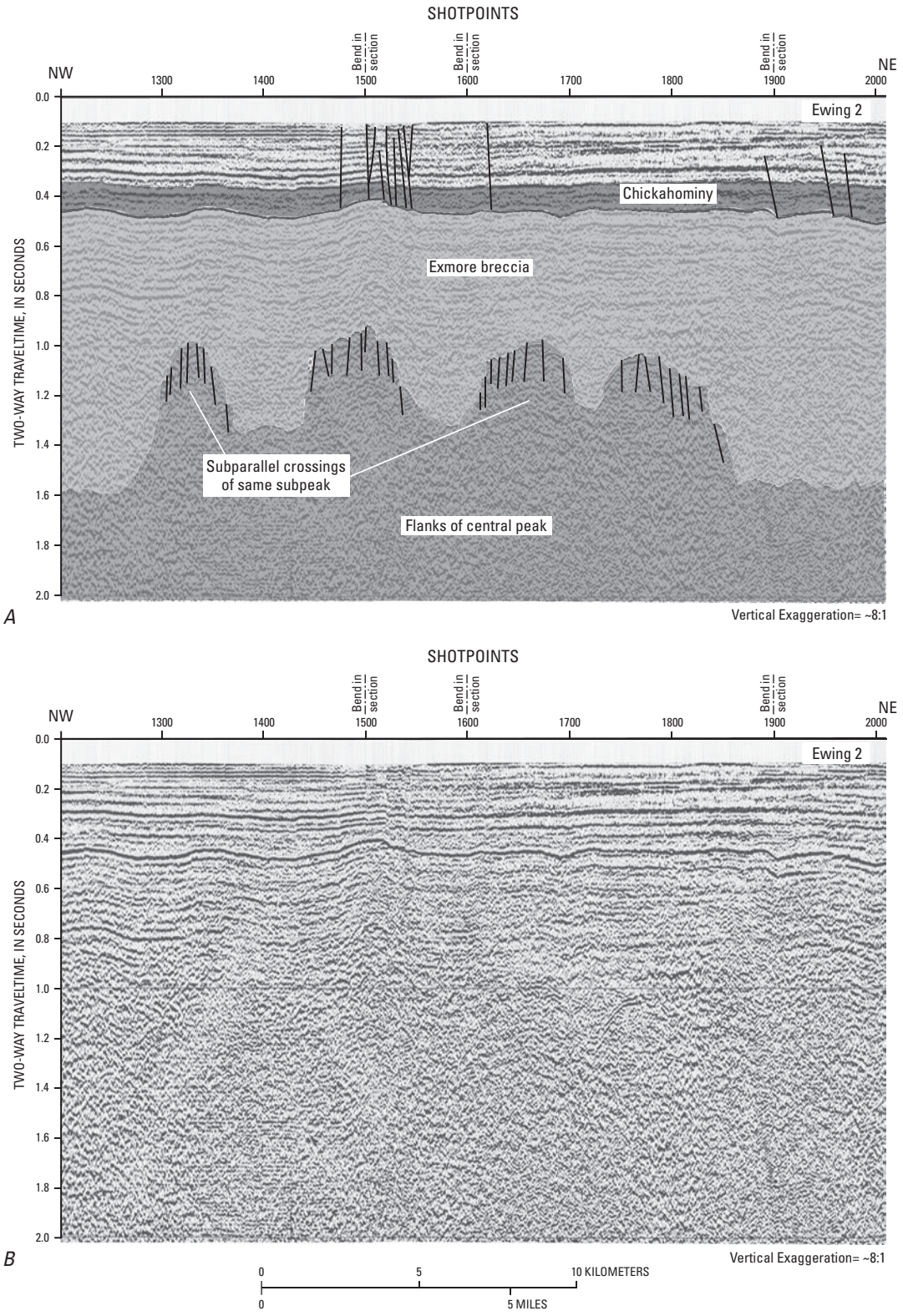

Figure F14. Second segment of two-channel seismic-reflection profile Ewing 2 collected in 1998 by the USGS in collaboration with the Lamont-Doherty Earth Observatory (LDEO). The profile segment crosses the flanks of the central peak of the Chesapeake Bay impact crater. Note that the Chickahominy Formation thins and rises structurally over basement highs. See figure F1 for location of profile. *A,* Interpreted segment of two-channel profile Ewing 2 (from Poag, Koeberl, and Reimold, 2004, fig. 4.32). *B,* Uninterpreted version of *A.*

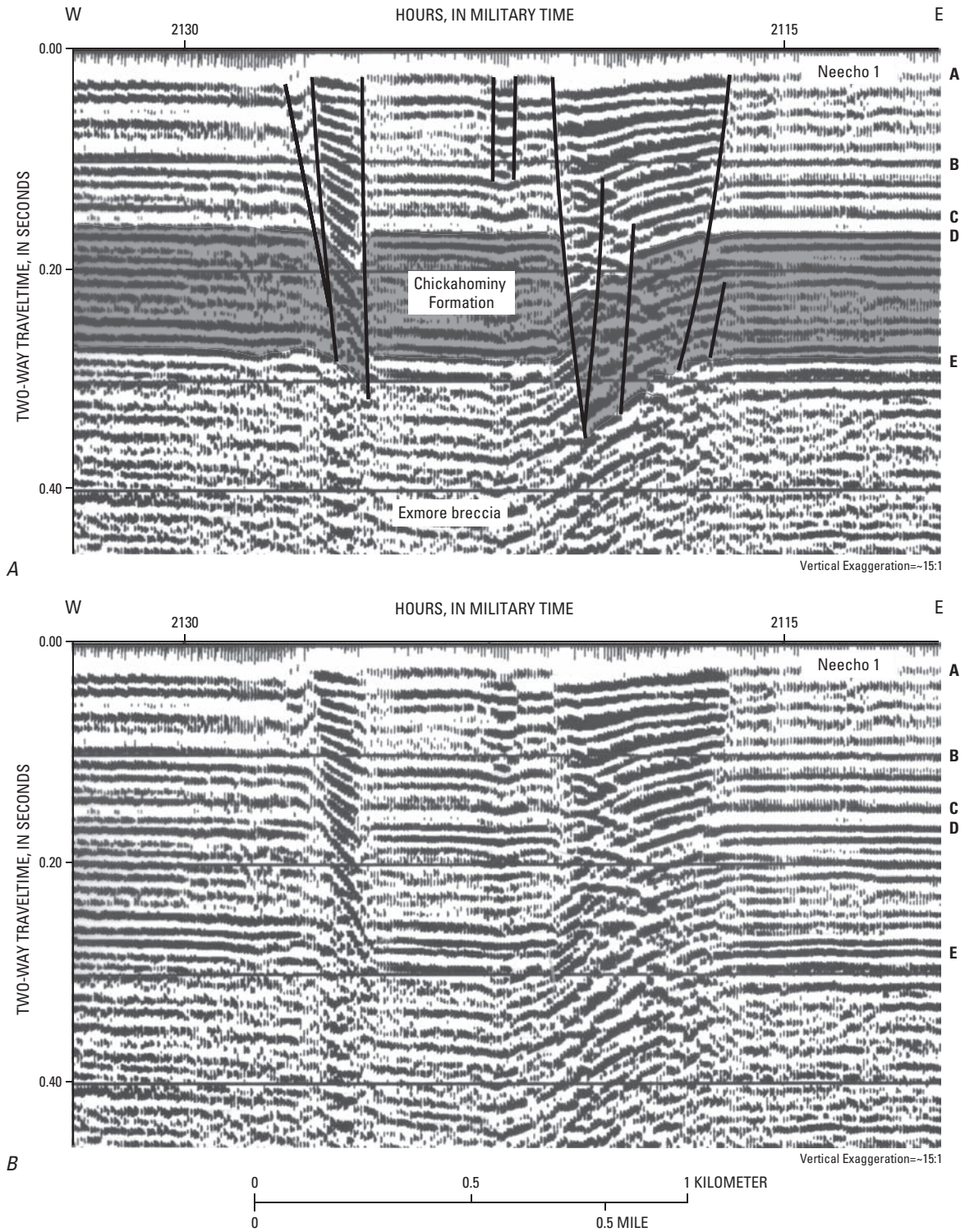

Figure F15. Segment of multichannel seismic-reflection profile Neecho 1 collected near the mouth of the York River by the USGS in 1982. The profile shows stratal offsets due to postimpact faults extending from the Chickahominy Formation. Letters A–E indicate seismic reflections traced across the profile to demonstrate upward decrease in fault throw. See figure F1 for location of profile. *A,* Interpreted segment of multichannel profile Neecho 1 (from Poag, Koeberl, and Reimold, 2004, fig. 7.12C). *B,* Uninterpreted version of *A.*

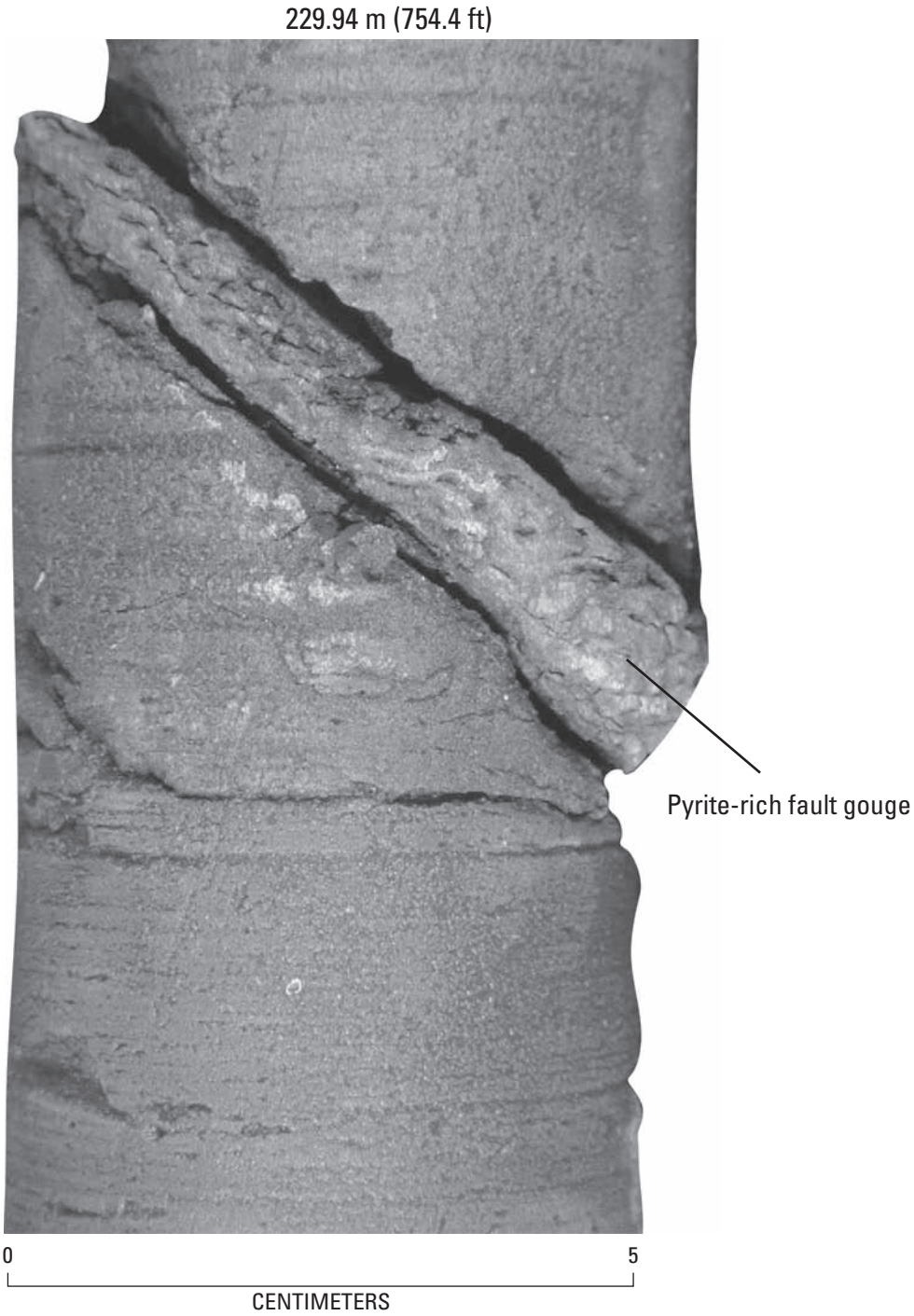

Figure F16. Photograph of a core segment of the Chickahominy Formation from the USGS-NASA Langley corehole showing a minor branch of the postimpact fault system. Leader indicates pyrite-rich fault gouge. Photograph by C.W. Poag (from Poag, Koeberl, and Reimold, 2004, fig. 7.10).

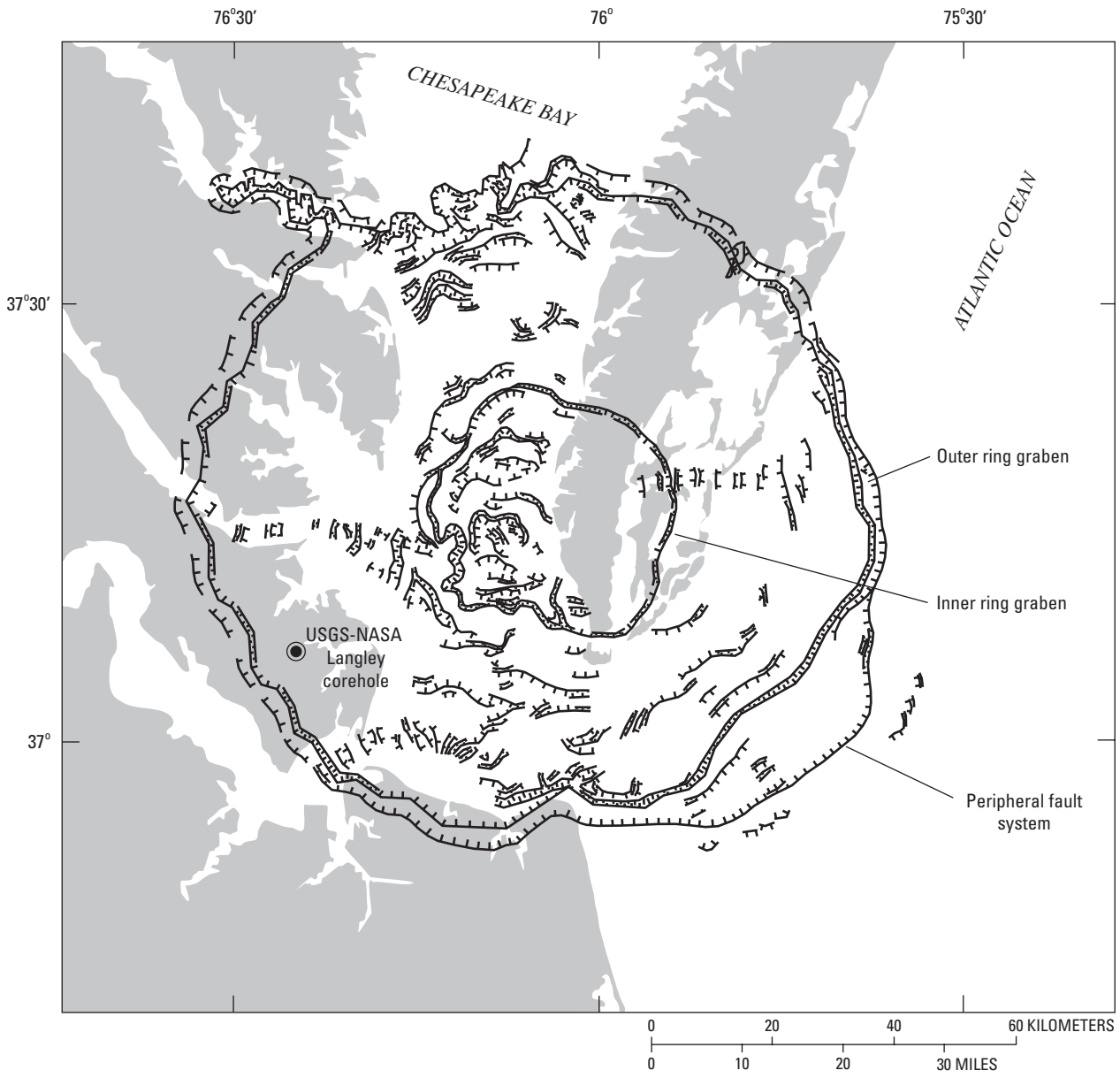

Figure F17. Map showing the general distribution of postimpact compaction faults (ticks on downthrown side) that cut the Chickahominy Formation at the Chesapeake Bay impact crater, as interpreted from seismic-reflection data. From Poag, Koeberl, and Reimold (2004, fig. 7.11).

indicates that sediment belonging to Zone P15 had been deposited prior to the impact.

The presence of *Turborotalia cunialensis* and *Cribrohantkenina inflata* in the Chickahominy at Kiptopeke is evidence that Zone P16 is represented in that core. The P15-P16 *biozonal* boundary was not recognized at Kiptopeke, however. Instead, Poag and Aubry (1995) identified the P15-P16 *biochronozone* on the basis of a thin concurrent-range biozone defined by the highest occurrence of *Bolboforma spinosa* and the lowest occurrence of *Bolboforma latdorfensis* (fig. F4; see also Poag, Koeberl, and Reimold, 2004). This bolboformid biozone has been established as approximately correlative with the P15-P16 biozonal boundary at Deep Sea Drilling Project (DSDP) Site 612 on the New Jersey Continental Slope (Poag and Aubry, 1995).

Poag, Koeberl, and Reimold (2004) also analyzed the stratigraphic distribution of benthic foraminifera in the Chickahominy Formation at Kiptopeke. They identified one calcareous benthic foraminiferal biozone (*Cibicidoides pippeni*) and four calcareous benthic foraminiferal subbiozones (*Bulimina jacksonensis, Lagenoglandulina virginiana, Uvigerina dumblei,* and *Bolivina tectiformis*) based on the stratigraphic ranges (presence-absence) of the nominate calcareous benthic foraminiferal species (fig. F5; pl. F1).

Poag, Koeberl, and Reimold (2004) defined the calcareous benthic foraminiferal zonation as follows:

- ***Cibicidoides pippeni*** **Taxon-Range Biozone**. That part of the Chickahominy Formation embracing the stratigraphic range of the nominate species. *Cibicidoides pippeni* appears to have a more extensive stratigraphic range in other localities, however, such as the Gulf of Mexico Coast and Caribbean (Van Morkhoven, Berggren, and Edwards, 1986) than it has at Kiptopeke.

- ***Bulimina jacksonensis*** **Interval Subbiozone**. That part of the Chickahominy Formation embracing the partial stratigraphic range of the nominate species between its lowest occurrence and the lowest occurrence of *Lagenoglandulina virginiana.*

- ***Lagenoglandulina virginiana*** **Interval Subbiozone**. That part of the Chickahominy Formation embracing the partial stratigraphic range of the nominate species between its lowest occurrence and the lowest occurrence of *Uvigerina dumblei*.

- ***Uvigerina dumblei*** **Interval Subbiozone**. That part of the Chickahominy Formation embracing the partial range of the nominate species between its lowest occurrence and the lowest occurrence of *Bolivina tectiformis*.

- ***Bolivina tectiformis*** **Taxon-Range Subbiozone.** That part of the Chickahominy Formation embracing the total range of the nominate species.

Poag, Koeberl, and Reimold (2004) also recognized a fifth subbiozone on the basis of agglutinated benthic foraminiferal taxa (fig. F5; pl. F1):

- ***Bathysiphon*** **Abundance Subbiozone**. That part of the Chickahominy Formation at the base of the *Bulimina jacksonensis* Subbiozone that contains the peak development (maximum specimen abundance and species diversity) of a suite of agglutinated benthic foraminifera in which *Bathysiphon* sp. is a notable (persistent and relatively abundant) constituent.

The USGS-NASA Langley Core

Lithostratigraphy

In the USGS-NASA Langley core, the Chickahominy Formation appears visually to be relatively uniform in composition. It is mainly a dense, dark-greenish-gray, highly fossiliferous marine clay (especially rich in microfossils); the unit is 52.37 m (171.8 ft) thick (see Powars and others, this volume, chap. G). On closer examination, the lithology is seen to be variable. For example, the relative amount of quartz silt and sand, mica flakes, and finely comminuted glauconite (as observed in washed foraminiferal samples) is not uniform through the cored section. Also, the unit is heavily burrowed at its top contact. The largest burrows contain sand and microfossils reworked downward from the overlying Oligocene Drummonds Corner beds. Fewer burrows are present at the base of the Chickahominy. The basal burrows contain sand and stratigraphically mixed microfossils reworked upward from the underlying Exmore breccia. Smaller burrows filled with framboidal pyrite are scattered throughout the formation but are more densely concentrated in some intervals than in others.

Log Correlations

Comparisons of downhole spontaneous-potential (SP) logs from the USGS-NASA Langley corehole and three other intracrater coreholes (North, Bayside, Kiptopeke; fig. F1) are useful in deciphering the thickness and distribution of lithofacies within the Chickahominy section. The logs from North, Bayside, and Kiptopeke indicate that the Chickahominy is notably less permeable (*negative* deflection of the SP curve) than the units that bound it (fig. F18). The Chickahominy section in the Langley corehole is an exception, however. There, the SP log is *positively* deflected relative to the log of the underlying Exmore breccia, which we infer to indicate greater permeability. Nevertheless, at all four core sites, the Chickahominy Formation can be partitioned into four principal subunits (SP–1 through SP–4) on the basis of log-defined SP deflections (relative permeability; fig. F18); a fifth subunit (SP–5) is recognized only at Kiptopeke.

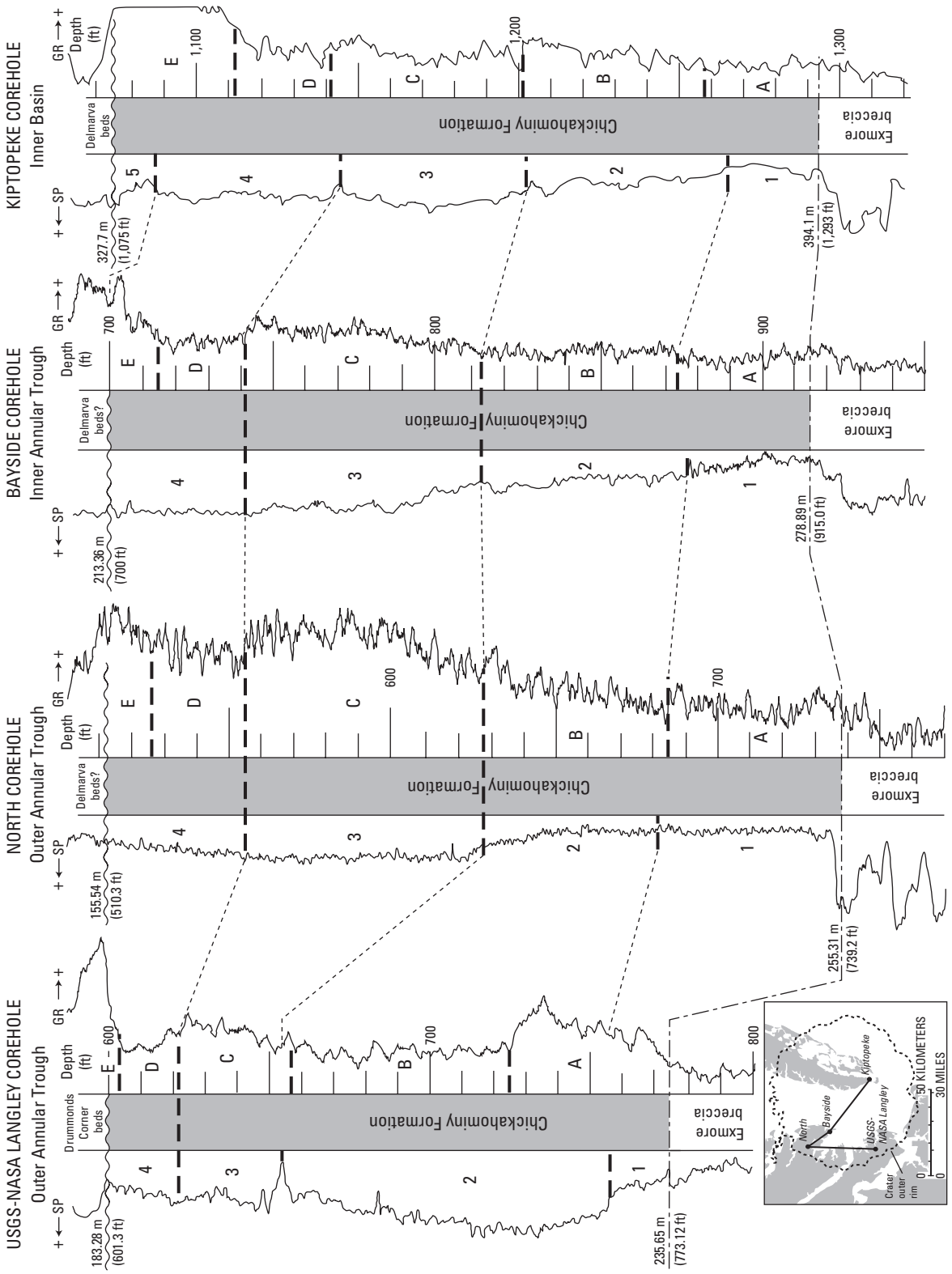

Figure F18. Downhole spontaneous-potential (SP) and gamma-ray (GR) logs, emphasizing log-defined lithic subunits within the Chickahominy Formation in the USGS-NASA Langley corehole and their correlations with subunits in the North, Bayside, and Kiptopeke coreholes (fig. F1). From Poag, Koeberl, and Reimold (2004, fig. 7.7A). Stratigraphic resolution is too coarse to show the dead zone. Vertical scales represent drill depths in feet. Negative deflections of the SP curves are interpreted to represent decreased permeability. Positive deflections of the GR curves are interpreted to represent increased amounts of clay or glauconite.

Subunits SP–1 through SP–5 are described below in ascending order:

- **Subunit SP–1.** At each site, subunit SP–1 (at the base) is characterized by the strongest negative deflections (lowest permeability).
- **Subunit SP–2.** At North, Bayside, and Kiptopeke, subunit SP–2 is characterized by SP values that become gradually more positive upcore (increasing permeability). In the Langley corehole, on the other hand, the positive SP deflection is abrupt at the base of SP–2, reaches highest values for this corehole, and then tapers off negatively, before declining steeply (becoming less permeable) at the top of SP–2 (fig. F18).
- **Subunit SP–3.** The log deflection in subunit SP–3 is more positive (greater permeability) than the deflection in SP–2 at North, Bayside, and Kiptopeke but is more negative (less permeability) than the deflection in SP–2 in the Langley corehole.
- **Subunit SP–4.** In subunit SP–4, the SP curve deflects negatively relative to the curve for SP–3 at North, Kiptopeke, and Langley but shows a relatively positive deflection at Bayside (fig. F18).
- **Subunit SP–5.** A fifth subunit (SP–5) at the top of the Chickahominy Formation can be recognized only at Kiptopeke. In subunit SP–5, the SP log deflects notably in the positive direction upsection.

Downhole gamma-ray (GR) logs, which reflect mainly the relative amount of clay and (or) glauconite in the Chickahominy Formation, provide a somewhat stronger definition of downhole lithic changes than do the SP curves (fig. F18); positive deflections of a GR log are interpreted to represent increased amounts of clay or glauconite. The GR curves at all four sites indicate a fivefold subdivision (GR–A through GR–E) of the Chickahominy. The upward succession of relative GR values, like that of the SP values, is similar at North, Bayside, and Kiptopeke.

Subunits GR–A through GR–E are described below in ascending order:

- **Subunit GR–A.** The basal GR subunit (GR–A) displays the greatest negative values at North, Bayside, and Kiptopeke, but in stark contrast, GR–A gives unusually high positive values at the Langley corehole.
- **Subunit GR–B.** Subunit GR–B shows upwardly increasing positive values at North and Kiptopeke, uniformly slightly higher values than GR–A at Bayside, and uniformly more negative values than GR–A at Langley (fig. F18).
- **Subunit GR–C.** In subunit GR–C, the GR values continue to increase positively upward at the Langley, North, and Bayside coreholes but decrease slightly before increasing again at Kiptopeke.
- **Subunit GR–D.** In subunit GR–D, GR values become negative at all sites relative to those of subunit GR–C.
- **Subunit GR–E.** Maximum positive GR values are reached at the top of the Chickahominy Formation in subunit GR–E at all four core sites (fig. F18).

The complex correlations of SP and GR subunits among different coreholes, combined with the marked stratigraphic variability within individual coreholes, are the results of laterally and vertically shifting Chickahominy lithotopes and suggest that the subunit boundaries are not likely to be synchronous from corehole to corehole. The most consistent intracorehole correlation is between SP–3 and GR–C, whose upper and lower boundaries coincide (or nearly coincide) at all four sites (fig. F18). There also is good correlation between SP–1 and GR–A and between SP–2 and GR–B at North, Bayside, and Kiptopeke, but these correlations break down at Langley. At the top of the Chickahominy section, SP–4 is equivalent to GR–D and GR–E, except at Kiptopeke, where SP–5 correlates with the top of GR–E.

In general, the logs indicate that during the early stages of Chickahominy deposition, the sedimentary regime at the USGS-NASA Langley site was distinctly different than that of the other three core sites. This difference is particularly manifested by subunit SP–2 (199–232 m; 653–760 ft) in the Langley corehole, which not only contains more sand-sized sediment than the basal (SP–1) and upper (SP–3, SP–4) subunits at Langley, but also contains much more sand-sized sediment than equivalent subunits farther downdip at the North corehole or farther toward the center of the crater at the Bayside and Kiptopeke coreholes (fig. F18). Moreover, the basal part of SP–2 at Langley also contains far more glauconite (subunit GR–A) than equivalent sections at the other three core sites (fig. F18).

Biostratigraphy

Planktonic Framework

In our Chickahominy samples from the USGS-NASA Langley core, we identified most of the same species of planktonic foraminifera and bolboformids (fig. F19) reported by Poag and Aubry (1995) for the Kiptopeke core. The planktonic foraminiferal succession in the Langley core is not sufficient to place the biozonal boundaries accurately, however, and so we followed Poag and Aubry (1995) and used the *Bolboforma spinosa-Bolboforma latdorfensis* biozone boundary to place the P15-P16 biochronozone boundary; in the Langley core, the boundary is between samples 24 and 25 at ~221.80 m (~727.70 ft) depth. See Edwards and others (this volume, chap. H) for stratigraphic distribution of additional planktonic microfossil groups.

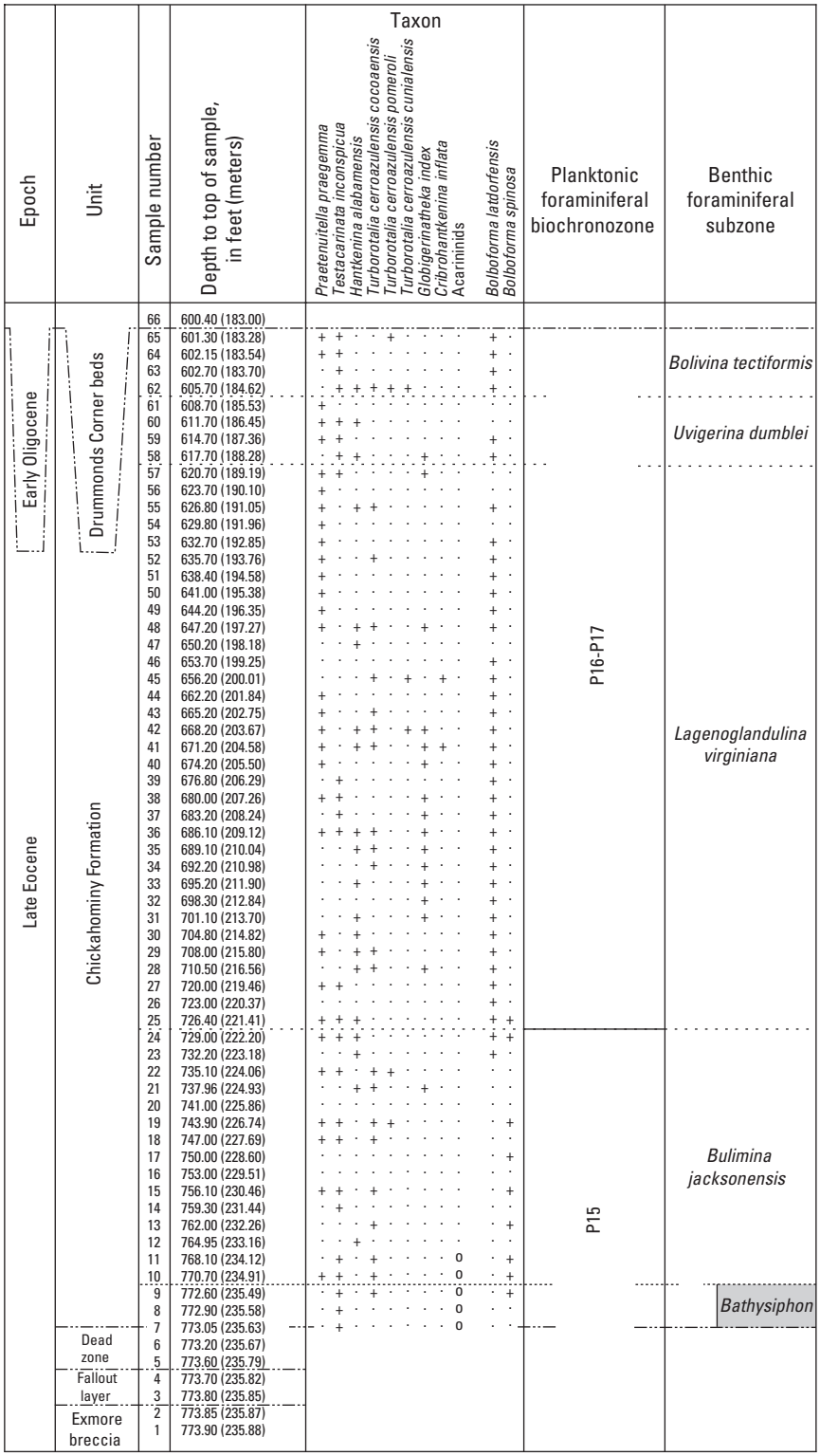

Figure F19. Chart showing planktonic biochronostratigraphic framework (based on occurrences of key planktonic foraminifera and bolboformids) for the Chickahominy Formation in the USGS-NASA Langley corehole correlated with benthic foraminiferal subzones. Symbols: +=present, .=absent, o= reworked specimen. Note that the contact between the dead zone and the Chickahominy Formation is near the middle of sample 7, whose top is at 235.63 m (773.05 ft) depth; the contact between the dead zone and the fallout layer is within sample 4 at ~235.84 m (~773.75 ft) (fig. F7). See also Edwards and others (this volume, chap. H).

Benthic Foraminifera

As in the Kiptopeke core, abundant benthic foraminiferal assemblages are present in the Chickahominy Formation samples from the Langley core and can be stratigraphically divided into the same *Cibicidoides pippeni* Zone and its five subzones (tables F4–F8; pl. F1; figs. F19, F20, and F21). Correlation of the benthic foraminiferal biozones of the Langley core with those of the Kiptopeke core is straightforward, but notable variations in the thickness of equivalent benthic subzones between the two core sites indicate that not all benthic subzone boundaries are isochronous horizons. Thickness disparities are particularly notable for the *Bulimina jacksonensis* and *Lagenoglandulina virginiana* Subzones, for example. The *Lagenoglandulina virginiana* Subzone is 12.6 m (41.3 ft) thick at Kiptopeke but is nearly three times as thick (33.07 m; 108.5 ft) at Langley. The benthic boundary that most closely approximates an isochronous boundary is that which separates the *Bulimina jacksonensis* Subzone from the *Lagenoglandulina virginiana* Subzone, because it is coincident with the planktonic foraminiferal P15-P16 zonal boundary at both Kiptopeke and Langley (fig. F22).

Age-Depth Model

Poag, Mankinen, and Norris (2003) and Poag, Koeberl, and Reimold (2004) used three biochronological datums and three magnetochronological datums to construct an age-depth model for the Kiptopeke core (fig. F23). Poag, Koeberl, and Reimold (2004) interpreted the two strongest deflections in the depth-age curve at Kiptopeke to represent significant changes in sediment accumulation rate (figs. F5, F22). We reassessed the Kiptopeke age-depth model and derived slightly different accumulation-rate values (fig. F23), but we identified the same two major shifts at the same stratigraphic horizons reported by Poag, Koeberl, and Reimold (2004).

At the Langley corehole, we are limited to the three biochronological datums: the base and top of the *Cibicidoides pippeni* Zone (35.78 Ma and 33.7 Ma, respectively) and the P15-P16 planktonic zonal boundary (35.2 Ma; Berggren and others, 1995; see fig. F3 of this chapter). We infer that erosion removed the base of planktonic foraminiferal chronozone Zone P18 from the very top of the intensely burrowed Chickahominy section; the lost record may have represented ~0.1 m.y. By using these datums, we identified a minor shift in sediment accumulation rate at the P15-P16 boundary at 221.8 m (~727.70 ft) depth (fig. F19), where the rate increases from 24 m/m.y. to 26 m/m.y. (78.7 ft/m.y. to 85.3 ft/m.y.). Given the imprecision of identifying stratigraphic boundaries on the basis of presence-absence data in core material and the relatively coarse sampling intervals, however, the differences between these two accumulation rates may not be significant. On the other hand, the largest rate shift at Kiptopeke takes place at the same stratigraphic level (P15-P16 boundary; fig. F22).

Even if the rate shift were significant, the resultant two-part sediment-accumulation record at the Langley corehole contrasts markedly with the three-part accumulation record at Kiptopeke (Poag, Koeberl, and Reimold, 2004; see figs. F5, F22, F23 of this chapter). The accumulation rate at Kiptopeke started out at an average of 56 m/m.y. (183.7 ft/m.y.) in the lowest 32 m (105 ft), decreased to 9 m/m.y. (29.5 ft/m.y.) in the succeeding 5 m (16.4 ft), and then increased to 32 m/m.y. (105 ft/m.y.) in the upper 27 m (88.6 ft). Even though the stratigraphic level of the sediment-accumulation-rate shift at the Langley site is coeval with the largest rate shift at Kiptopeke (fig. F22), the latter shift is a six-fold *decrease*, rather than a minor *increase*.

If one assumes that the sediment accumulation rate did not vary significantly between successive datums at the Langley site, then one can derive a rough estimate of the duration of each benthic foraminiferal subzone and the postimpact age of each benthic subzonal boundary (fig. F21). These estimates would support the hypothesis that some benthic subzonal boundaries are diachronous between the Langley and Kiptopeke coreholes. Such diachroneity would be further supported by comparing these boundary positions graphically (fig. F24). In the graphic correlation, the top of the *Bulimina jacksonensis* Subzone appears to be the only unequivocally isochronous benthic horizon, because its plot coincides with that of the planktonic P15-P16 boundary at both sites. The top of the *Uvigerina dumblei* Subzone plots close to the line of isochroneity, however, and may be truly isochronous, given the coarse sample spacing at both sites. The other two benthic foraminiferal subzonal boundaries are significantly distant from the line of isochroneity. One must keep in mind, however, that the SP and GR logs strongly indicate that the rate of sediment accumulation during Chickahominy time at the Langley site varied considerably, though perhaps not in concert with the rate changes at Kiptopeke. Clearly an analysis of the paleomagnetic record (or some other reliable set of datums) is needed at the Langley site to provide a more detailed record of sediment accumulation rates there.

Species Richness

In their study of Chickahominy benthic foraminifera in the Kiptopeke core, Poag, Koeberl, and Reimold (2004) demonstrated quantitatively that species richness (number of species represented in a sample) varied cyclically in approximate concert with the three intervals of distinctly different sediment accumulation rates (fig. F5). In the USGS-NASA Langley core, we find no equivalent cycles of species richness (fig. F25). Instead, there is a twofold subdivision, with higher average species richness (56) below 201.84 m (662.20 ft) and lower average species richness (47) above this level. This richness shift does not correspond to any obvious biostratigraphic boundary but takes place near the middle of the *Lagenoglandulina virginiana* Subzone. Most of the interval of higher average species richness corresponds, however, to the section of greatest positive SP deflection (SP–2; greatest permeability) in the Chickahominy Formation in the Langley corehole (fig. F18). In contrast, the

Text continues on page F43.

Table F4. Important benthic foraminiferal species of the *Cibicidoides pippeni* Zone in the Chickahominy Formation in the USGS-NASA Langley core.

[The benthic foraminiferal assemblages of the Chickahominy Formation are encompassed in a single biozone, the *Cibicidoides pippeni* Zone, which is represented by 126 calcareous and agglutinated species in the Chickahominy Formation (postimpact) in the USGS-NASA Langley core (fig. F20). Species listed in this table are those whose specimens are persistently present and (or) abundant in the *Cibicidoides pippeni* Zone in the Langley core. An asterisk (*) indicates species that were also present during the earliest late Eocene (preimpact) in the region later affected by the Chesapeake Bay impact. The *Cibicidoides pippeni* Zone was defined for the Kiptopeke core and preimpact species were identified by Poag, Koeberl, and Reimold (2004, tables 13.2 and 13.3). Quotation marks indicate provisory trivial names used by Poag, Koeberl, and Reimold (2004)]

*Bulimina jacksonensis**
*Caucasina marylandica**
*Charltonina madrugaensis**
*Cibicidoides pippeni**
*Epistominella minuta**
*Globobulimina ovata**
*Globulina gibba**
*Grigelis annulospinosa**
Grigelis cookei
Grigelis “elongata”
*Guttulina hantkeni**
*Guttulina irregularis**
*Gyroidinoides byramensis**
*Gyroidinoides planatus**
Hanzawaia blanpiedi
Lenticulina americana
*Lenticulina virginiana**
Loxostomina vicksburgensis f. “spinosa”*
*Marginulina cocoaensis**
*Melonis planatus**
Nodosaria capitata
Nodosaria cooperensis
*Oridorsalis umbonatus**
Proxyfrons virginiana
Sigmoidella plummerae
*Spiroplectinella mississippiensis**
*Stilostomella cocoaensis**
*Uvigerina gardnerae**
Vaginulina longiforma

Table F5. Important calcareous benthic foraminiferal species of the *Bulimina jacksonensis* Subzone in the Chickahominy Formation in the USGS-NASA Langley core.

[Species listed are those whose specimens are persistently present and (or) abundant in this subzone or are restricted (or nearly so) to this subzone. Quotation marks indicate provisory trivial names used by Poag, Koeberl, and Reimold (2004)]

Bolivina gardnerae	*Lenticulina americana*
Bolivina gracilis	*Lenticulina* "carinata"
Bolivina jacksonensis	*Loxostomina vicksburgensis* f. "spinosa"
Bolivina "praevirginiana"	*Marginulina cocoaensis*
Bolivina striatella	*Marginulina karreriana*
Bulimina jacksonensis	*Melonis planatus*
Caucasina marylandica	*Nodosaria capitata*
Charltonina madrugaensis	*Nodosaria cooperensis*
Cibicidoides "chickahominyanus"	*Nuttallides* sp.
Cibicidoides pippeni	*Oridorsalis umbonatus*
Epistominella minuta	*Parafrondicularia cookei*
Globobulimina ovata	*Sigmoidella plummerae*
Globulina gibba	*Spiroplectinella mississippiensis*
Grigelis annulospinosa	*Stilostomella* "aduncocostata"
Grigelis cookei	*Stilostomella cocoaensis*
Grigelis "elongata"	*Trifarina cooperensis*
Grigelis "tubulosa"	*Uvigerina gardnerae*
Grigelis "tumerosa"	*Valvulineria texana*
Guttulina hantkeni	
Guttulina irregularis	
Gyroidinoides aequilateralis	
Gyroidinoides byramensis	
Gyroidinoides planatus	
Hanzawaia blanpiedi	
Hoeglundina elegans	

Table F6. Important benthic foraminiferal species of the *Lagenoglandulina virginiana* Subzone in the Chickahominy Formation in the USGS-NASA Langley core.

[Species listed are those whose specimens are persistently present and (or) abundant in this subzone or are restricted (or nearly so) to this subzone. Quotation marks indicate provisory trivial names used by Poag, Koeberl, and Reimold, (2004)]

Bolivina "carinocostata"	*Lagenoglandulina virginiana*
Bolivina jacksonensis	*Lenticulina americana*
Bulimina cooperensis	*Lenticulina* "carinata"
Bulimina jacksonensis	*Lenticulina crassilimbata*
Caucasina marylandica	*Lenticulina virginiana*
Ceratobulimina perplexa	*Loxostomina vicksburgensis* f. "spinosa"
Charltonina madrugaensis	*Marginulina cocoaensis*
Cibicidoides pippeni	*Marginulina karreriana*
Epistominella minuta	*Melonis planatus*
Frondovaginulina tenuissima	*Nodosaria capitata*
Globobulimina ovata	*Nodosaria cooperensis*
Globulina gibba	*Nodosaria vertebralis*
Grigelis annulospinosa	*Nuttallides* sp.
Grigelis cookei	*Oridorsalis umbonatus*
Grigelis "elongata"	*Proxyfrons virginiana*
Grigelis "tubulosa"	*Sigmoidella plummerae*
Grigelis "tumerosa"	*Siphonina tenuicarinata*
Guttulina hantkeni	*Spiroplectinella mississippiensis*
Guttulina irregularis	*Stilostomella cocoaensis*
Gyroidinoides aequilateralis	*Uvigerina gardnerae*
Gyroidinoides byramensis	*Uvigerina jacksonensis* f. alata
Gyroidinoides planatus	*Uvigerina jacksonensis* f. typica
Hanzawaia blanpiedi	*Valvulineria texana*
Hoeglundina elegans	*Vasiglobulina alabamensis*
Hopkinsina danvillensis	

Table F7. Important benthic foraminiferal species of the *Uvigerina dumblei* Subzone in the Chickahominy Formation in the USGS-NASA Langley core.

[Species listed are those whose specimens are persistently present and (or) abundant in this subzone or are restricted (or nearly so) to this subzone. Quotation marks indicate provisory trivial names used by Poag, Koeberl, and Reimold (2004)]

Bolivina "carinocostata"	*Lenticulina virginiana*
Bulimina jacksonensis	*Loxostomina vicksburgensis* f. "spinosa"
Buliminellita curta	*Marginulina cocoaensis*
Caucasina marylandica	*Marginulina karreriana*
Charltonina madrugaensis	*Massilina decorata*
Cibicidina mauricensis	*Melonis planatus*
Cibicidoides pippeni	*Nodosaria cooperensis*
Epistominella minuta	*Nodosaria vertebralis*
Globobulimina ovata	*Oridorsalis umbonatus*
Globulina gibba	*Proxyfrons virginiana*
Grigelis annulospinosa	*Saracenaria hantkeni*
Grigelis cookei	*Sigmoidella plummerae*
Grigelis "elongata"	*Siphonina tenuicarinata*
Grigelis "tumerosa"	*Spiroplectinella mississippiensis*
Guttulina irregularis	*Stilostomella cocoaensis*
Gyroidinoides aequilateralis	*Uvigerina gardnerae*
Gyroidinoides byramensis	*Valvulineria texana*
Gyroidinoides planatus	
Hanzawaia blanpiedi	
Hoeglundina elegans	
Hopkinsina danvillensis	
Lagenoglandulina virginiana	
Lenticulina americana	
Lenticulina americana f. "spinosa"	
Lenticulina "carinata"	

Table F8. Important benthic foraminiferal species of the *Bolivina tectiformis* Subzone in the Chickahominy Formation in the USGS-NASA Langley core.

[Species listed are those whose specimens are persistently present and (or) abundant in this subzone or are restricted (or nearly so) to this subzone. Quotation marks indicate provisory trivial names used by Poag, Koeberl, and Reimold (2004)]

Bolivina regularis	*Loxostomina vicksburgensis* f. "spinosa"
Bolivina tectiformis	*Marginulina cocoaensis*
Bulimina jacksonensis	*Massilina decorata*
Buliminellita curta	*Melonis planatus*
Cassidulinoides braziliensis	*Nodosaria capitata*
Caucasina marylandica	*Nodosaria cooperensis*
Charltonina madrugaensis	*Nodosaria vertebralis*
Cibicidina mauricensis	*Oridorsalis umbonatus*
Cibicidoides pippeni	*Proxyfrons virginiana*
Epistominella minuta	*Sigmoidella plummerae*
Globobulimina ovata	*Siphonina tenuicarinata*
Globulina gibba	*Spiroplectinella mississippiensis*
Grigelis cookei	*Stilostomella* "aduncocostata"
Grigelis "elongata"	*Stilostomella cocoaensis*
Grigelis "tumerosa"	*Uvigerina gardnerae*
Guttulina hantkeni	*Vaginulina longiforma*
Gyroidinoides byramensis	
Gyroidinoides planatus	
Hanzawaia blanpiedi	
Hopkinsina danvillensis	
Lagenoglandulina virginiana	
Lenticulina americana	
Lenticulina americana f. "spinosa"	
Lenticulina "carinata"	
Lenticulina virginiana	

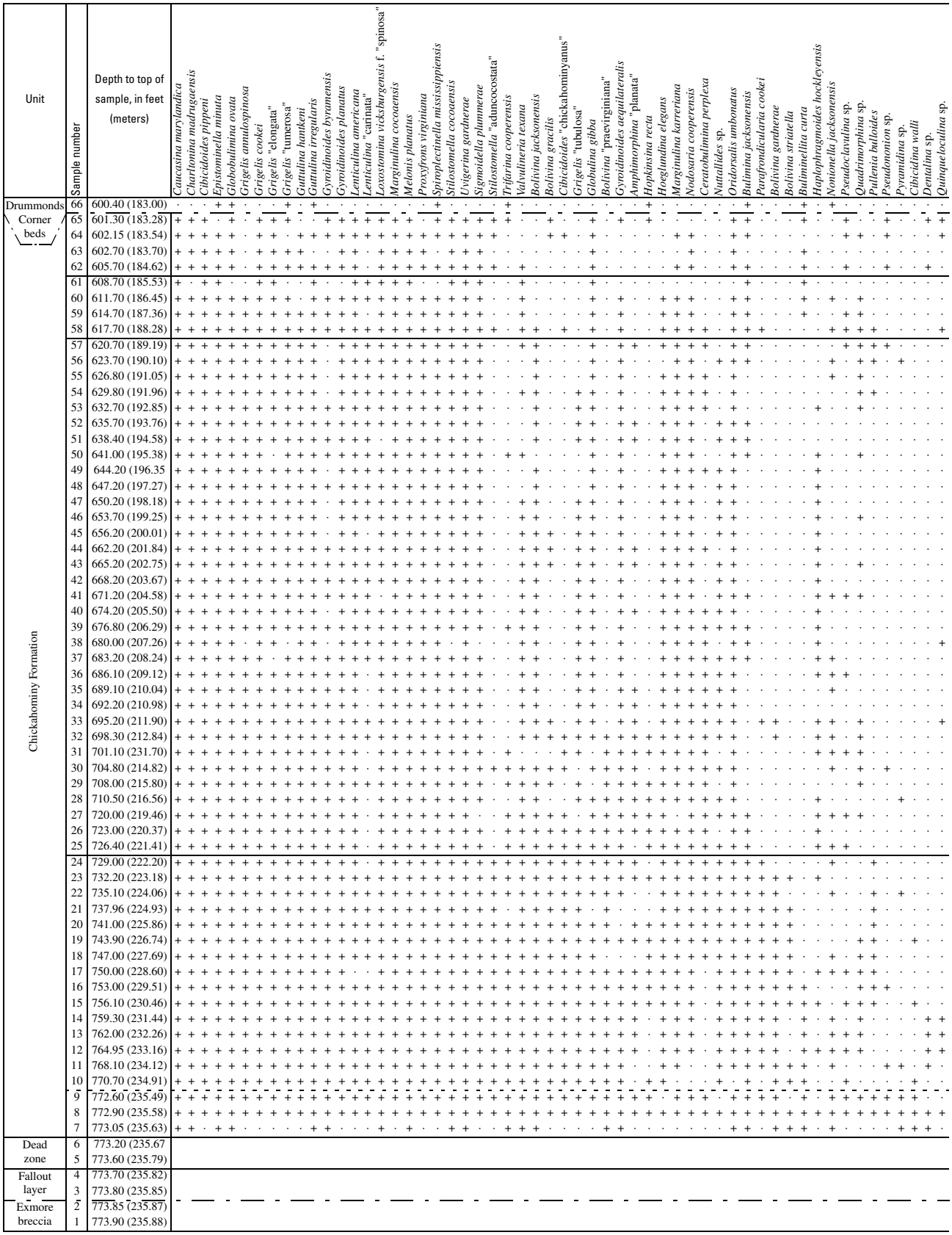

Unit	Sample number	Depth to top of sample, in feet (meters)
Drummonds Corner beds	66	600.40 (183.00)
	65	601.30 (183.28)
	64	602.15 (183.54)
	63	602.70 (183.70)
	62	605.70 (184.62)
	61	608.70 (185.53)
	60	611.70 (186.45)
	59	614.70 (187.36)
	58	617.70 (188.28)
Chickahominy Formation	57	620.70 (189.19)
	56	623.70 (190.10)
	55	626.80 (191.05)
	54	629.80 (191.96)
	53	632.70 (192.85)
	52	635.70 (193.76)
	51	638.40 (194.58)
	50	641.00 (195.38)
	49	644.20 (196.35
	48	647.20 (197.27)
	47	650.20 (198.18)
	46	653.70 (199.25)
	45	656.20 (200.01)
	44	662.20 (201.84)
	43	665.20 (202.75)
	42	668.20 (203.67)
	41	671.20 (204.58)
	40	674.20 (205.50)
	39	676.80 (206.29)
	38	680.00 (207.26)
	37	683.20 (208.24)
	36	686.10 (209.12)
	35	689.10 (210.04)
	34	692.20 (210.98)
	33	695.20 (211.90)
	32	698.30 (212.84)
	31	701.10 (231.70)
	30	704.80 (214.82)
	29	708.00 (215.80)
	28	710.50 (216.56)
	27	720.00 (219.46)
	26	723.00 (220.37)
	25	726.40 (221.41)
	24	729.00 (222.20)
	23	732.20 (223.18)
	22	735.10 (224.06)
	21	737.96 (224.93)
	20	741.00 (225.86)
	19	743.90 (226.74)
	18	747.00 (227.69)
	17	750.00 (228.60)
	16	753.00 (229.51)
	15	756.10 (230.46)
	14	759.30 (231.44)
	13	762.00 (232.26)
	12	764.95 (233.16)
	11	768.10 (234.12)
	10	770.70 (234.91)
	9	772.60 (235.49)
	8	772.90 (235.58)
	7	773.05 (235.63)
Dead zone	6	773.20 (235.67
	5	773.60 (235.79)
Fallout layer	4	773.70 (235.82)
	3	773.80 (235.85)
Exmore breccia	2	773.85 (235.87)
	1	773.90 (235.88)

Figure F20. Occurrence chart showing the presence of benthic foraminifera identified in the Chickahominy Formation in the USGS-NASA Langley core. Symbols: +=present, . =absent. The placement of the P15-P16 planktonic foraminiferal biochronozone boundary was approximated by the overlapping ranges of *Bolboforma latdorfensis* and *Bolboforma spinosa* (fig. F19). Note that the contact between the dead zone and the Chickahominy Formation is near the middle of sample 7, whose top is at 235.63 m (773.05 ft) depth.

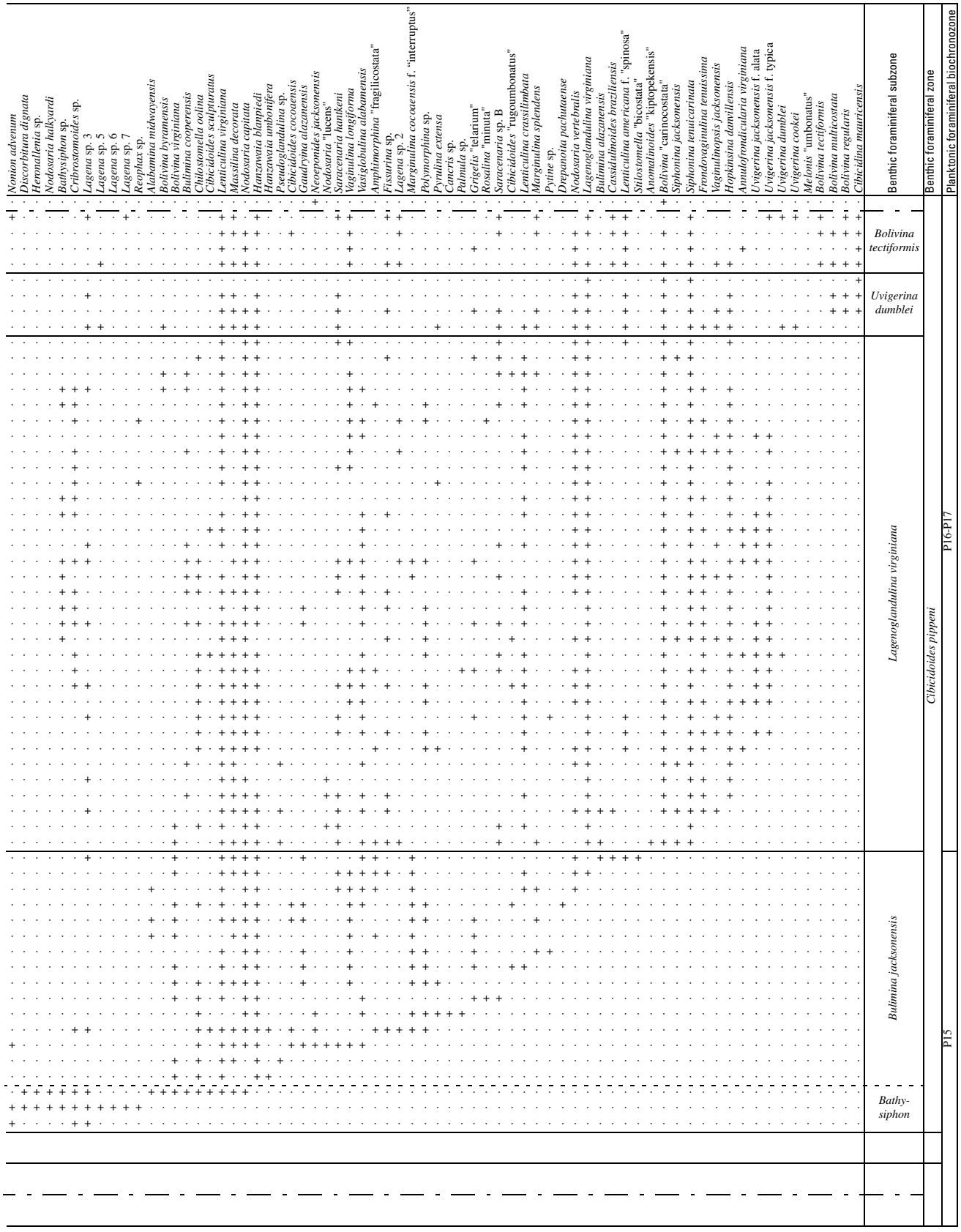

Figure F20. Continued.

Kiptopeke core

Zone	Subzone	Boundary depth (m)	Postimpact age	Approximate duration (k.y.)
		327.7	2.10 m.y.	
Cibicidoides pippeni	*Bolivina tectiformis*			134
		332.0	1.98 m.y.	
	Uvigerina dumblei			506
		348.2	1.47 m.y.	
	Lagenoglandulina virginiana			837
		360.8	596 k.y.	
	Bulimina jacksonensis			593
		370.3	426 k.y.	
	Bathysiphon			423
		394.0	3 k.y.	
Dead zone				<1–3
		394.2	0.0 y.	

USGS-NASA Langley core[1]

Zone	Subzone	Boundary depth (m)	Postimpact age	Approximate duration (k.y.)
		183.28	2.10 m.y.	
Cibicidoides pippeni	*Bolivina tectiformis*			69
		185.07	2.02 m.y.	
	Uvigerina dumblei			141
		188.73	1.88 m.y.	
	Lagenoglandulina virginiana			1,272
		221.80	604 k.y.	
	Bulimina jacksonensis			577
		235.19	27 k.y.	
	Bathysiphon			19
		235.65	8 k.y.	
Dead zone				<1–8
		235.84	0.0 y.	

[1]If the rate at the Langley core site was 24 m/m.y., then 1 m of sediment accumulated in 42 k.y. If the rate at the Langley core site was 26 m/m.y., then 1 m of sediment accumulated in 39 k.y.

Figure F21. Chart showing boundary depths, postimpact ages, and approximate durations of five benthic foraminiferal subzones recognized in the Chickahominy Formation at the Kiptopeke and USGS-NASA Langley core sites. The time scale for the Kiptopeke core was derived from magnetochronology, biochronology, and sediment accumulation rates recalculated from those shown in figure F5. The time scale for the USGS-NASA Langley core was derived from biochronology and sediment accumulation rates.

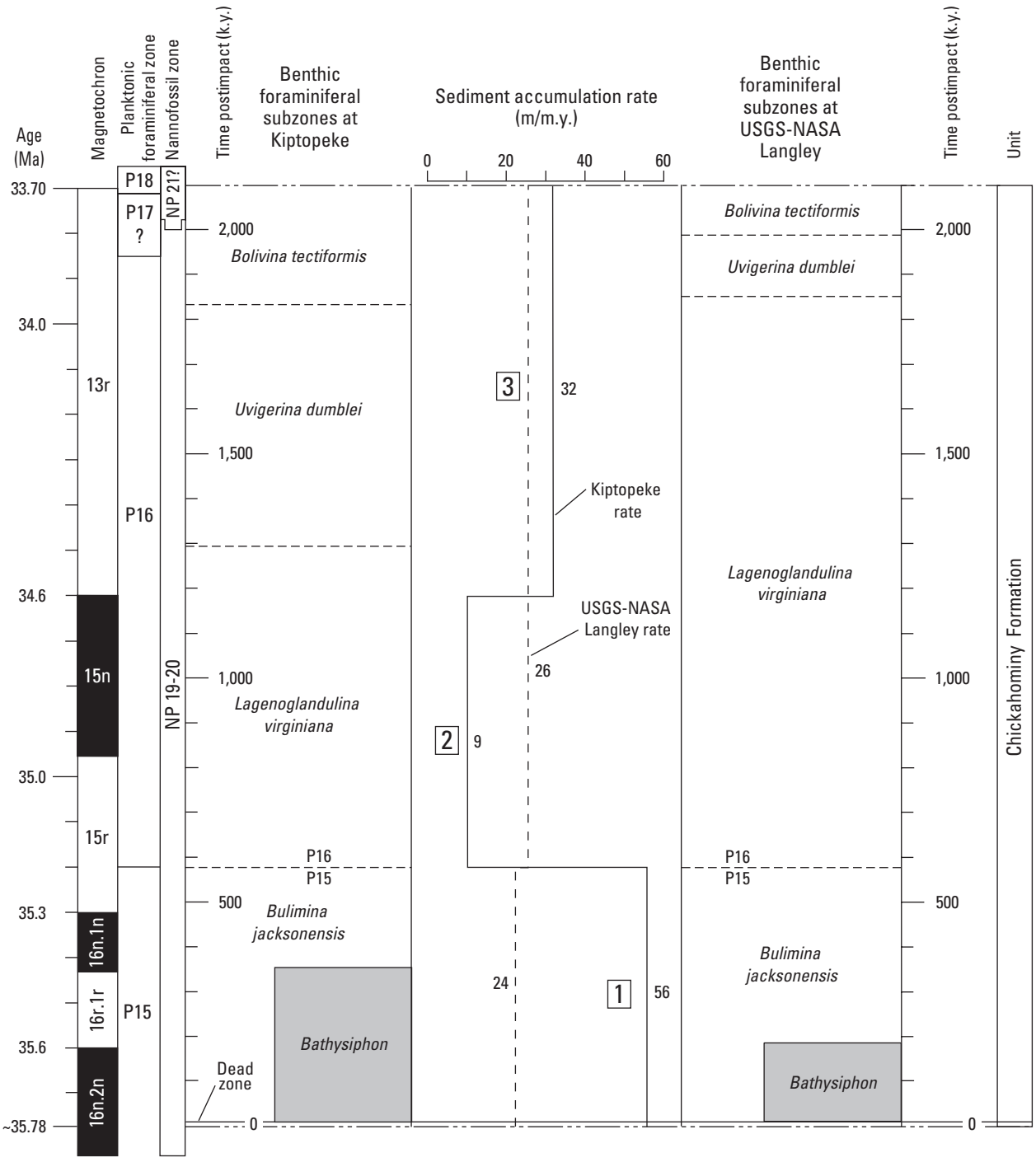

Figure F22. Chart showing geochronological correlation of benthic foraminiferal subzones and sediment accumulation rates for the Chickahominy Formation in the USGS-NASA Langley corehole compared with those in the Kiptopeke corehole (modified from Poag, Koeberl, and Reimold, 2004). Scale at right indicates time in thousands of years (k.y.) postimpact; see figure F5. Note that the top of the *Bulimina jacksonensis* Subzone (coincident with the planktonic foraminiferal P15-P16 biochronozone boundary) is the only benthic subzone boundary (other than the base and top of the Chickahominy section) that is isochronous between these two core sites. Numbers 1, 2, and 3 in squares indicate the three depositional episodes at Kiptopeke; the sediment accumulation rates for these episodes are revised from rates shown in figure F5 and reported by Poag, Koeberl, and Reimold (2004, table 13.1).

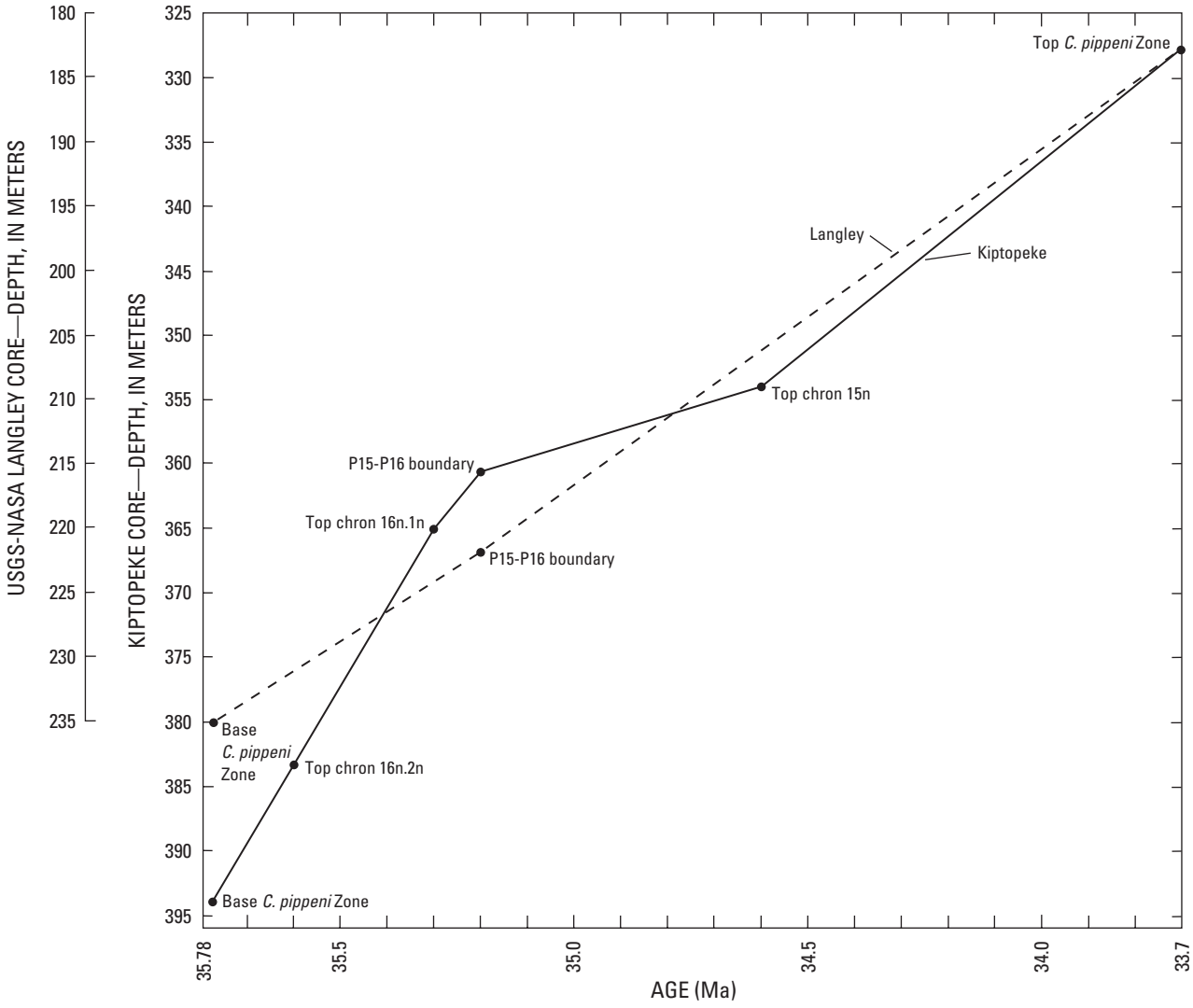

Figure F23. Graph showing depth-age models for the Chickahominy Formation in the Kiptopeke and USGS-NASA Langley cores. Kiptopeke data are from Poag, Koeberl, and Reimold (2004, p. 392, 393). The Langley model shows fewer control points because magnetochron boundaries in the Langley core have not been determined. The time scale is from figure F22.

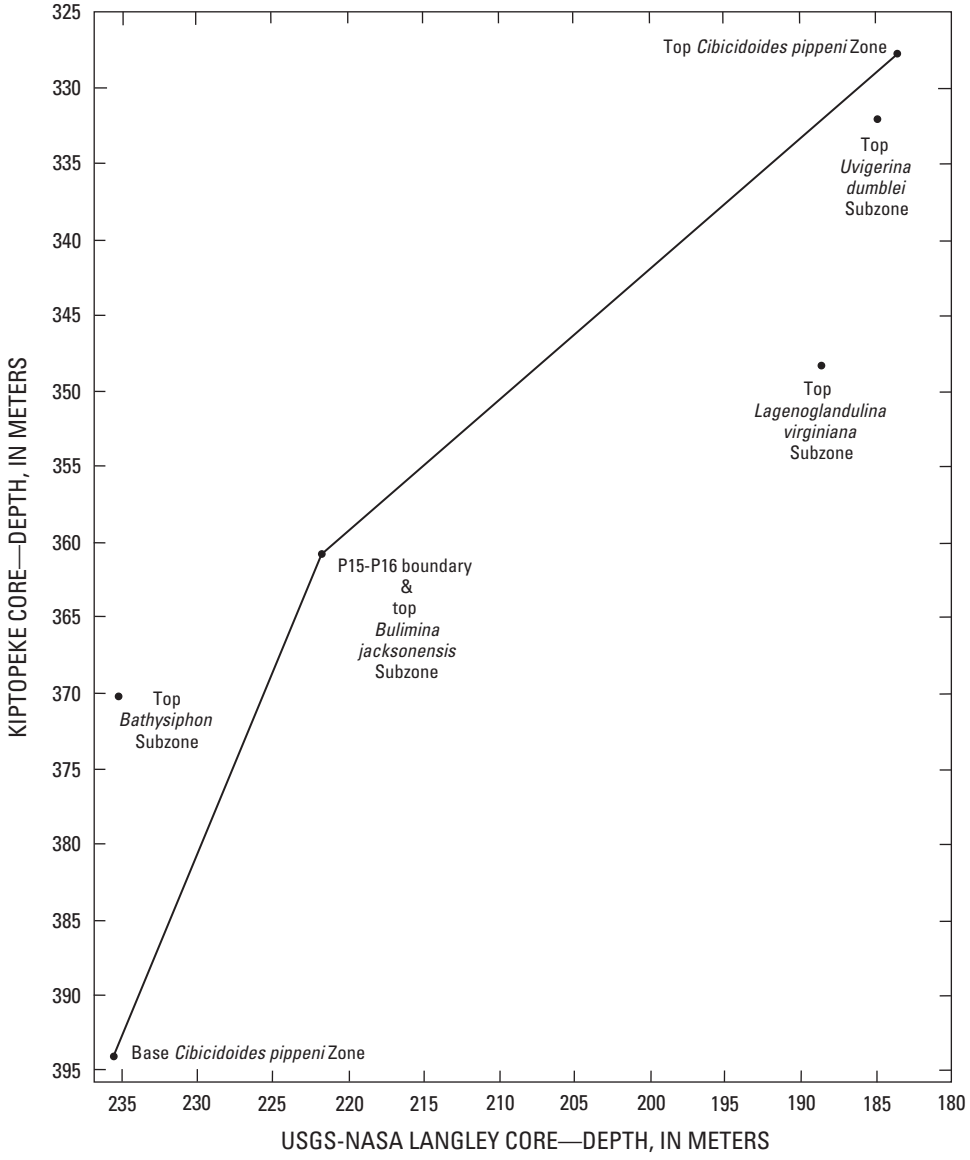

Figure F24. Graph showing correlation of three correlative stratigraphic boundaries in the Kiptopeke and USGS-NASA Langley cores. The bend in the line of correlation results from the marked shift in sediment accumulation rate at the P15-P16 boundary in the Kiptopeke core (see fig. F22). The top boundaries of the *Bathysiphon, Lagenoglandulina virginiana,* and *Uvigerina dumblei* Subzones plot well away from the line of correlation, which indicates that the subzone boundaries are not isochronous horizons between these two core sites.

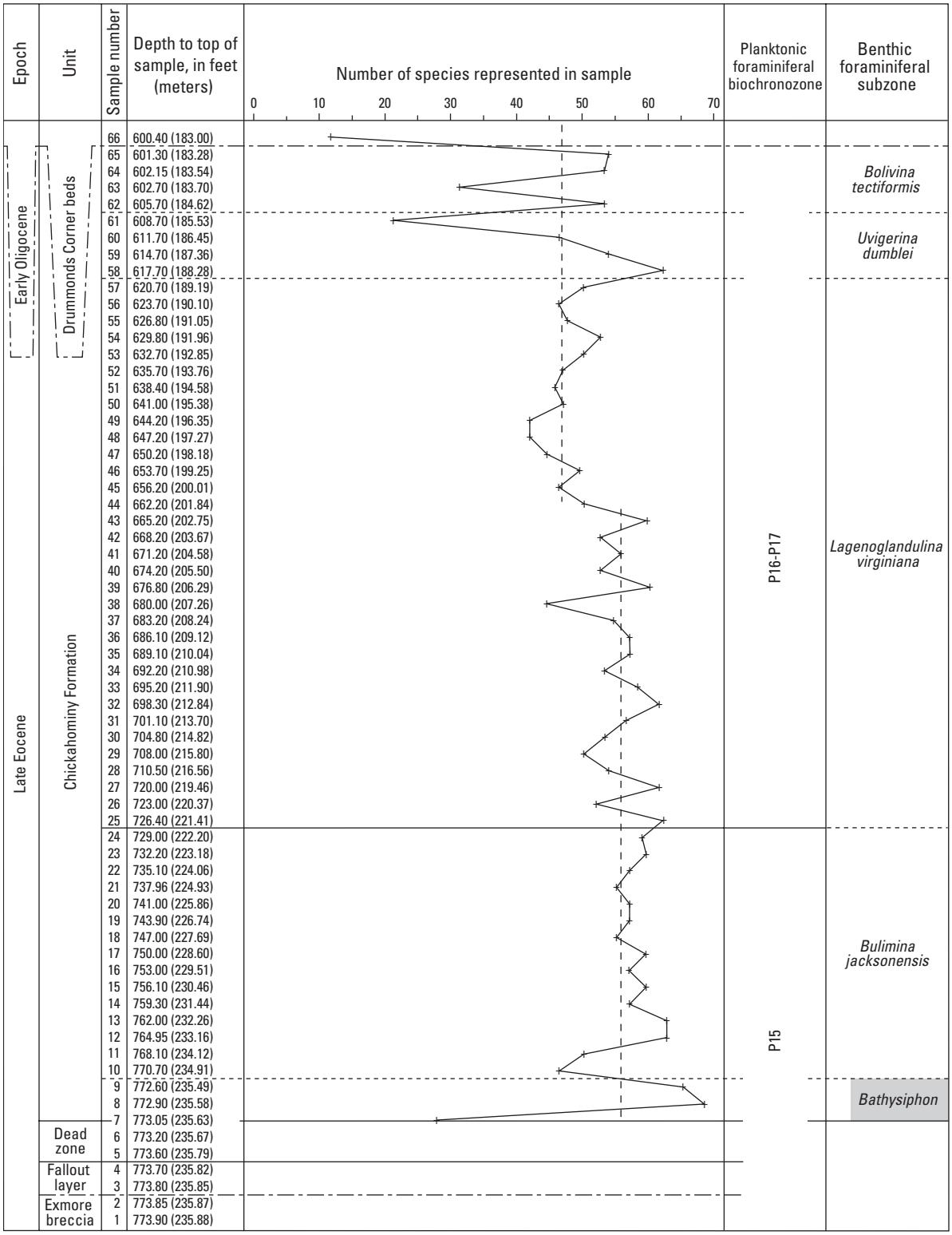

Figure F25. Graph showing species-richness curve (number of species represented in sample) for the Chickahominy Formation in the USGS-NASA Langley core. Occurrence data are from figure F20. P15-P16 is the planktonic foraminiferal biochronozone boundary approximated by the overlapping ranges of *Bolboforma latdorfensis* and *Bolboforma spinosa*. Note that the average species richness (indicated by dashed vertical lines) shifts to persistently lower values in samples higher than the middle of the *Lagenoglandulina virginiana* Subzone. Note also that the contact between the dead zone and the Chickahominy Formation is near the middle of sample 7, whose top is at 235.63 m (773.05 ft) depth.

highest values for species richness (65, 67) occur at the base of the section (fig. F25), where permeability is lowest (SP–1; fig. F18). The two highest values of species richness at the base of the section can be explained by the added presence of several species of agglutinated foraminifera that constitute the *Bathysiphon* Subzone.

Stable-Isotope Analyses

Poag (1997b) hypothesized that an impact-generated pulse of warm climate could be recognized in late Eocene marine and terrestrial records. Poag, Mankinen, and Norris (2003) supported that idea with stable-isotope ($\delta^{18}O$) analyses from the Chickahominy Formation at Kiptopeke. The Kiptopeke $\delta^{18}O$ record showed three pulses of relatively warm climate in the late Eocene, rather than a single long-lasting pulse (figs. F5, F26). The amplitude of the $\delta^{18}O$ variation is ~0.2‰–0.3‰ and suggests temperature variations of ~1°C or slightly more. The first pulse (W–1) was identified at the base of the Chickahominy and probably lasted 0–200 k.y. postimpact; a second pulse (W–2) was identified in the middle of the Chickahominy (350–600 k.y. postimpact), and a third (W–3), at the top of the Chickahominy (1,400–2,000 k.y. postimpact; figs. F5, F26). Poag, Mankinen, and Norris (2003) correlated these three pulses with a similar tripartite subdivision of the global record of late Eocene climate. Poag, Mankinen, and Norris (2003) interpreted the $\delta^{18}O$ record as an indication of impact-generated climatic warming maintained by a 2-m.y.-long late Eocene comet shower, which had previously been inferred from an unusual abundance of extraterrestrial ^{3}He within the Eocene-Oligocene boundary stratotype at Massignano, Italy (Farley and others, 1998).

The $\delta^{18}O$ record in the USGS-NASA Langley core is nearly identical to that of the Kiptopeke core (fig. F26) and shows the same three principal negative excursions identified by Poag, Mankinen, and Norris (2003). This similarity reinforces Poag's (1997b) hypothesis that a relatively warm late Eocene climate (see also Kobashi and others, 2001; Pearson and others, 2001) was initiated or reinforced by the Chesapeake Bay and Popigai (northern Siberia, Russia) impacts and was maintained during the following ~2 m.y. by a prolonged succession of impacts during the comet shower.

Poag, Mankinen, and Norris (2003) also analyzed the $\delta^{13}C$ record at Kiptopeke and found a small (single-point) negative excursion associated with the basal Chickahominy warm pulse and another, much larger and longer lasting negative excursion, nearly coincident with biochronozone P16-P17 (figs. F5, F26). We found an identical pair of negative excursions in the Chickahominy record in the USGS-NASA Langley core (fig. F26). The stratigraphically highest negative $\delta^{13}C$ excursion has been documented at several other sites around the globe and indicates a significant net decrease in global carbon burial. This negative $\delta^{13}C$ excursion also promises to provide good correlations in areas where other stratigraphic data may be weak or missing (Poag, Mankinen, and Norris, 2003). The positive extensive $\delta^{13}C$ excursion in the lower part of the Chickahominy Formation can be interpreted as a net exhumation of carbon (decrease in global carbon storage). The single-point negative $\delta^{13}C$ excursion at the base of the Chickahominy section at Langley matches that at Kiptopeke, giving support to its validity, but additional sampling in the basal section is needed for corroboration.

Paleoenvironmental Interpretations

Postimpact Microfaunal Recovery

Poag (2002) interpolated the maximum duration of the dead zone at the USGS-NASA Langley site to be <1–10 k.y. by extrapolating the sediment accumulation rate of 21 m/m.y. (68.9 ft/m.y.) in the lower part of the Langley core. We slightly reduced the maximum duration estimate to ~8 m.y. by using a sediment accumulation rate of 24 m/m.y. (78.7 ft/m.y.). Poag, Koeberl, and Reimold (2004) took only one sample in the dead zone at Kiptopeke and were not able to measure the thickness of the dead zone there because the core had been disrupted between the time it was drilled (1989) and the time it was sampled (1992).

Samples analyzed above the dead zone at Kiptopeke (Poag, Koeberl, and Reimold, 2004) show relatively slow repopulation of that site by the *Cibicidoides pippeni* assemblage (*Bulimina jacksonensis* subassemblage). The Kiptopeke *Bulimina jacksonensis* subassemblage did not reach preimpact species richness (as documented by Poag, Koeberl, and Reimold, 2004) until 3.4 m (11.1 ft) above the top of the dead zone (at 390.5 m; 1,281 ft), which is equivalent to ~36 k.y. postimpact, if one uses the basal Kiptopeke sediment accumulation rate of 67 m/m.y. (220 ft/m.y.) (Poag, Koeberl, and Reimold, 2004; see original and revised rates in figs. F5 and F22 of this chapter). In contrast, the *Cibicidoides pippeni* assemblage (*Bulimina jacksonensis* subassemblage) reoccupied the USGS-NASA Langley site immediately following deposition of the dead zone, appearing in the top third of sample 7 (235.63–235.65 m; 773.06–773.13 ft depth), which is the base of the Chickahominy Formation (figs. F7, F19, and F20; table F1). Though the precision of these rate calculations is low, the relative difference suggests that postimpact paleoenvironments normalized faster near the western rim of the crater (at Langley) than farther toward the crater center (inside the peak ring at Kiptopeke; fig. F1).

Paleobathymetry

The USGS-NASA Langley and Kiptopeke core sites occupied the middle part of a broad, gently sloping continental shelf before the impact (Poag, 1997b). After the impact, the two sites were inside the crater, a partly filled, subcircular excavation, whose upper surface formed a depression or closed basin in the sea floor. Presumably, the depression was somewhat deeper in the center than along the periphery, but the bathymetric differ-

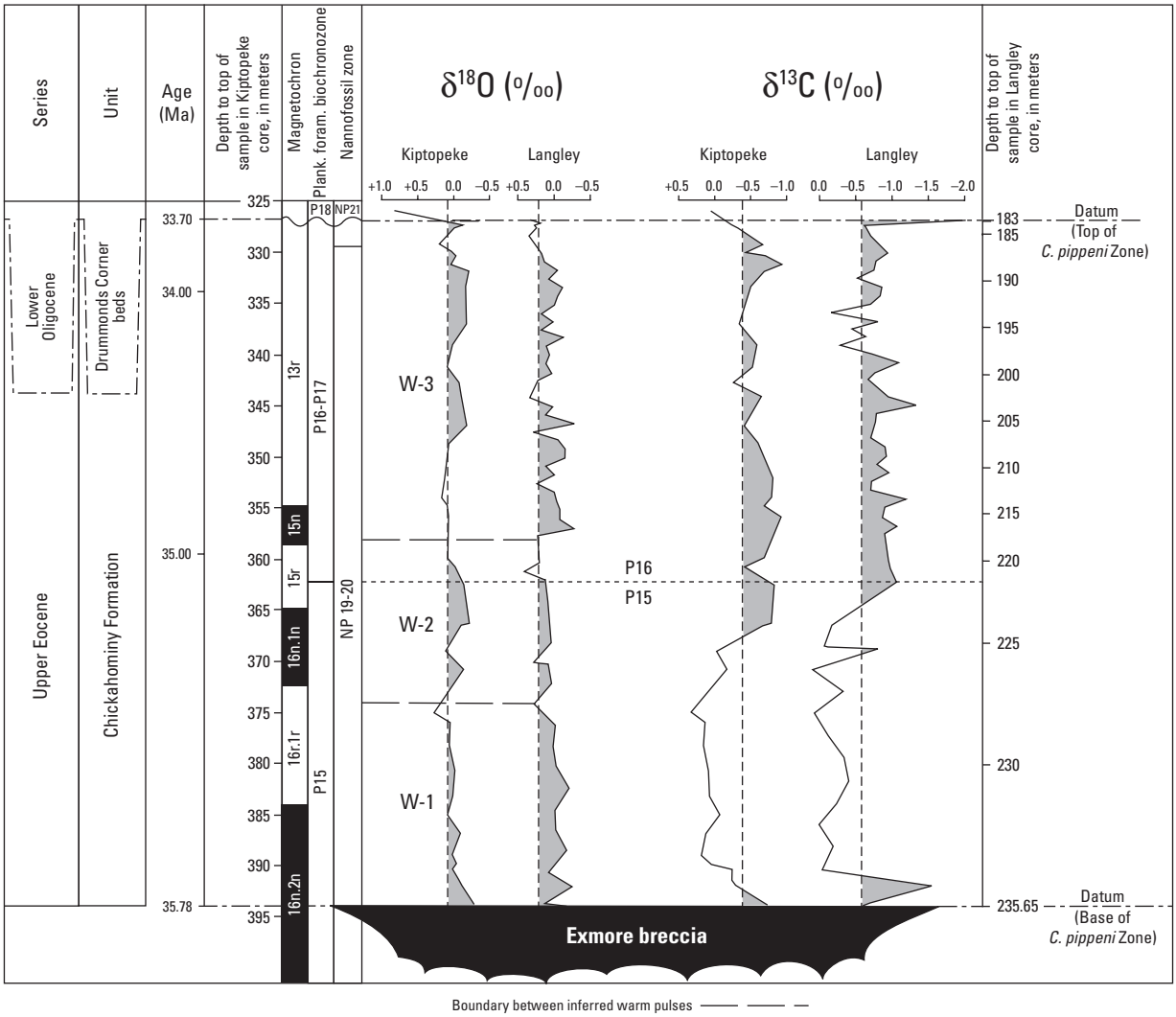

Figure F26. Diagram showing correlation of stable-isotope records from the Chickahominy Formation in the USGS-NASA Langley core with those in the Kiptopeke core. P15-P16 is the planktonic foraminiferal biochronozone boundary approximated by the overlapping ranges of *Bolboforma latdorfensis* and *Bolboforma spinosa*. W–1, W–2, and W–3 are warm pulses inferred from relatively negative $\delta^{18}O$ values. The lower part of the depth scale for the USGS-NASA Langley core and corresponding segments of isotope curves have been uniformly stretched because the part of the Chickahominy Formation below the P15-P16 boundary is much thicker at Kiptopeke than at Langley; the stretching enables the three isochronous correlation horizons (base and top of *Cibicidoides pippeni* Zone and P15-P16 biochronozone boundary) to be displayed as horizontal lines on this diagram. The vertical dashed lines and shading are provided to aid the reader in visualizing the grouping of positive and negative excursions of the isotope data.

ence, if any, is beyond the resolution of the current foraminiferal analysis.

Nearly all the Chickahominy species at Kiptopeke and Langley have modern counterparts; in fact, some are still extant (Poag, Koeberl, and Reimold, 2004). Most of these modern species are abundant (individually and in similar species associations) in outer neritic to upper bathyal marine biotopes, and the fossil counterparts indicate paleodepths of 150–500 m (~500–~1,600 ft) (table F9; Charletta, 1980; Poag, 1981; Van Morkhoven, Berggren, and Edwards, 1986). Many of the Chickahominy species at Kiptopeke and Langley (such as *Bulimina jacksonensis*, *Siphonina tenuicarinata*, *Hoeglundina elegans*, *Turrilina robertsi*, *Bolivina byramensis*, *Grigelis* spp., *Stilostomella* spp.) also occur in other widely distributed Paleogene outer neritic-bathyal deposits (Beckmann, 1954; Tjalsma and Lohmann, 1983; Van Morkhoven, Berggren, and Edwards, 1986). From these data, Poag, Koeberl, and Reimold (2004) estimated that the paleodepth at Kiptopeke was ~300 m (~1,000 ft) during deposition of the Chickahominy Formation. We infer that the paleodepth was essentially identical at Langley.

Benthic Habitats

Most of the predominant genera and species in the Chickahominy benthic foraminiferal assemblages from the Langley and Kiptopeke cores have modern counterparts that are notable for opportunistic life strategies and tolerance of (or preference for) oxygen-depleted (disoxic, microxic, anoxic) muds rich in organic detritus (Poag, Koeberl, and Reimold, 2004). Among the best documented of these modern taxa are the calcareous genera that predominate in the *Cibicidoides pippeni* assemblage: *Epistominella*, *Bolivina*, *Bulimina*, *Globobulimina*, *Uvigerina*, and *Buliminella* (modern counterpart of *Caucasina*) (Phleger and Soutar, 1973; Douglas and Heitman, 1979; Mackensen and Douglas, 1989; Jorissen and others, 1992; Kaminski and others, 1995; Sen Gupta and others, 1996; Bernhard and Sen Gupta, 1999; Loubere and Fariduddin, 1999; table F9; pls. F1, F2). Most of the members of the Chickahominy *Bathysiphon* Subassemblage also are typical inhabitants of oxygen-depleted, nutrient-rich substrates (Gooday, 1994; Kaminski and others, 1995).

Nutrient Supply

There is considerable evidence from the modern oceans that the geographic distribution, test size, and abundance (absolute and relative) of certain benthic foraminiferal species and genera are strongly correlative with the flux of organic detritus to the sea floor (Caralp, 1989; Corliss and Fois, 1990; Corliss and Silva, 1993; Pfannkuche, 1993; Linke and others, 1995; Gooday, 1996). This correlation exists because outer neritic, bathyal, and abyssal benthic foraminifera are dependent upon the flux of labile organic carbon for their food source (Gooday, 1994; Loubere and Fariduddin, 1999).

Most of the predominant Chickahominy calcareous genera (and those of the *Bathysiphon* subassemblage) at the Langley and Kiptopeke core sites have modern counterparts that are most abundant, and often have largest test sizes, in organic-matter-rich muds, which commonly also are oxygen depleted (Poag, Koeberl, and Reimold, 2004). The Chickahominy assemblages also are notable for unusually large test sizes, especially among the lenticulinids, nodosariids, and stilostomellids.

Of special note in the Chickahominy assemblages is an association of small, smooth, thin-walled, hyaline, opportunistic genera, such as *Epistominella*, which in modern oceans live epifaunally within aggregates of phytodetritus (a gelatinous matrix containing the remains of phytoplankton and zooplankton) on the sea floor (Gooday, 1993, 1994). These species have opportunistic feeding strategies and grow explosively into large concentrations during peak development of phytodetritus. Among the predominant Chickahominy taxa, species of *Epistominella* and *Caucasina* are probably representative of this lifestyle (pl. F2, figs. 1, 6).

Paleoenvironmental Summary

Overall, the Chickahominy benthic foraminiferal associations documented in the USGS-NASA Langley corehole represent consistently diverse, species-rich communities living within the upper 10 cm (4 in.) of fine-grained substrates, in paleodepths of ~300 m (~1,000 ft), generally typified by high flux rates of organic carbon and by oxygen deficiency. The development of five successive subassemblages, however, points to marked temporal changes in environmental properties other than paleodepth. The principal variable properties that we have considered are sediment delivery rates, permeability (volume of sand-sized particles), glauconite content, marked to subtle changes in substrate chemistry and nutrient flux, and broad-scale shifts in climate indicated by $\delta^{18}O$ variations and in the local and global carbon budget indicated by $\delta^{13}C$ variations. However, coincident temporal changes in the measured or calculated values of these properties do not necessarily establish a one-to-one cause-and-effect relationship.

For example (indicated by stars in fig. F27), a change in the composition of benthic foraminiferal assemblages at the boundary between the *Bulimina jacksonensis* and *Lagenoglandulina virginiana* Subzones coincides (or nearly coincides) with shifts in several properties, including a minor increase in rate of sediment accumulation, a brief positive excursion in $\delta^{18}O$, a sustained negative excursion in $\delta^{13}C$ (increased burial of carbon), a significant positive deflection in the SP curve (peak in permeability), and a negative deflection in the GR curve (reduction in glauconite content). A major paleoceanographic change also took place at that level, as indicated by the changes in planktonic foraminifera and bolboformid assemblages.

Similar correlations at this horizon apply to the Kiptopeke corehole (fig. F27), though the depositional lithofacies there (indicated by differences in geophysical logs) were quite different from those at Langley, and some of the log-derived lithic

Table F9. Benthic foraminiferal species used for interpretation of Chickahominy paleoenvironments at the USGS-NASA Langley and Kiptopeke core sites.

[Core sites are shown in figure F1. Species names in quotation marks are provisory. Abbreviations in the microhabitat column for infaunal depths: s=shallow (depth below sediment-water interface of 0–2 cm; 0–0.8 in.), i=intermediate (depth of 2–4 cm; 0.8–1.6 in.), d=deep (depth of 4–10 cm; 1.6–3.9 in.). Table from Poag, Koeberl, and Reimold (2004, table 13.9)]

Species	Test construction	Microhabitat	Oxygen/ nutrient tolerance	Preferred paleodepth	Opportunist
Ammobaculites sp.	agglutinated	infaunal	low/high	outer neritic-upper bathyal	
Amphimorphina "fragilicostata"	calcite	infaunal	low/high	outer neritic-upper bathyal	
Amphimorphina "planata"	calcite	infaunal	low/high	outer neritic-upper bathyal	
Bathysiphon sp.	agglutinated	epifaunal	low/high	bathyal-abyssal	
Bolivina byramensis	calcite	s infaunal	low/high	outer neritic-upper bathyal	
Bolivina gardnerae	calcite	s infaunal	low/high	outer neritic-upper bathyal	yes
Bolivina gracilis	calcite	i-d infaunal	low/high	outer neritic-upper bathyal	
Bolivina jacksonensis	calcite	i-d infaunal	low/high	outer neritic-upper bathyal	yes
Bolivina multicostata	calcite	s infaunal	low/high	outer neritic-upper bathyal	
Bolivina plicatella	calcite	s infaunal	low/high	outer neritic-upper bathyal	
Bolivina "postvirginiana"	calcite	s infaunal	low/high	outer neritic-upper bathyal	yes
Bolivina "praevirginiana"	calcite	s infaunal	low/high	outer neritic-upper bathyal	
Bolivina regularis	calcite	i-d infaunal	low/high	outer neritic-upper bathyal	
Bolivina striatella	calcite	s infaunal	low/high	outer neritic-upper bathyal	
Bolivina tectiformis	calcite	s infaunal	low/high	outer neritic-upper bathyal	
Bolivina virginiana	calcite	s infaunal	low/high	outer neritic-upper bathyal	yes
Bulimina alazanensis	calcite	i-d infaunal	low/high	outer neritic-upper bathyal	
Bulimina cooperensis	calcite	i-d infaunal	low/high	outer neritic-upper bathyal	
Bulimina jacksonensis	calcite	i-d infaunal	low/high	outer neritic-upper bathyal	yes
Caucasina marylandica	calcite	phytodetrital	low/high	outer neritic-upper bathyal	yes
Charltonina madrugaensis	calcite	d infaunal	low/high	outer neritic-upper bathyal	yes
Cibicidoides pippeni	calcite	epifaunal	high/low	outer neritic-upper bathyal	
Cribrostomoides sp.	agglutinated	s infaunal	low/high	outer neritic-upper bathyal	
Cyclammina cancellata	agglutinated	s infaunal	low/high	outer neritic-upper bathyal	
Dorothia sp.	agglutinated	d infaunal	low/high	outer neritic-upper bathyal	
Epistominella minuta	calcite	epifaunal	low/high	outer neritic-upper bathyal	yes
Gaudryina alazanensis	agglutinated	d infaunal	low/high	outer neritic-upper bathyal	
Globobulimina ovata	aragonite?	i-d infaunal	low/high	outer neritic-upper bathyal	
Globocassidulina subglobosa	calcite	phytodetrital	low/high	outer neritic-upper bathyal	
Grigelis annulospinosa	calcite	infaunal	low/high	outer neritic-upper bathyal	
Grigelis cookei	calcite	infaunal	low/high	outer neritic-upper bathyal	
Grigelis "curvicostata"	calcite	infaunal	low/high	outer neritic-upper bathyal	
Grigelis "elongata"	calcite	infaunal	low/high	outer neritic-upper bathyal	
Grigelis "elongostriata"	calcite	infaunal	low/high	outer neritic-upper bathyal	
Grigelis "gigas"	calcite	infaunal	low/high	outer neritic-upper bathyal	
Grigelis "tubulosa"	calcite	infaunal	low/high	outer neritic-upper bathyal	
Grigelis "tumerosa"	calcite	infaunal	low/high	outer neritic-upper bathyal	
Gyroidinoides aequilateralis	calcite	s infaunal	low/high	outer neritic-upper bathyal	
Gyroidinoides byramensis	calcite	s infaunal	low/high	outer neritic-upper bathyal	
Gyroidinoides octocameratus	calcite	s infaunal	low/high	outer neritic-upper bathyal	
Gyroidinoides planatus	calcite	s infaunal	low/high	outer neritic-upper bathyal	
Hoeglundina elegans	aragonite	epifaunal	low/high	outer neritic-upper bathyal	
Marginulina cocoaensis	calcite	infaunal	low/high	outer neritic-upper bathyal	
Marginulina karreriana	calcite	infaunal	?/?	outer neritic-upper bathyal	

Table F9. Benthic foraminiferal species used for interpretation of Chickahominy paleoenvironments at the USGS-NASA Langley and Kiptopeke core sites.—Continued

Species	Test construction	Microhabitat	Oxygen/ nutrient tolerance	Preferred paleodepth	Opportunist
Melonis planatus	calcite	i-d infaunal	low/high	outer neritic-upper bathyal	
Nodosaria capitata	calcite	infaunal	low/high	outer neritic-upper bathyal	
Nodosaria pustulosa	calcite	infaunal	low/high	outer neritic-upper bathyal	
Nodosaria saggitula	calcite	infaunal	low/high	outer neritic-upper bathyal	
Nodosaria soluta	calcite	infaunal	low/high	outer neritic-upper bathyal	
Nodosaria vertebralis	calcite	infaunal	low/high	outer neritic-upper bathyal	
Oridorsalis umbonatus	calcite	epifaunal	low/high	outer neritic-upper bathyal	
Reophax sp.	agglutinated	i-d infaunal	low/high	inner neritic-upper bathyal	
Spiroplectinella mississippiensis	agglutinated	d infaunal	low-high	outer neritic-upper bathyal	
Stilostomella "aduncocostata"	calcite	infaunal	low/high	outer neritic-upper bathyal	
Stilostomella annulospinosa	calcite	infaunal	low/high	outer neritic-upper bathyal	
Stilostomella "bicostata"	calcite	infaunal	low/high	outer neritic-upper bathyal	
Stilostomella cocoaensis	calcite	infaunal	low/high	outer neritic-upper bathyal	
Stilostomella "exilispinata"	calcite	infaunal	low/high	outer neritic-upper bathyal	
Stilostomella "juvenocostata"	calcite	infaunal	low/high	outer neritic-upper bathyal	
Stilostomella "multispiculata"	calcite	infaunal	low/high	outer neritic-upper bathyal	
Technitella sp.	agglutinated	infaunal	low/high	outer neritic-upper bathyal	
Turrilina robertsi	calcite	infaunal	low/high	outer neritic-upper bathyal	
Uvigerina cookei	calcite	s infaunal	low/high	outer neritic-upper bathyal	
Uvigerina dumblei	calcite	s infaunal	low/high	outer neritic-upper bathyal	
Uvigerina gardnerae	calcite	s infaunal	low/high	outer neritic-upper bathyal	yes
Uvigerina jacksonensis	calcite	s infaunal	low/high	outer neritic-upper bathyal	
Uvigerina spinicostata	calcite	s infaunal	low/high	outer neritic-upper bathyal	

boundaries and benthic foraminiferal subzonal boundaries are shown to be diachronous. For example, application of the depth-age model indicates that subunits SP–2 and SP–3 at Kiptopeke are equivalent geochronologically to SP–2 at Langley. This correlation implies further that SP–4 and SP–5 at Kiptopeke are equivalent to SP–3 and SP–4, respectively, at Langley. Likewise, the depth-age model indicates that log subunits GR–A and GR–B at Kiptopeke are equivalent to GR–A at Langley, requiring consequent reassignment of GR–C (now GR–B) and the combination of GR–D and GR–E (now GR–C) at Kiptopeke.

On the other hand, however, significant shifts in some of these same physico-chemical properties take place near the middle of the *Lagenoglandulina virginiana* Subzone (indicated by filled triangles in fig. F27) without a corresponding change in the benthic foraminiferal populations (other than an upward shift in average species diversity).

Summary and Conclusions

The transition from synimpact to postimpact deposition at the USGS-NASA Langley core site began with an airfall of shock-melted glass microspherules, which collected as a fallout layer, 3 cm (1.2 in.) thick, in tranquil conditions on the floor of the 300-m-deep (~1,000-ft-deep) crater basin. Marine deposition resumed at the site, but hostile bottom conditions prevented a normal marine benthic community from migrating into the crater. Instead, a succession of submillimeter-scale clay, silt, and sand laminae accumulated, in which the sand laminae contained reworked specimens of microfossils (mainly foraminifera and ostracodes). The reworked specimens apparently were derived from the apron of Exmore breccia that surrounded the crater rim. The hostile conditions lasted no more than ~8 k.y. (the duration could have been less than 1 k.y.) and were replaced by fertile, clay-dominated marine lithotopes that supported a rich assemblage of benthic microbiota whose fossils are found in cores of the Chickahominy Formation.

Upon visual examination, the Chickahominy Formation in the USGS-NASA Langley core appears to be a uniform, massive marine clay unit that is 52.37 m (171.8 ft) thick. Likewise, acoustic impedance properties of the Chickahominy yield a generally uniform signature on seismic-reflection profiles. This seismic signature enables us to easily trace the Chickahominy over the entire impact crater, to determine the structural geometry of its upper surface, and to extrapolate its stratigraphic thickness in areas where no cores are available.

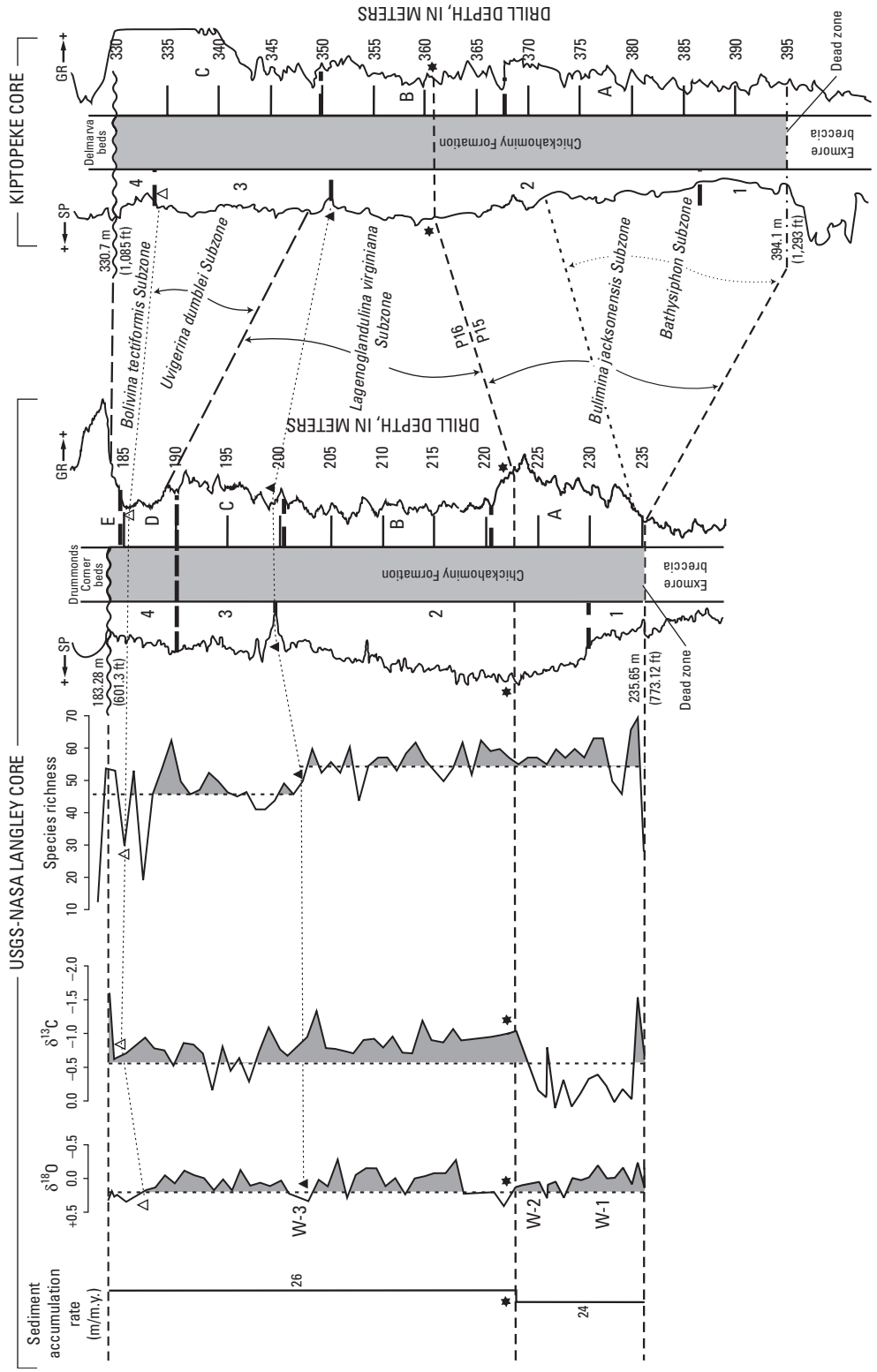

Figure F27. Chart showing correlations of principal properties of the Chickahominy Formation studied in the USGS-NASA Langley corehole with geophysical logs and benthic foraminiferal stratigraphy from the Kiptopeke corehole. The best (closest to isochronous) correlations (indicated by stars) are among the upward increase in sediment accumulation rate, the positive excursion in $\delta^{18}O$, the negative excursion in $\delta^{13}C$, the maximum positive deflection in the spontaneous-potential (SP) curve (peak in permeability), and the maximum positive deflection in the gamma-ray (GR) curve (peak in glauconite content) at Langley and the top of the *Bulimina jacksonensis* Subzone (coincident with the P15-P16 boundary) at Langley and Kiptopeke. A secondary (approximate) correlation (indicated by filled triangles) exists among the upward species-richness decrease, the major negative deflection of the SP curve (permeability decrease), and the moderate positive shift in the GR curve (glauconite increase) near the middle of the *Lagenoglandulina virginiana* Subzone at Langley and the boundary between subunits SP–2 and SP–3 at Kiptopeke. Another possible secondary correlation (indicated by open triangles) exists at the top of the Chickahominy section among the positive $\delta^{18}O$ deflection, the negative $\delta^{13}C$ deflection, the increase in stratigraphic variability of species richness, and the negative deflection in the GR curve (glauconite decrease) at Langley and the top of the *Uvigerina dumblei* Subzone at both Langley and Kiptopeke.

The Chickahominy can be stratigraphically subdivided rather easily, however, on the basis of downhole geophysical logs and foraminifera (both planktonic and benthic). The spontaneous-potential (SP) log curve allows a fourfold subdivision, whereas the gamma-ray (GR) log curve defines a fivefold subdivision. These subdivisions can be also recognized in the North, Bayside, and Kiptopeke coreholes, but not all subunit boundaries can be considered coeval at the different core sites. In the middle of the formation, the SP and GR unit boundaries are closely correlative from corehole to corehole, but lithic boundary correlations are poor at the top and base of the Chickahominy. On the basis of these log characteristics, the Chickahominy in the USGS-NASA Langley corehole is anomalous with regard to the unit in the other three intracrater coreholes, mainly because of the unusually great permeability and thickness of subunit SP–2 and the significantly greater glauconite volume in subunit GR–A. Another anomaly in the USGS-NASA Langley corehole is the fact that the basal part of the Chickahominy is significantly more permeable than the top part of the underlying Exmore breccia, whereas, the opposite relationship characterizes the transition in the other three coreholes.

The planktonic foraminiferal record at the USGS-NASA Langley site yields no clear subdivision of the Chickahominy. Elements of Zones P15, P16, and P17 are present but not in enough abundance or stratigraphic persistence to identify their mutual boundary. We, therefore, identified the approximate P15-P16 biochronozonal boundary by proxy, by using the short overlap interval between the highest occurrence of *Bolboforma spinosa* and the lowest occurrence of *Bolboforma latdorfensis*.

A suite of 126 benthic foraminiferal species in the Chickahominy Formation in the Langley core represents a single, easily recognizable biozone (*Cibicidoides pippeni* Zone), which embraces five distinct subbiozones (from base to top, the *Bathysiphon, Bulimina jacksonensis, Lagenoglandulina virginiana, Uvigerina dumblei,* and *Bolivina tectiformis* Subzones). Both planktonic and benthic zonations correlate well with equivalent zonations in the Kiptopeke core, but only one of the benthic boundaries (top of the *Bulimina jacksonensis* Subzone) appears to be isochronous.

The dominant benthic foraminiferal assemblages in the Chickahominy Formation at Langley contain both calcareous and agglutinated species, whose modern counterparts and ancient equivalents have been studied in many other localities. The key paleoenvironmental indicators point to epifaunal and shallow infaunal microhabitats characterized by oxygen deprivation and high flux rates of organic matter to the sea floor. At the USGS-NASA Langley site, the *Cibicidoides pippeni* assemblage reoccupied the crater floor a relatively short time (<1 to 8 k.y.) after tumultuous deposition of the Exmore breccia had abated.

Stable-isotope records derived from the benthic foraminifer *Cibicidoides pippeni* show three negative excursions in $\delta^{18}O$ (interpreted as pulses of warm paleoclimate) and two negative excursions in $\delta^{13}C$ (interpreted as variations in the global burial of carbon). This stable-isotope record matches that previously documented at Kiptopeke and supports the hypothesis of Poag (1997b) that the Chesapeake Bay and Popigai (Russia) bolide impacts significantly influenced the long-term atmospheric dynamics of the late Eocene-early Oligocene time interval and may have helped trigger a globally recognized mass extinction event in the early Oligocene.

Acknowledgments

U.S. Geological Survey (USGS) investigations of the Chesapeake Bay impact structure are conducted in cooperation with the Hampton Roads Planning District Commission, the Virginia Department of Environmental Quality, and the National Aeronautics and Space Administration (NASA) Langley Research Center. The Hampton Roads Planning District Commission and the USGS provided funds for the drilling of the USGS-NASA Langley corehole. The NASA Langley Research Center provided extensive operational and logistical support for the drilling operation. The Virginia Department of Environmental Quality and the Department of Geology of the College of William and Mary provided extensive operational support at the drill site.

We thank the other members of the Chesapeake coring team for acquiring and sampling the USGS-NASA Langley core, Stephen E. Curtin (USGS) and Richard E. Hodges (USGS) for providing the geophysical logs of the Langley, North, and Bayside coreholes, Texaco, Inc., for providing multichannel seismic-reflection profiles, Judith Commeau (USGS) and Louie Kerr (Marine Biological Laboratory) for providing scanning-electron microscopy, and Emily Denham (USGS) for preparing the samples for analysis. We are indebted to the National Geographic Society for funding the collection of single-channel seismic profiles, to the Woods Hole Oceanographic Institution for use of its mass spectrometer, and to the Marine Biological Laboratory (Woods Hole, Mass.) for use of its scanning-electron-microscope facilities. Lucy E. Edwards, Harry J. Dowsett, J. Wright Horton, Jr., David S. Powars, and Gregory S. Gohn, all of the USGS, reviewed early versions of the manuscript of this chapter.

References Cited

Bandy, O.L., 1949, Eocene and Oligocene foraminifera from Little Stave Creek, Clarke County, Alabama: Bulletins of American Paleontology, v. 32, no. 131, 210 p.

Beckmann, J.P., 1954, Die Foraminferen der Oceanic Formation (Eocaen-Oligocaen) von Barbados, Kl. Antillen: Eclogae Geologicae Helvetiae, v. 46, no. 2, p. 301–412, 15 pls. (In German with English summary.)

Berggren, W.A., Kent, D.V., Swisher, C.C., III, and Aubry, M.P., 1995, A revised Cenozoic geochronology and chronostratigraphy, *in* Berggren, W.A., Kent., D.V., Aubry, M.-P., and Hardenbol, Jan, eds., Geochronology, time scales, and global stratigraphic correlation: SEPM (Society for Sedimentary Geology) Special Publication 54, p. 129–212.

Berggren, W.A., and Miller, K.G., 1988, Paleogene tropical planktonic foraminiferal biostratigraphy and magnetobiochronology: Micropaleontology, v. 34, no. 4, p. 362–380.

Bernhard, J.M., and Sen Gupta, B.K., 1999, Foraminifera of oxygen-depleted environments, *in* Sen Gupta, B.K., ed., Modern foraminifera: Boston, Kluwer Academic Publishers, p. 201–216.

Brown, P.M., Miller, J.A., and Swain, F.M., 1972, Structural and stratigraphic framework and spatial distribution of permeability of the Atlantic Coastal Plain, North Carolina to New York: U.S. Geological Survey Professional Paper 796, 79 p.

Bukry, David, 1973, Low-latitude coccolith biostratigraphic zonation, *in* Edgar, N.T., and others, Initial reports of the Deep Sea Drilling Project, v. 15: Washington. D.C., U.S. Government Printing Office, p. 685–703.

Bukry, David, 1975, Coccolith and silicoflagellate biostratigraphy, northwestern Pacific Ocean, Deep Sea Drilling Project, Leg 32, *in* Initial reports of the Deep Sea Drilling Project, v. 32: College Station, Tex., Texas A&M University, Ocean Drilling Program, p. 677–701.

Caralp, M.H., 1989, Abundance of *Bulimina exilis* and *Melonis barleeanum*; Relationship to the quality of marine organic matter: Geo-Marine Letters, v. 9, no. 1, p. 37–43.

Charletta, A.C., 1980, Eocene benthic foraminiferal paleoecology and paleobathymetry of the New Jersey continental margin: New Brunswick, N.J., Rutgers, the State University of New Jersey, Ph.D. thesis, 82 p.

Corliss, B.H., and Fois, Elisabetta, 1990, Morphotype analysis of deep-sea benthic foraminifera from the northwest Gulf of Mexico: Palaios, v. 5, no. 6, p. 589–605.

Corliss, Bruce, and Silva, K.A., 1993, Rapid growth of deep-sea benthic foraminifera: Geology, v. 21, no. 11, p. 991–994.

Cushman, J.A., 1925, Eocene foraminifera from the Cocoa Sand of Alabama: Contributions from the Cushman Laboratory for Foraminiferal Research, v. 1, p. 65–70.

Cushman, J.A., 1926, Some fossil Bolivinas from Mexico: Contributions from the Cushman Laboratory for Foraminiferal Research, v. 1, p. 81–84.

Cushman, J.A., 1933, New foraminifera from the Upper Jackson Eocene of the southeastern coastal plain of the United States: Contributions from the Cushman Laboratory for Foraminiferal Research, v. 9, p. 1–21.

Cushman, J.A., 1935, Upper Eocene foraminifera of the southeastern United States: U.S. Geological Survey Professional Paper 181, 88 p.

Cushman, J.A., and Applin, E.R., 1926, Texas Jackson foraminifera: American Association of Petroleum Geologists Bulletin, v. 10, no. 2, p. 154–189, 6 pls.

Cushman, J.A., and Bermúdez, P.T., 1948, Some Paleocene foraminifera from the Madruga Formation of Cuba: Contributions from the Cushman Laboratory for Foraminiferal Research, v. 24, p. 68–75.

Cushman, J.A., and Cederstrom, D.J., 1945, An upper Eocene foraminiferal fauna from deep wells in York County, Virginia: Virginia Geological Survey Bulletin 67, 58 p., 6 pls.

Cushman, J.A., and Garrett, J.B., 1938, Three new rotaliform foraminifera from the lower Oligocene and upper Eocene of Alabama: Contributions from the Cushman Laboratory for Foraminiferal Research, v. 14, p. 62–66.

Cushman, J.A., and Todd, R., 1946, A foraminiferal fauna from the Byram Marl at its type locality: Contributions from the Cushman Laboratory for Foraminiferal Research, v. 22, p. 76–102.

Douglas, R.G., and Heitman, H.L., 1979, Slope and basin benthic foraminifera of the California borderland, *in* Doyle, L.J., and Pilkey, O.H., eds., Geology of continental slopes: Society of Economic Paleontologists and Mineralogists Special Publication 27, p. 231–246.

Farley, K.A., Montanari, A., Shoemaker, E.M., and Shoemaker, C.S., 1998, Geochemical evidence for a comet shower in the late Eocene: Science, v. 280, no. 5367, p. 1250–1253.

Gooday, A.J., 1993, Deep-sea benthic foraminiferal species which exploit phytodetritus; Characteristic features and controls on distribution: Marine Micropaleontology, v. 22, no. 3, p. 187–205.

Gooday, A.J., 1994, The biology of deep-sea foraminifera; A review of some advances and their applications to paleoceanography: Palaios, v. 9, no. 1, p. 14–31.

Gooday, A.J., 1996, Epifaunal and shallow infaunal foraminiferal communities at three abyssal NE Atlantic sites subject to differing phytodetritus input regimes: Deep-Sea Research, v. 43, p. 1395–1421.

Jones, M.H., 1990, Middle Eocene foraminifera from the Piney Point Formation of the Virginia and Maryland Coastal Plain: Norfolk, Va., Old Dominion University, masters thesis, 243 p.

Jorissen, F.J., Barmawidjaja, D.M., Puskaric, S., and van der Zwaan, G.J., 1992, Vertical distribution of benthic foraminifera in the northern Adriatic Sea; The relation with the organic flux: Marine Micropaleontology, v. 19, no. 1–2, p. 131–146.

Kaminski, M.A., Boersma, Ann, Tyszka, Jaroslaw, and Holbourn, A.E.L., 1995, Response of deep-water agglutinated foraminifera to dysoxic conditions in the California borderland basins, *in* Kaminski, M.A., Geroch, Stanislaw, and Gasinski, M.A., eds., Proceedings of the Fourth International Workshop on Agglutinated Foraminifera, Krakow, Poland,

September 12–19, 1993: Grzybowski Foundation Special Publication 3, p. 131–140, 1 pl.

Kobashi, Takuro, Grossman, E.L., Yancey, T.E., and Dockery, D.T., III, 2001, Reevaluation of conflicting Eocene tropical temperature estimate; Molluskan oxygen isotope evidence for warm low latitudes: Geology, v. 29, no. 11, p. 983–986.

Linke, P., Altenbach, A.V., Graf, G., and Heeger, T., 1995, Response of deep-sea benthic foraminifera to a simulated sedimentation event: Journal of Foraminiferal Research, v. 25, no. 1, p. 75–82.

Loubere, P., and Fariduddin, M., 1999, Benthic foraminifera and the flux of organic carbon to the seabed, *in* Sen Gupta, B.K., ed., Modern foraminifera: Boston, Kluwer Academic Publishers, p. 181–199.

Mackensen, Andreas, and Douglas, R.G., 1989, Down-core distribution of live and dead deep-water benthic foraminifera in box cores from the Weddell Sea and the California continental borderland: Deep-Sea Research, v. 36, no. 6, p. 879–900.

Martini, Erlend, 1971, Standard Tertiary and Quaternary calcareous nannoplankton zonation, *in* Farinacci, Anna, and Matteucci, R., eds., Proceedings of the II Planktonic Conference, Roma, 1970: Rome, Edizioni Tecnoscienza, v. 2, p. 739–785, 4 pls.

Nogan, D.S., 1964, Foraminifera, stratigraphy, and paleoecology of the Aquia Formation of Maryland and Virginia: Cushman Foundation for Foraminiferal Research Special Publication 7, 50 p.

Olsson, R.K., 1960, Foraminifera of latest Cretaceous and earliest Tertiary age in the New Jersey Coastal Plain: Journal of Paleontology, v. 34, no. 1, p. 1–58.

Orbigny, Alcide d', 1846, Foraminifères fossiles du bassin tertiare de Vienne: Paris, 312 p.

Pearson, P.N., Ditchfield, P.W., Singano, Joyce, Harcourt-Brown, K.G., Nicholas, C.J., Olsson, R.K., Shackleton, N.J., and Hall, M.A., 2001, Warm tropical sea surface temperatures in the Late Cretaceous and Eocene epochs: Nature, v. 413, no. 6855, p. 481–487.

Pfannkuche, O., 1993, Benthic response to the sedimentation of particulate organic matter at the BIOTRANS station, 47°N, 20°W: Deep-Sea Research, v. 40, p. 135–139.

Phleger, F.B, and Soutar, Andrew, 1973, Production of benthic foraminifera in three east Pacific oxygen minima: Micropaleontology, v. 19, no. 1, p. 110–115.

Plummer, H.J., 1927, Foraminifera of the Midway Formation in Texas: Texas University Bulletin 2644, 205 p., 15 pls.

Poag, C.W., 1981, Ecologic atlas of benthic foraminifera of the Gulf of Mexico: Woods Hole, Mass., Marine Science International, 174 p.

Poag, C.W., 1997a, The Chesapeake Bay bolide impact; A convulsive event in Atlantic Coastal Plain evolution: Sedimentary Geology, v. 108, no. 1–4, p. 45–90.

Poag, C.W., 1997b, Roadblocks on the kill curve; Testing the Raup hypothesis: Palaois, v. 12, no. 6, p. 582–590.

Poag, C.W., 2002, Synimpact-postimpact transition inside Chesapeake Bay crater: Geology, v. 30, no. 11, p. 995–998.

Poag, C.W., and Aubry, M.-P., 1995, Upper Eocene impactites of the U.S. East Coast; Depositional origins, biostratigraphic framework, and correlation: Palaios, v. 10, no. 1, p. 16–43.

Poag, C.W., and the Chesapeake Coring Team, 2001, Drilling to basement inside the Chesapeake Bay crater [abs.]: Lunar and Planetary Science Conference, 32d, Houston, Tex., March 12–16, 2001, Abstract 1203, available online at http://www.lpi.usra.edu/meetings/lpsc2001/pdf/1203.pdf.

Poag, C.W., and Commeau, J.A., 1995, Paleocene to middle Miocene planktonic foraminifera of the southwestern Salisbury embayment, Virginia and Maryland; Biostratigraphy, allostratigraphy, and sequence stratigraphy: Journal of Foraminiferal Research, v. 25, no. 2, p. 134–155, 9 pls.

Poag, C.W., Gohn, G.S., and Powars, D.S., 2001, From shocked basement to fallout spherules; The coring record at the Chesapeake Bay crater [abs.]: Geological Society of America Abstracts with Programs, v. 33, no. 6, p. A–433.

Poag, C.W., Hutchinson, D.R., Colman, S.M., and Lee, M.W., 1999, Seismic expression of the Chesapeake Bay impact crater; Structural and morphologic refinements based on new seismic data, *in* Dressler, B.O., and Sharpton, V.L., eds., Large meteorite impacts and planetary evolution; II: Geological Society of America Special Paper 339, p. 149–164.

Poag, C.W., Koeberl, Christian, and Reimold, W.U., 2004, The Chesapeake Bay crater—Geology and geophysics of a late Eocene submarine impact structure: New York, Springer-Verlag, 522 p. plus CD-ROM.

Poag, C.W., Mankinen, E., and Norris, R.D., 2003, Late Eocene impacts; Geologic record, correlation, and paleoenvironmental consequences, *in* Prothero, D.R., Ivany, L.C., and Nesbitt, E.R., eds., From greenhouse to icehouse; The marine Eocene-Oligocene transition: New York, Columbia University Press, p. 495–510.

Powars, D.S., and Bruce, T.S., 1999, The effects of the Chesapeake Bay impact crater on the geologic framework and the correlation of hydrogeologic units of the lower York-James Peninsula, Virginia: U.S. Geological Survey Professional Paper 1612, 82 p., 9 oversize pls. (Also available online at http://pubs.usgs.gov/prof/p1612/).

Powars, D.S., Mixon, R.B., and Bruce, Scott, 1992, Uppermost Mesozoic and Cenozoic geologic cross section, outer coastal plain of Virginia, *in* Gohn, G.S., ed., Proceedings of the 1988 U.S. Geological Survey Workshop on the Geology and Geohydrology of the Atlantic Coastal Plain: U.S. Geological Survey Circular 1059, p. 85–101.

Sen Gupta, B.K., Turner, R.E., and Rabalais, N.N., 1996, Seasonal oxygen depletion in continental-shelf waters of Louisi-

ana; Historical record of benthic foraminifers: Geology, v. 24, no. 3, p. 227–230.

Tjalsma, R.C., and Lohmann, G.P., 1983, Paleocene-Eocene bathyal and abyssal benthic foraminifera from the Atlantic Ocean: Micropaleontology Special Publication 4, 90 p., 22 pls.

Van Morkhoven, F.P.C.M., Berggren, W.A., and Edwards, A.S., 1986, Cenozoic cosmopolitan deep-water benthic foraminifera: Bulletin des Centres de Recherches Exploration-Production Elf-Aquitaine, Mémoire 11, 421 p.

Plates F1, F2

Plate F1

Nominate Species for Benthic Foraminiferal Zone and Subzones Recognized in the Chickahominy Formation

[Scale bars are 100 micrometers (μm). These species are represented in the Chickahominy Formation in all cores obtained from the Chesapeake Bay impact crater. Sites where cores were obtained are shown in figure F1. Plate from Poag, Koeberl, and Reimold (2004, fig. 13.3)]

Figure
1. *Cibicidoides pippeni* (Cushman and Garrett) 1938. Chickahominy Formation, Exmore core, umbilical view.
2. *Bulimina jacksonensis* Cushman 1925. Chickahominy Formation, Exmore core, lateral view.
3. *Lagenoglandulina virginiana* (Cushman and Cederstrom) 1945. Chickahominy Formation, Newport News Park 2 core, lateral view.
4. *Uvigerina dumblei* Cushman and Applin 1926. Chickahominy Formation, Exmore core, lateral view.
5. *Bolivina tectiformis* Cushman 1926. Chickahominy Formation, Exmore core, lateral view.
6. *Bathysiphon* sp. Chickahominy Formation, Kiptopeke core, lateral view.

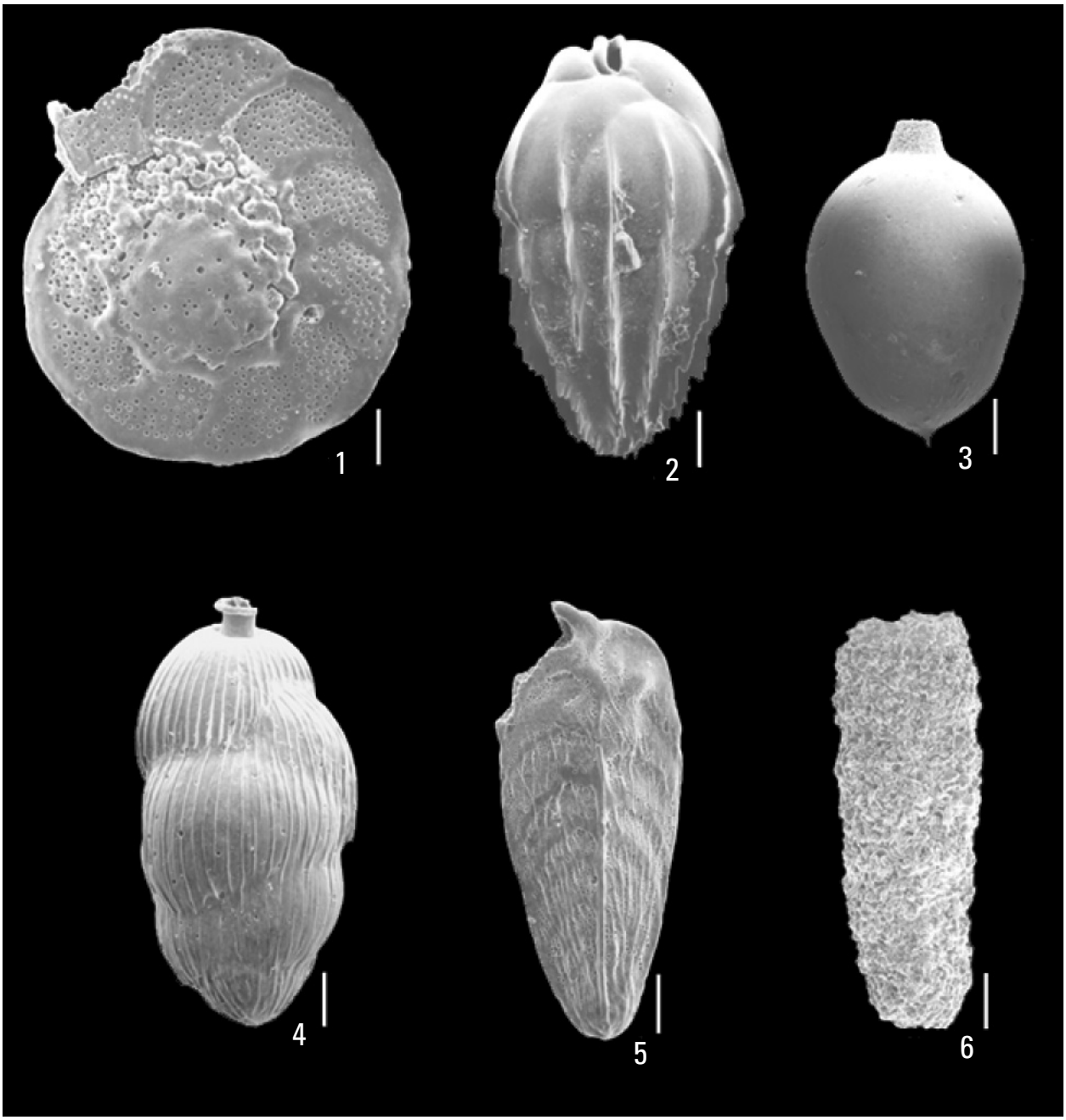

Nominate Species for Benthic Foraminiferal Zone and Subzones Recognized in the Chickahominy Formation

Plate F2

Important Benthic Foraminiferal Species from the Chickahominy Formation Used for Paleoenvironmental Interpretations

[Scale bars are 100 μm. Illustrated specimens are from the Exmore core; specimens of the same species in the Kiptopeke and USGS-NASA Langley cores are used for paleoenvironmental interpretations (table F9). The Exmore, Kiptopeke, and Langley corehole locations are shown in figure F1. Plate from Poag, Koeberl, and Reimold (2004, fig. 13.7). Quotation marks indicate provisory trivial name]

Figure
1. *Epistominella minuta* Olsson 1960. Chickahominy Formation, Exmore core, umbilical view.
2. *Charltonina madrugaensis* (Cushman and Bermúdez) 1948. Chickahominy Formation, Exmore core, umbilical view.
3. *Gyroidinoides aequilateralis* (Plummer) 1927. Chickahominy Formation, Exmore core, umbilical view.
4. *Gyroidinoides byramensis* (Cushman and Todd) 1946. Chickahominy Formation, Exmore core, umbilical view.
5. *Uvigerina gardnerae* Cushman 1926. Chickahominy Formation, Exmore core, lateral view.
6. *Caucasina marylandica* (Nogan) 1964. Chickahominy Formation, Exmore core, lateral view.
7. *Bolivina gracilis* Cushman and Applin 1926. Chickahominy Formation, Exmore core, lateral view.
8. *Bolivina virginiana* Cushman and Cederstrom 1945. Chickahominy Formation, Exmore core, lateral view.
9. *Bolivina* "praevirginiana." Chickahominy Formation, Exmore core, lateral view.
10. *Globobulimina ovata* (d'Orbigny) 1846. Chickahominy Formation, Exmore core, lateral view.
11. *Grigelis cookei* (Cushman) 1933. Chickahominy Formation, Exmore core, lateral view, final two chambers.
12. *Grigelis annulospinosa* (Bandy) 1949. Chickahominy Formation, Exmore core, lateral view.
13. *Stilostomella* "exilispinata." Chickahominy Formation, Exmore core, lateral view.
14. *Stilostomella cocoaensis* (Cushman) 1925. Chickahominy Formation, Exmore core, lateral view.

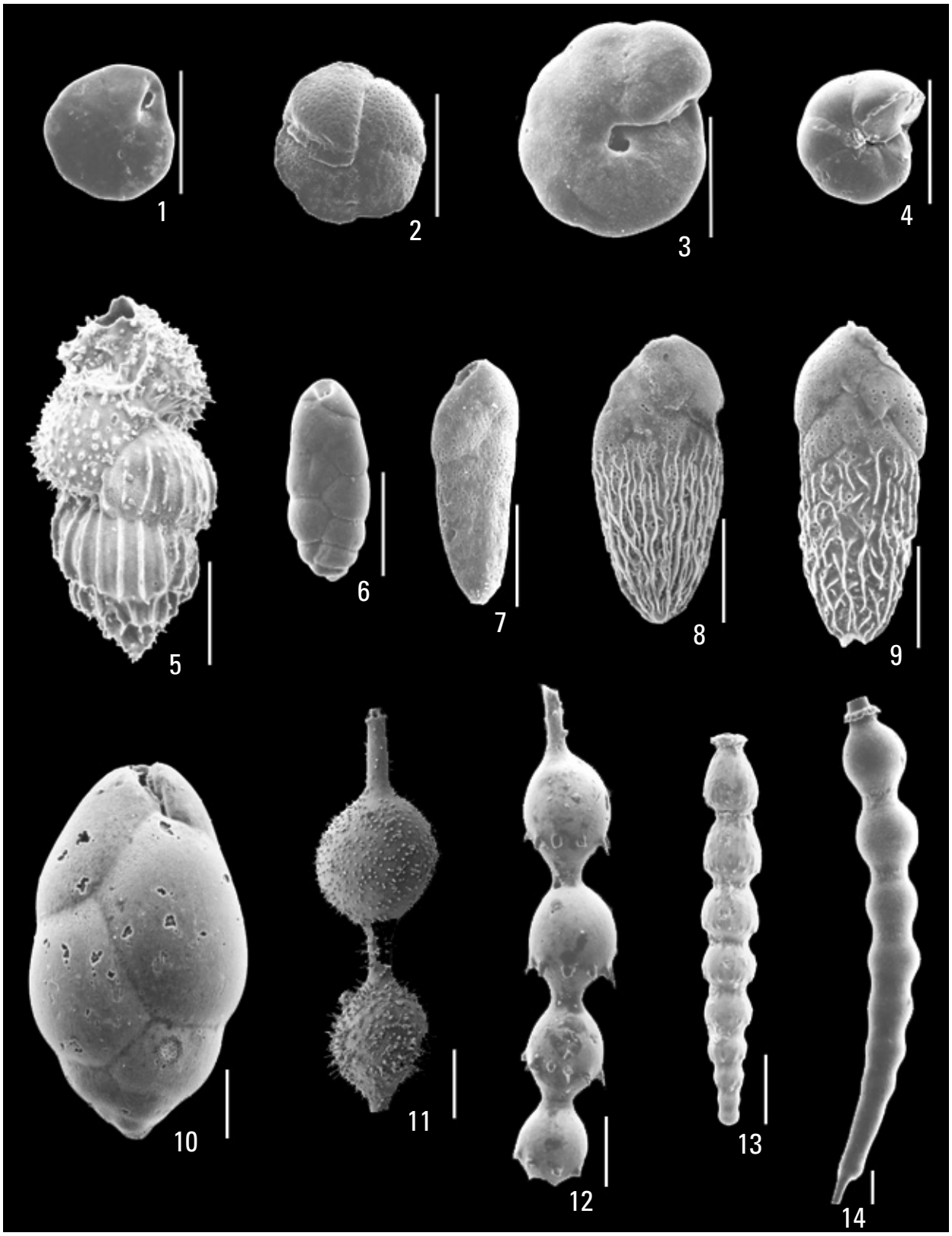

Important Benthic Foraminiferal Species from the Chickahominy Formation Used for Paleoenvironmental Interpretations